SEEING THROUGH THE EYES OF A SMALL FISH: THE ROLE OF VISION IN THE PERCEPTION OF SOCIAL INFORMATION

by

Diana Caroline Pita

A Dissertation

Submitted to the Faculty of Purdue University

In Partial Fulfillment of the Requirements for the degree of

Doctor of Philosophy

Department of Biological Sciences

West Lafayette, Indiana

December 2020

THE PURDUE UNIVERSITY GRADUATE SCHOOL
STATEMENT OF COMMITTEE APPROVAL

Dr. Esteban Fernández-Juricic, Chair

Department of Biological Sciences

Dr. Jeffrey R. Lucas

Department of Biological Sciences

Dr. Yuk Fai Leung

Department of Biological Sciences

Dr. Reuben R. Goforth

Department of Forestry and Natural Resources

Approved by:

Dr. Janice P. Evans

To my family: Mom, Dad, Layla, Porter, Violet and Peter

ACKNOWLEDGMENTS

I am thankful to the many people who supported me on my Ph.D. journey. First, my advisor, Dr. Esteban Fernández-Juricic for guiding me in my development as a scientist and critical-thinker and teaching me how to communicate effectively both verbally and through writing. I am also very grateful for Esteban's support in allowing me to pursue a Doctor of Veterinary Medicine (D.V.M.) while being enrolled simultaneously in the Ph.D. program.

I am thankful to my committee: Dr. Yuk Fai Leung, Dr. Jeff Lucas and Dr. Reuben Goforth for their diverse and constructive feedback. Through their combined expertise I have been able to strengthen the work of this dissertation.

My amazing lab members past and present have functioned as an unwavering support system and continuous source of knowledge. I feel honored to have worked alongside them and lucky to have learned from them: Rebecca Trapp, Morgan Chaney, Deona Harris, Ryan Lunn, Carlay LaTour, Benny Goller, Patrice Baumhardt, Yue Liu, Andrea Kress, Arden Blumenthal, Kelly Ronald, Luke Tyrrell, Shannon Butler, Megan Doppler, Ellie Sheridan, Bret Moore, Amanda Ensminger, Jessica Yorzinski, Adam Keener, Jeff Radloff, Javier Lenzi, and Yuanxing Ye.

Several dedicated undergraduate students have also contributed to this work: Megan Bock, Rachel Lim and Elizabeth Brewer. I am very grateful for their assistance in conducting endless hours of video coding and animal care duties. I am also grateful to the faculty and graduate students of the EEB Department who have functioned as respected colleagues and wonderful friends.

Lastly, I am thankful to the zebrafish and other animals that contributed to the work in this dissertation.

TABLE OF CONTENTS

ABSTRACT

In group-living animals social information is essential to survival, providing indirect information about the environment, such as predator presence. An individual's ability to acquire social information is mediated by its sensory system. In visually-oriented species, different visual dimensions provide rapid information about conspecifics. However, we know relatively little about how the uptake of visual social information mediates the formation of coordinated patterns of group movement, referred to as collective behavior. Using two species of birds (i.e., European starling (*Sturnus vulgaris*) and red-winged blackbird (*Agelaius phoeniceus*)) and fish (i.e., zebrafish (*Danio rerio*) and golden shiner (*Notemigonus crysoleucas*)), I determine how the structure of social interactions are facilitated by the capabilities imposed by the visual system from a theoretical point of view. With a focus on zebrafish (*Danio rerio*), a visually-oriented, social cyprinid, I further explore the role of vision in mediating social interactions. Specifically, I characterize several relevant visual dimensions in zebrafish that have the potential to influence the uptake of social information: visual coverage, visual resolution and visual contrast. With insights gained from theoretical modelling and a series of behavioral experiments, I discuss the constraints that these visual dimensions might impose on social interactions and develop predictions for collective behavior.

INTRODUCTION

Animals form groups when the benefits of association outweigh the costs of living alone (Krause and Ruxton, 2002). These benefits can include enhanced mating opportunities, food localization, energy efficiency, and antipredator defense (Krause and Ruxton, 2002). One consequence of group formation is the coordinated assemblage of individuals within the group, referred to as collective behavior (Sumpter, 2010). Collective behavior represents the large-scale patterns of coordinated movement that arise as individuals respond to environmental changes while attempting to remain attached to the group (Couzin and Krause, 2003; Sumpter, 2010). Different forms of collective behavior can be identified based on the group's emergent properties such as size (i.e. total number of individuals), density (i.e. number of individuals per unit area/volume), polarity (i.e. degree to which group members are facing the same direction) and shape (i.e. length and width of the group) (Sumpter et al., 2008; Katz et al., 2011; Lopez et al., 2012). The important function of collective behavior is that can amplify the benefits that an individual receives from being in a group, especially regarding antipredator defense. For example, in fish, low-density aggregations (i.e., shoals) can increase the survival of its individual members through enhanced vigilance (i.e., many eyes hypothesis) and reduced attack probability (i.e., dilution effect). However, if the group assembles into a more organized configuration with higher polarity (i.e., school) these advantages are enhanced along with the added benefit of decreasing the capture efficiency of the predator (i.e., confusion effect) (Pitcher and Parrish, 1993).

The persistence of collective behavior relies on the individual's ability to remain attached to the group (Sumpter, 2006). To accomplish this, individuals must maintain updated and reliable social information through the use of their sensory system (Warburton, 1997; King and Cowlishaw, 2007). Therefore, the key to understanding the formation and persistence of collective behavior depends on understanding the role of the sensory system in the perception of social information.

Much of our current understanding of collective behavior stems from the insights gained from theoretical modeling (Couzin et al., 2002). However, models make simplistic assumptions regarding how individuals should perceive and interact with conspecifics in their environment and often do not consider the relevant sensory components needed to replicate species-specific perception. As a result, we may be misrepresenting our understanding of collective behavior which

introduces the question: how do the various sensory dimensions contribute to the uptake of social information leading to collective behavior?

For my dissertation, I evaluate how the structure of collective interactions are mediated by the capabilities imposed by the visual system. I focus on the visual system because vision is a particularly reliable modality to gather social information due to its rapid propagation through the environment (Stevens, 2013). Additionally, visually-oriented species can receive indirect information about immediate threats through visual cues like the changes in the position, orientation, distance, and the saliency of conspecifics (Kelley et al., 2012) Within the visual system I examine certain dimensions that have the potential to influence the perception of social information. In visually-oriented species, the visual field configuration defines an individual's capacity to acquire social information while visual acuity and visual contrast limit information quality and content (Fernández-Juricic and Kacelnik, 2004; Martin, 2007; Fernández-Juricic and Kowalski, 2011).

In chapter 1 I evaluate the role that the sensory system plays in structuring collective behavior from a theoretical point of view by revaluating the visual assumptions of two ubiquitous collective behavior models, the distance-based metric model and number-based topological model. To accomplish this, I compare a set of classic visual assumptions for birds and fish with a set of realistic visual assumptions from two species of birds (i.e., European starling (*Sturnus vulgaris*) and red-winged blackbird (*Agelaius phoeniceus*)) and fish (i.e., zebrafish (*Danio rerio*) and golden shiner (*Notemigonus crysoleucas*)) that are known to display collective behavior (Røskaft and Rohwer, 1987; Saverino and Gerlai, 2008; Polverino et al., 2013; Butler and Fernández-Juricic, 2014). Following the insights gained from modeling, I further explore the role of specific visual dimensions on the uptake of social information and develop predictions for collective behavior. Specifically, in chapter 2 I focus my efforts to the zebrafish (*Danio rerio*), a visually-oriented, social cyprinid that is known to engage in various forms of collective behavior (Miklosi and Andrew, 2006; Saverino and Gerlai, 2008). Using the zebrafish, I characterize the components of two visual dimensions that have the potential to influence the uptake of social information: visual coverage and visual resolution. By characterizing these different visual dimensions, I determine how the structure of social interactions are facilitated by the capabilities imposed by the visual system, generating specific predictions for social interactions based on the perception of social information. To evaluate the validity of these predictions, I then conduct behavior experiments to

evaluate the constraints that these different visual dimensions might impose on social behavior. Specifically, I use a series of playback experiments to manipulate the visual resolution (chapter 3) and visual contrast (chapter 4) of animated conspecifics in order to determine how individuals respond behaviorally to changes in information quality and content.

References:

Butler, S. R., and Fernández-Juricic, E. (2014). European starlings recognize the location of robotic conspecific attention. *Biol. Lett.* 10, 20140665.

Couzin, I. D., and Krause, J. (2003). Self-organization and collective behavior in vertebrates. *Adv. Study Behav.* 32, 1–75.

Couzin, I. D., Krause, J., James, R., Ruxton, G. D., and Franks, N. R. (2002). Collective memory and spatial sorting in animal groups. *J. Theor. Biol.* 218, 1–11. doi:10.1006/yjtbi.3065.

Fernández-Juricic, E., and Kacelnik, A. (2004). Information transfer and gain in flocks: The effects of quality and quantity of social information at different neighbour distances. *Behav. Ecol. Sociobiol.* 55, 502–511. doi:10.1007/s00265-003-0698-9.

Fernández-Juricic, E., and Kowalski, V. (2011). Where does a flock end from an information perspective? A comparative experiment with live and robotic birds. *Behav. Ecol.* 22, 1304–1311. doi:10.1093/beheco/arr132.

Katz, Y., Tunstrøm, K., Ioannou, C. C., Huepe, C., Couzin, I. D., Tunstrom, K., et al. (2011). Inferring the structure and dynamics of interactions in schooling fish. *Proc. Natl. Acad. Sci.* 108, 18720–18725. doi:10.1073/pnas.1107583108.

Kelley, J. L., Phillips, B., Cummins, G. H., and Shand, J. (2012). Changes in the visual environment affect colour signal brightness and shoaling behaviour in a freshwater fish. *Anim. Behav.* 83, 783–791. doi:10.1016/j.anbehav.2011.12.028.

King, A. J., and Cowlishaw, G. (2007). When to use social information: the advantage of large group size in individual decision making. *Biol. Lett.* 3, 137–9. doi:10.1098/rsbl.2007.0017.

Krause, J., and Ruxton, G. D. (2002). *Living in groups*. Oxford: Oxford University Press.

Lopez, U., Gautrais, J., Couzin, I. D., and Theraulaz, G. (2012). From behavioural analyses to models of collective motion in fish schools. *Interface Focus* 2, 693–707. doi:10.1098/rsfs.2012.0033.

Martin, G. R. (2007). Visual fields and their functions in birds. *J. Ornithol.* 148, 547–562. doi:10.1007/s10336-007-0213-6.

Miklosi, A., and Andrew, R. J. (2006). The Zebrafish as a Model for Behavioral Studies. *Zebrafish* 3, 227–234.

Pitcher, T. J., and Parrish, J. K. (1993). "Functions of shoaling behaviour in teleosts," in *Behaviour of Teleost Fishes* (London: Chapman & Hall), 363–439.

Polverino, G., Phamduy, P., and Porfiri, M. (2013). Fish and robots swimming together in a water tunnel: robot color and tail-beat frequency influence fish behavior. *PLoS One* 8, e77589. doi:10.1371/journal.pone.0077589.

Røskaft, E., and Rohwer, S. (1987). An experimental study of the function of the red epaulettes and the black body colour of male red-winged blackbirds. *Anim. Behav.* 35, 1070–1077. doi:10.1016/S0003-3472(87)80164-1.

Saverino, C., and Gerlai, R. (2008). The social zebrafish: Behavioral responses to conspecific, heterospecific, and computer animated fish. *Behav. Brain Res.* 191, 77–87. doi:10.1016/j.bbr.2008.03.013.

Stevens, M. (2013). *Sensory ecology, behaviour and evolution*. Oxford University Press.

Sumpter, D., Buhl, J., Biro, D., and Couzin, I. (2008). Information transfer in moving animal groups. *Theory Biosci.* 127, 177–86. doi:10.1007/s12064-008-0040-1.

Sumpter, D. J. T. (2006). The principles of collective animal behaviour. *Philos. Trans. R. Soc. Lond. B. Biol. Sci.* 361, 5–22. doi:10.1098/rstb.2005.1733.

Sumpter, D. J. T. (2010). *Collective Animal Behavior*. Princeton, N.J.: Princeton University Press.

Warburton, K. (1997). "Social forces in animal congregations: interactive, motivational and sensory aspects," in *Animal Groups in Three Dimensions: How Species Aggregate*, ed. W. M. H. Julia K. Parrish (Cambridge University Press), 312–336.

CHAPTER 1. COLLECTIVE BEHAVIOR IN VERTEBRATES: A SENSORY PERSPECTIVE

Diana Pita[1], Bertrand Collignon[2], José Halloy[2] and Esteban Fernández-Juricic[1]

[1]Department of Biological Sciences, Purdue University, West Lafayette, Indiana, USA
[2]Université Paris Diderot, Sorbonne Paris Cité, LIED, UMR 8236, 75013 Paris, France

Citation:
A version of this chapter was originally published in The Royal Society Open Science and is reproduced here with permission.

Pita, D., Collignon, B., Halloy, J., and Fernández-Juricic, E. (2016). Collective behaviour in vertebrates: a sensory perspective. *R. Soc. Open Sci.* 3, 160377. doi:10.1098/rsos.160377.

1.1 Abstract

Collective behavior models can predict behaviors of schools, flocks, and herds. However, in many cases, these models make biologically unrealistic assumptions in terms of the sensory capabilities of the organism, which are applied across different species. We explored how sensitive collective behavior models are to these sensory assumptions. Specifically, we used parameters reflecting the visual coverage and visual acuity that determine the spatial range over which an individual can detect and interact with conspecifics. Using metric and topological collective behavior models, we compared the classic sensory parameters, typically used to model birds and fish, with a set of realistic sensory parameters obtained through physiological measurements. Compared with the classic sensory assumptions, the realistic assumptions increased perceptual ranges, which led to fewer groups and larger group sizes in all species, and higher polarity values and slightly shorter neighbor distances in the fish species. Overall, classic visual sensory assumptions are not representative of many species showing collective behavior and constrain unrealistically their perceptual ranges. More importantly, caution must be exercised when empirically testing the predictions of these models in terms of choosing the model species, making realistic predictions, and interpreting the results.

1.2 Introduction

For many species, social interactions play an important role in life history, often leading to the formation of social groups (Sumpter, 2010b). From an individual's perspective, joining groups can be beneficial (i.e., enhancing mating opportunities, food localization and predator detection) (Krause and Ruxton, 2002). Additionally, many of these benefits depend on the group structure as groups can vary in size (i.e., number of individuals), density (i.e., number of individuals per unite area/volume), spacing (i.e., distance between group mates), shape (i.e., length and width of the group), polarity (i.e., individuals face similar or different directions, leading to high or low alignment, respectively) (Giardina, 2008; Sumpter et al., 2008).

One fundamental aspect of group structure is understanding how individuals interact within the group (Sumpter, 2010b), as these interactions can lead to large-scale patterns of coordinated movement, known as collective behavior. For example, when group mates vary their distance, position or speed relative to their nearest neighbors, the density and shape of the group can change (Couzin and Krause, 2003; Sumpter, 2006, 2010b). Many fish species are known to organize themselves into two main types of collective states, shoals and schools (Pitcher and Parrish, 1993). Shoals are loose aggregations (i.e., random orientation, alignment and spacing of individuals) often formed during low stress contexts (i.e. foraging). Schools often form when a predator is detected, resulting in individuals maintaining high alignment and close spacing, increasing cohesiveness and consequently, reducing the changes of mortality (Pitcher and Parrish, 1993). Other forms of collective behavior, particularly in fish, include swarms and toruses (Krause and Ruxton, 2002).

The persistence of collective behavior relies on individuals being able to acquire, interpret and make use of relevant social information (Sumpter, 2006; King and Cowlishaw, 2007). Social information conveys aspects about the sender's current state, encoded in the form of inadvertent cues (e.g., shift in body position of a neighbor) or intended signals (e.g., alarm call) (Danchin et al., 2004). Considering that information is costly to obtain, species are thought to have evolved sensory systems that may be efficient in acquiring information under particular ecological conditions (Dall et al., 2005; Gordon, 2014). Therefore, in some species, individuals may rely on certain sensory modalities (e.g. visual system) or certain dimensions within a sensory modality (e.g. visual resolution) to acquire specific types of social information (Warburton, 1997; Hogan and Laskowski, 2013; Ben-Shaul, 2015). Variations in sensory input can influence the interactions between group members. For instance, studies conducted with saithe (*Pollachius virens*) found

that eliminating mechanosensory information decreased neighbor distances and increased the number of collisions between group members, while eliminating visual information led to an increase in neighbor distance (Partridge and Pitcher, 1980).

Despite the role that the sensory systems may play in the acquisition of social information, our current understanding of collective behavior does not consider the sensory constraints of different species (Lemasson et al., 2009). In the past, many models used to study collective behavior followed simplistic assumptions and interaction rules largely based off inanimate particles (Vicsek et al., 1995). Some recent models have considered aspects of sensory systems such as chemotaxis (Amorim, 2015) and vision (Kunz and Hemelrijk, 2012; Harpaz and Schneidman, 2014). Despite these attempts, many theoretical models still (i) limit an entire sensory modality to one dimension and do not include key aspects of sensory filtering relative to collective behavior (ii) generalize a single sensory configuration to multiple species or (iii) inaccurately represent the sensory system of the study species (Strandburg-Peshkin et al., 2013; Harpaz and Schneidman, 2014; Rosenthal et al., 2015). Establishing the role of different sensory system configurations in collective behavior from a theoretical perspective can provide novel insights into how sensory filtering may influence some of the mechanisms underlying collective behavior in different taxa.

In this study, we investigated how sensitive collective behavior models (metric model (MM) and topological model TM)) are to the constraints of the sensory system in different species by focusing on one sensory modality (i.e., vision) and assessing the role of two sensory components (i.e. visual coverage and visual acuity). We used models with metric-interaction rules and topological-based rules because they have been used frequently and continue to serve as a foundation for developing new models of collective behavior (Ballerini et al., 2008; Niizato and Gunji, 2011; Vicsek and Zafeiris, 2012). We established the influence of visual assumptions on the predictions of these models relative to the number of groups in the population, group size (i.e. total number of interacting individuals), polarity (i.e. degree of individual alignment), and nearest neighbor distance (i.e., spacing between individuals), speed at which group properties stabilized (i.e. speed of social information transfer) and the internal structural stability of the group (i.e. degree to which individuals maintain their position relative to neighbors in the group). We compared the model outputs based on (i) a set of visual assumptions used often throughout the literature and applied across species despite their likely very different sensory configurations

(hereafter, classic assumptions) and (ii) a set of assumptions from direct measurements of the visual systems of four vertebrates (two fish and two birds) that engage in collective behavior and predominantly use vision during social interactions (hereafter, realistic assumptions).

1.2.1 Visual sensory assumptions in collective behavior

In visually oriented species, visual coverage and visual acuity are two components of the visual sensory dimension that can mediate social interactions. For example, an individual's capacity to detect the presence of surrounding neighbors is influenced by the degree of visual coverage or visual field (i.e. the inverse of its blind area at the rear of the head (Martin, 2007)), while the ability to resolve subtle differences in neighbor identity and behavior at a given distance is dependent upon the spatial resolving power of the retina (i.e. visual acuity) (Fernández-Juricic and Kowalski, 2011).

Collective behavior models are often not species-specific when they attempt to incorporate vision-based parameters. For example, many models often use a 60° blind area for modeling fish and a 90° blind area for modeling birds (Hall et al., 1986; Hildenbrandt et al., 2010). The origin of these values can be traced back to measurements obtained from single species through direct observation of group behavior or inferred indirectly without taking measurements of the projections of the retinal boundaries in space. In the case of fish, blind area values have been obtained from indirect estimates assumed to apply to species with a body shape similar to gadoid fish (Hall et al., 1986) while visual acuity values (i.e., 0.5 – 2 body lengths) have been inferred from nearest neighbor distance ranges observed in minnow (*Phoxinus phoxinus*) groups (Partridge, 1980; Huth and Wissel, 1992, 1994). In the case of birds, blind area and visual acuity values were largely inferred without taking direct measurements from any species (e.g., Hildenbrandt, Carere & Hemelrijk, 2010). Additionally, some studies estimated visual coverage from the projections of the eyes (Strandburg-Peshkin et al., 2013; Rosenthal et al., 2015), but this method does not provide precise assessments of the actual projections of the retinal boundaries in space (Martin, 2007).

One of the consequences of using these inferred visual parameters in collective behavior models is that the outputs may be constrained to the same type of sensory filtering. However, there is a large amount of between-species variation in the configuration of the visual system (Walls, 1942; Hughes, 1977; Hart, 2001; Litherland and Collin, 2008; Thewissen and Nummela, 2008). Additionally, it is unclear whether the classic sensory parameters used in the models accurately

represent all species within each respective taxonomic group. For example, one avian species often used in collective behavior research, the European starling (*Sturnus vulgaris*) has a blind area of 64° (Martin, 1986), which is 26° lower than the assumed 90° blind area used to model its flocking behavior (e.g., Hildenbrandt, Carere & Hemelrijk, 2010; Hemelrijk & Hildenbrandt, 2012). Golden shiners (*Notemigonus crysoleucas*) and zebrafish (*Danio rerio*) have blind areas of only 21° and 25° (Pita et al., 2015), respectively, which is about half the values commonly used in studies that model fish collective behavior (Huth and Wissel, 1994; Hemelrijk and Kunz, 2005; Viscido et al., 2005; Wood and Ackland, 2007). Employing the same set of sensory assumptions across species could potentially impair our ability to (i) make informed predictions about collective behavior in different taxa, (ii) choose the right species to empirically test those predictions (i.e., species whose sensory configuration matches the model assumptions), (iii) interpret the mismatches between theoretical predictions and empirical data, and ultimately (iv) fail to isolate the mechanisms driving group member interactions.

1.3 Methods

The MM and TM we used belong to the family of individual-based models, which provide a way of understanding the mechanisms that lead to different emerging group configurations (Sumpter, 2010a; Lopez et al., 2012). Additionally, individual-based models allow scientists to compare the output of simulations where agents follow different local interaction rules (Vicsek and Zafeiris, 2012; Perna et al., 2014). The metric-based interaction rules (Reynolds, 1987; Huth and Wissel, 1994) define three metric zones that radiate from the center of the individual: a (i) repulsion, (ii) alignment and (iii) attraction. Neighbors located within the repulsion zone are avoided. Neighbors located within the alignment and attraction zones are used to determine the individual's successive movement decisions, either by matching its heading to that of its neighbors or moving closer to them (Couzin et al., 2002).

Models that follow topological-based rules were introduced after empirical evidence showed that starlings respond to a set number of neighbors independent of their metric neighbor distance (Ballerini et al., 2008). Topological-based rules allow individuals to weigh information equally from a set number of near or distant neighbors while incorporating similar principles of attraction, repulsion and alignment (Tian et al.; Niizato and Gunji, 2011).

We studied the effects two components of the visual system: visual coverage and visual acuity and incorporated both as the basis for the realistic assumptions. We operationally defined visual coverage as the area around an individual's head along the horizontal plane of the body from which it can gather visual information (Martin, 2007), and visual acuity as the maximum distance than an individual can spatially resolve social cues, which can be used as a proxy for an individual's social interaction range (Fernández-Juricic and Kowalski, 2011; Pita et al., 2015). Our proxy of visual acuity is not the maximum distance an individual can perceive the whole body of a conspecific, but rather the distance it can resolve specific morphological cues of a neighbor (i.e., head height for birds and body height for fish) that would lead to the recognition of a member of the same species. Consequently, our proxy of visual acuity is assumed to more closely resemble the distance that animals react to neighbors. In Appendix A, we explain how we calculated the interaction range of each species using each species' anatomically derived visual acuity and visual coverage to generate the realistic assumptions.

As study systems, we used two bird species from the Order Passeriformes (Family Sturnidae: European starling *Sturnus vulgaris*; Family Icteridae: red-winged blackbird *Agelaius phoeniceus*) and two fish species from the order Cypriniformes (Family Cyprinidae: golden shiner *Notemigonus crysoleucas* and zebrafish *Danio rerio*) (Table 1.1Table 1.1). These species are excellent systems for the purposes of our study because they all engage in social interactions using visual cues (Røskaft and Rohwer, 1987; Saverino and Gerlai, 2008; Polverino et al., 2013; Butler et al., 2014), and have measured descriptions of their visual system configurations (Fernández-Juricic; Martin, 1986; Dolan and Fernández-Juricic, 2010; Pita et al., 2015). Additionally, some of these species have empirical data available on their grouping behavior (Table 1.2), which we used to increase the level of species-specificity in the models. We examined the following group parameters: (i) number of groups in the population (ii) average group size (i.e. the average number of individuals per each group calculated from the total simulated population) (iii) the polarity (i.e., degree to which all individuals in the population are facing the same direction), (iv) the average nearest neighbor distance between all individuals in the population, (v) speed at which the group stabilized and (vi) the internal structural stability of the group. A group was defined as a subset of individuals that interact with at least one other member within this subset. Polarity was computed as:

$$P(t) = \frac{1}{N}\left|\sum_{i=1}^{N} v_i(t)\right|$$

with $P(t)$ the polarity of the group at time step t, N the total number of agents, and $v_i(t)$ the unit direction vector of the agent i at time step t.

We assessed the time it took for the group to stabilize into its final configuration for certain group properties (i.e. number of groups, group size, polarity and nearest neighbor distance), which we associated to the speed of information transfer within the group. The lapse of time to stabilization can be regarded as a proxy of the speed of social information transfer in the group. For example, it has been shown that species with greater perceptual ranges (i.e. higher visual acuity) are capable of detecting social cues from farther away, which can potentially enhance the speed at which information travels through the group (Fernández-Juricic and Kowalski, 2011). The speed of information transfer is a relevant component to collective interactions because it indicates how efficiently individuals uptake social information and modify their behavior (Dall et al., 2005), ultimately leading to the final group configurations. Finally, we examined the spatial distribution of neighbors surrounding an individual in order to determine the probability of neighbor presence. This parameter provides an indication of the internal structural stability of a group (i.e. higher peak neighbor probability, we computed a normalized two-dimensional histogram of the positions of the neighbors surrounding each individual at each time step of the simulation. We translated and rotated the positions of all the individuals to bring the focal agent towards the origins of the two axes, oriented towards the zenith (90° uppermost region of the virtual environment). We measured the positions of all neighbors and sorted them in a two-dimensional normalized histogram that provided the probability to find a neighbor in a specific position of the space surrounding the focal individual.

We coded a self-propelled agent model to simulate groups of virtual agents that moved on a two-dimensional torus surface of size L^2 with $L = 43$ (Vicsek et al., 1995). These agents interacted with each other during collective motion. At each time step, the agents perceived other individuals in their perceptual range and updated their position according to the neighbors' position and orientation. The perceptual range of an agent was characterized by an interaction zone delimited by (i) a "vision-cone" parameter, and (ii) a "vision-distance" parameter. The "vision-cone" can be thought of as the individual's visual field (excluding the blind area), and the "vision-distance" was represented as the maximum metric distance that an individual can interact with its neighbors (i.e.

as a proxy of visual acuity). For example, if a group member was beyond the "vision-distance" threshold of the focal individual, it was not considered in its future movement decisions. In addition to their perceptual range, the agents were also surrounded by a short-range repulsion zone (i.e. 1 body length) and tend to avoid the conspecifics situated in this zone. The agents update their positions X_i with a velocity vector V_i though a discrete time process:

$$X_i(t + \delta t) = X_i(t) + V_i(t)\delta t$$

$$V_i(t + \delta t) = v_i(t + \delta t)\Theta_i(t + \delta t)$$

with v_i, the linear speed of the agent i and Θ_i its orientation. In our simulations, the linear speed of the agent was constant and species-specific (Table 1.2). The orientation was computed according to the position and orientation of the neighbors. To determine the subset of neighbors that influenced the next orientation of the focal agent, we implemented two different methods: the metric perception approach and the topological perception approach. In the metric perception approach, all individuals situated in the perception zone of the focal agent influenced its future orientation. In the topological perception approach, only the n proximate agents in the perception zone influenced the focal agent's future orientation. In the topological perception approach, only the n proximate agents in the perception zone influenced the focal agent's future orientation, with n being species-specific. Once this subset of neighbors was identified, the model evaluated the presence of neighbors in the repulsion zone of the focal agent. If a neighbor was detected in this zone, then the focal agent would only interact (i.e. move towards and align) with neighbors located in other regions of its perception zone (Couzin et al., 2002).

For each species, we ran 50 simulations of 3600-time steps with each perception approach (metric or topological) and each set of parameter values (classic or realistic) for each of the four studied species.

1.4 Results

Overall, the results of the modeling simulations indicate that in many cases, both the MM and TM are sensitive to modifications of the sensory assumptions (Figure 1.1 - Figure 1.4; Appendix A Table A1). In the European starling and the red-winged blackbird, both models yielded several small groups with the classic sensory assumptions compared with the realistic sensory assumptions, which yielded one large group composed of all members of the simulated population (Figure 1.1

& Figure 1.2;, Appendix A Table A1a,b). Both models yielded similar polarity and nearest neighbor distance values upon stabilization irrespective of the type of sensory assumption (Figure 1.1 & Figure 1.2; Appendix A Table A1a,b). However, for both bird species, it took longer to achieve a stable polarity and nearest neighbor distance in both models with the classic than the realistic sensory assumptions (Figure 1.1 & Figure 1.2).

In the golden shiner and zebrafish, both models yielded several smaller groups with the classic compared with the realistic sensory assumptions (Figure 1.3 & Figure 1.4; Appendix A Table A1c,d). Additionally, both species groups achieved lower polarity and took longer to reach the stable polarity values with the classic than with the realistic sensory assumptions (Figure 1.3 & Figure 1.4; Appendix A Table A1c,d). Furthermore, in the golden shiner, both models produced similar results in terms of neighbor distance considering both sensory assumptions (Figure 1.3; Appendix A Table A1c). However, in the zebrafish, both models yielded slightly longer neighbor distances with the classic than with the realistic sensory assumptions (Figure 1.4; Appendix A Table A1d). Lastly, for both fish species, models with the classic assumptions took a longer period of time to reach to the stable neighbor distance values than models with the realistic sensory assumptions (Figure 1.3 & Figure 1.4).

In terms of the probability of neighbor presence surrounding an individual, we found that in all the species, the realistic assumptions resulted in groups with higher structural stability. For both fish species, the peak probability of neighbor presence was higher in the TM using realistic assumptions. However, for both bird species, the probability of neighbor presence reached a higher peak probability value with the MM using realistic sensory assumptions (Appendix A Figure A1). Additionally, the area encompassing high probability of neighbor presence (red color in Figure 1.5) tended to be higher in the models with realistic assumptions, particularly for birds.

1.5 Discussion

We found that the classic sensory assumptions often used in collective behavior models yielded different outcomes in terms of key parameters describing group structure (e.g. mostly group size and total number of groups, and in some cases polarity, neighbor distance, group stability, along with the speed to reach stable values).

The main reason for the discrepancy between the modeling outcomes is that the classic sensory assumptions appear to substantially underestimate values of visual acuity and visual

coverage for both species of birds and fish. Figure 1.6 shows the different positions of the classic versus the realistic assumptions in a visual space bounded by visual acuity and visual coverage. This figure not only shows the four species used in this study, but also other species that have both visual parameters measured. Realistic sensory assumptions result in a greater area available for social interactions because species appear to have higher visual coverage and visual acuity than often assumed by collective behavior models (Huth and Wissel, 1992, 1994; Wood and Ackland, 2007; Hildenbrandt et al., 2010).

Our collective behavior models with realistic assumptions led in general to fewer groups and larger group sizes for both bird and fish species than the models with the classic sensory assumptions. Greater perceptual area ranges can increase the volume of space individuals have to interact with others because of the higher changes of detecting them and resolving their subtle behavior, thereby increasing the number of neighbors that are taken into consideration in movement decisions. This finding appears to support some empirical evidence showing that groups of golden shiners tend to organize into a single large group as opposed to assembling into several smaller groups (Tunstrøm et al., 2013). Furthermore, our results agree with previous modeling studies that explored variations in an individual's perceptual range by altering a single visual dimension, such as visual coverage (i.e. through variations in the width of the blind area). For example, (Romey and Vidal, 2013) found that larger blind areas caused large groups to break up into smaller, more numerous groups with lower density. Similarly, (Newman and Sayama, 2008) found that increasing the size of an individual blind area resulted in the abolishment of certain types of collective behavior (i.e. milling patterns) and (Couzin et al., 2002) demonstrated that a variety of different types of collective behaviors could be produced by altering the radius of the individual's interaction range (i.e. orientation and attraction).

In both fish species, we also found differences in polarity between models with different sensory assumptions. For example, in both fish species, the model with the realistic sensory assumptions yielded higher polarity values (i.e. group tended to move in the same direction) than the one with the classic sensory assumptions. In both models, a group was defined when two or more individuals interacted with each other. As group members continue to factor in the behavior of an individual during the running time of the model, all members of the group tended to coalesce into similar directional headings, resulting in an increase in polarity. In the case of the realistic sensory assumptions, where the entire population formed one large group, polarity was very high

(i.e., close to 1). However, for the classic sensory assumptions, polarity was comparatively lower due to the multiple, independent groups formed in the population with different directional headings among them. This finding is somewhat supported by empirical evidence. For instance, European starlings have been shown to maintain large flock sizes with high polarity (i.e. greater than 0.9) (Hemelrijk and Hildenbrandt, 2011). Similarly, golden shiner groups also tend to associate in higher polar configurations (Tunstrøm et al., 2013).

The realistic sensory assumptions also predicted fish species to produce groups with slightly shorter neighbor distances compared with the classic sensory assumptions. According to the interaction rules that define the minimum neighbor separation (i.e. repulsion zone), individuals are limited to having a separation distance of approximately 1 body length in size (Couzin et al., 2002). Therefore, as the simulation proceeds, and the group increases in size with the realistic sensory assumptions, individuals would tend to reduce the neighbor distances closed to the 1 body length threshold. On the other hand, for small, sparse groups, like the situation observed with the classic sensory assumptions, the nearest neighbor distance would be larger than 1 body length as individuals are separated farther in space.

We also found that in all the species considered, models with the realistic assumptions yielded groups with higher internal group stability (i.e., higher peak surrounding neighbor probability), which is probably also a function of the higher perceptual range of the realistic assumptions. Interestingly, groups that achieved the highest stability were obtained with the MM for the bird species and the TM for the fish species. This difference in stability predictions between birds and fish is likely explained by birds having higher average speeds than fish in our simulations (Figure 1.2). For instance, by moving at higher speeds, birds can take into account perceptually, and interact with, a greater number of neighbors within the confines of their metric-interaction range. Since the TM limits the total number of neighbors that an individual can interact with, it ends up producing lower peak neighbor probability values than the MM. However, for the fish species, it takes longer for individuals to detect neighbors metrically, probably due to their slower speeds. On the other hand, with the TM, individuals care capable of immediately interacting with neighbors in the population, moving closer to them, even if they are separated farther than the metric distance in space. Therefore, for both fish species, the TM ends up producing more stable groups (i.e. higher peak surrounding neighbor probability values) compared with the MM.

Our models provided a series of very specific predictions about collective behavior: higher visual acuity and wider visual coverage is expected to lead to lower numbers of groups in the population, each with larger group size, higher polarity, shorter neighbor distance, higher structural stability and a faster spread of social information. These predictions can be tested at the comparative level across species (e.g. birds, fish) with different visual field configuration and/or visual acuity. However, the results of comparative tests may be confounded by other differences between species in ecology, physiology and degree of shared ancestry. Our predictions could also be tested experimentally within species (i.e. different age classes in some fish, amphibians and reptiles or different mutants in some model organisms like zebrafish) by manipulating visual coverage and visual acuity. Studies on birds have used eye caps to fully or partially occlude vision (Clayton and Krebs, 1994; Prior et al., 2004; Templeton and Christensen-Dykema, 2008; Martinho et al., 2015). Therefore, visual coverage could be manipulated by applying eye caps to increase the size of the blind area, and visual acuity could be manipulated by using transparent eye caps with different refractive indices. In fish, a combination of eye caps and artificial lens designs have been used to manipulate various visual dimensions (Rowland, 1999), and consequently, these tools can also be used to test our predictions. In model species, like zebrafish, genetic mutants may also be used to determine the influence of specific retinal cell types implicated in visual acuity on behavior. For example, one study examined the foraging success of zebrafish mutants with a reduced population of ultraviolet sensitive cones to assess their ability to visually detect and capture prey when their perception of ultraviolet cues was reduced (Flamarique, 2016). A similar approach using zebrafish mutants with decreased retinal ganglion cell populations (Catalano et al., 2007; Emran et al., 2007; Sherpa et al., 2011) could be used to assess if variations in visual acuity between mutants and wild type changes the range necessary to perceive conspecific cues.

Current technology is also likely to facilitate the assessment of some of the grouping parameters measured in the model. For example, group size, polarity and neighbor distance can be measured in laboratory conditions with specialized tracking software that can isolate and identify the movements of group members in three dimensions (Katz et al., 2011; Delcourt et al., 2013). Similarly, sonar technology can be used to measure comparable parameters of large fish schools in the wild (Gerlotto et al., 2006). For birds, tracking individual trajectories among large groups in the field is done with small tracking devices, allowing one to estimate group size and neighbor distance (Nagy et al., 2010). Additionally, stereo photography can also be used to reconstruct the

spatial configuration of the flock through time (Ballerini et al., 2008), which can estimate group size, neighbor distance, polarity, structural stability and speed of information transfer (Ballerini et al., 2008; Cavagna et al., 2010).

Our results also have implications for interpreting the results of previous empirical studies by establishing the matching or mismatching of the theoretical predictions versus empirical findings in the light of the sensory assumptions. For example, in zebrafish, it has been found that group sizes in the wild are much larger (i.e. up to 300 individuals, (Suriyampola et al., 2015)) than group sizes commonly used in laboratory experiments. Our model with the realistic sensory assumptions can be run with realistic group sizes to generate predictions that can then be compared with empirical data. Ultimately, bringing the sensory approach to collective behavior will allow us to generate species-specific predictions with more realistic assumptions.

We examined only two properties of the visual system (i.e. visual acuity and visual coverage), but in reality, social interactions can be influenced by many other factors (e.g. chromatic contrast, achromatic contrast, position, type and number of centers of acute vision). Some of these factors may actually be quite relevant in collective behavior. For instance, both MM and TM assume the quality of visual perception is the same across all regions of the visual field, and consequently, irrespective of the position of the neighbor, the information will have the same weight in influencing the successive movement decisions of the focal individual. In reality, some parts of the visual field have higher acuity than others, because they are subtended in the retina by the centers of acute vision (i.e. areas with high density of photoreceptors, such as the fovea, area (Hughes, 1977; Pettigrew and Manger, 2008)).

The implication is that neighbors that are visually tracked with the center of acute vision may have higher weight in the movement decisions of focal individuals than neighbors tracked with the peripheral area of the retina (i.e. lower visual acuity). For instance, golden shiners typically maintain close distances with neighbors located directly ahead of them (i.e. 60° bearing angle) (Katz et al., 2011) (Appendix A Figure A2), and they seem to use their center of acute vision (an area that projects in approximately the same direction) to track neighbors visually (Pita et al., 2015). On the other hand, in European starlings and homing pigeons, nearest neighbors are often located directly adjacent to the forward direction of motion of the focal individual (i.e. 90° bearing angle) (Ballerini et al., 2008; Pettit et al., 2013). However, the projection of the centers of acute vision along the horizontal place occurs more forward (i.e. 60° for starlings, 66° for pigeons)

(Martin, 1984; Butler et al., 2014), suggesting that these birds are not tracking neighbors with their centers of acute vision (Appendix A Figure A2). Although some models have aimed to incorporate the idea of neighbors having different weight in the decision-making of the focal individual (Lemasson et al., 2009; Gao et al., 2010; Wang et al., 2013), none have done so in the context of the centers of acute vision and their position in visual space.

By challenging previous sensory assumptions, our results suggest that the sensory system is a relevant component of collective interactions, at least from a theoretical perspective. Our findings have important implications for future theoretical and empirical collective behavior research. First, classic visual assumptions are not necessarily representative of the visual system of the species that show some form of social behavior. Second, classic visual assumptions unrealistically constrain the social visual space (i.e. the area around an individual from which it can get information about group mates) that animals have to coordinate their movements with group mates. Third, not all sensory configurations may be well represented by the same model. For instance, the metric-based interaction rules, in which an individual responds to all neighbors within a defined concentric range, may accurately reflect the visual limitations of species with narrow visual coverage and reduced acuity. However, a species with high visual coverage and acuity may instead follow topological rules where instead of responding to all neighbors within a particular zone, individuals respond to a set number of neighbors regardless of their separation distance (Giardina, 2008).

1.6 Tables and Figures

Table 1.1 Comparison of the classic visual assumptions assumed throughout the literature for birds and fish along with the realistic visual assumptions determined physiologically from species representatives (i.e. European starling, red-winged blackbird, golden shiner and zebrafish).Visual coverage corresponds to regions of the visual field configuration, excluding the blind area in the horizontal plane of the head. The visual acuity reflects the minimum visual acuity necessary to resolve social cues from conspecifics (i.e. head for birds and body for fish) of each species represented in units of body length (BL) (see Appendix A). Parameters applied to the interaction rules of both MM and TM. (Hildenbrandt et al., 2010)[a], (Ballerini et al., 2008)[b], (Martin, 1986)[c], (Dolan and Fernández-Juricic, 2010)[d], (Fernández-Juricic unpublished data)[e], (Hall et al., 1986)[f], (Partridge, 1980)[g], (Pita et al., 2015)[h].

Species	Classic Visual Assumptions		Realistic Visual Assumptions	
	Visual Coverage	Visual Acuity	Visual Coverage	Visual Acuity
European Starling	270°[a]	6 BL[b]	296°[c]	15.5 BL[d]
Red-winged Blackbird			314°[e]	19.5 BL[e]
Golden Shiner	300°[f]	2 BL[g]	335°[g]	16.5 BL[g]
Zebrafish			339°[h]	7.7 BL[h]

Table 1.2 Species assumptions that remained constant across both models and sets of visual assumptions (i.e. classic versus realistic). Values obtained from the literature according to: group size (number of individuals in the group), speed (body lengths per second, BL s−1), minimum separation distance in terms of body length (BL) and the maximum turning angle per each species measured in degrees (see Appendix A), analyzed from video (See Appendix A). (Fischl and Caccamise, 1985)[a], (Videler, 2005)[b], (Ballerini et al., 2008)[c], analyzed from video (See Appendix A)[d], (Yasukawa and Searcy, 1995)[e], (Sarkar, 2003)[f], (Werner et al., 1978)[g], (Tunstrøm et al., 2013)[h], (Burgess and Shaw, 1981)[i], (Pritchard et al., 2001)[j], (Plaut and Gordon, 1994)[k], (Miller and Gerlai, 2012)[l].

Species	Group Size	Speed	Minimum Separation	Maximum Turning Angle
European Starling	30[a]	50 BL/sec[b]	1 BL[c]	131°[d]
Red-winged Blackbird	100[e]	40 BL/sec[f]	1 BL[e]	132°[d]
Golden Shiner	45[g]	1 BL/sec[h]	1 BL[i]	134°[d]
Zebrafish	10[j]	5 BL/sec[k]	1 BL[l]	87°[d]

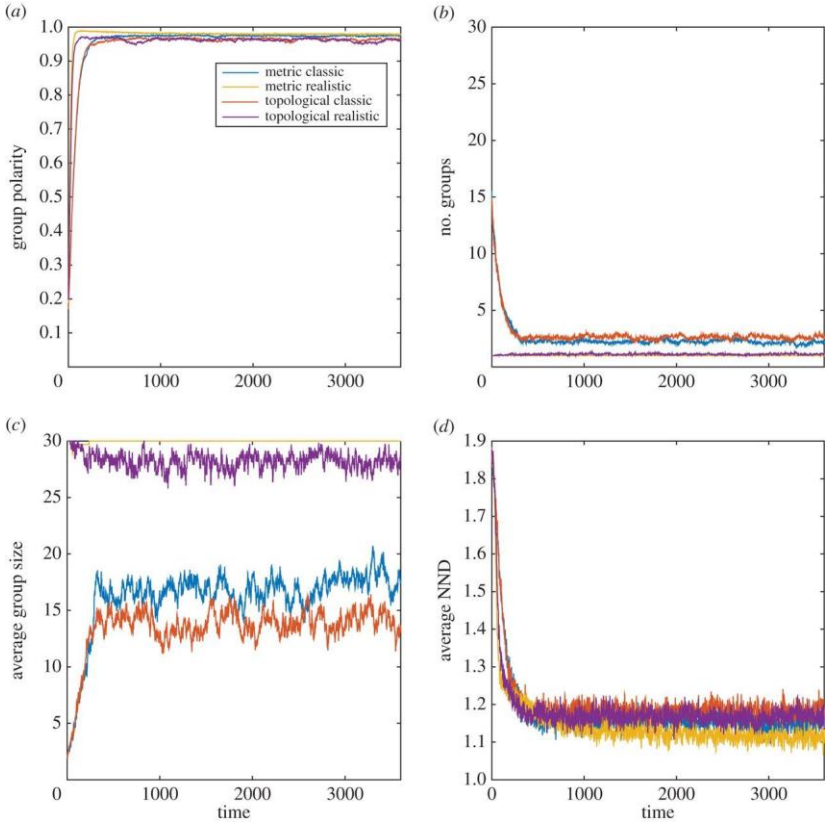

Figure 1.1 MM and TM outputs comparing the group properties: a) group polarity, b) number of groups, c) average group size and d) average nearest neighbor distance (NND) for the classic and realistic visual assumptions in the European starling.

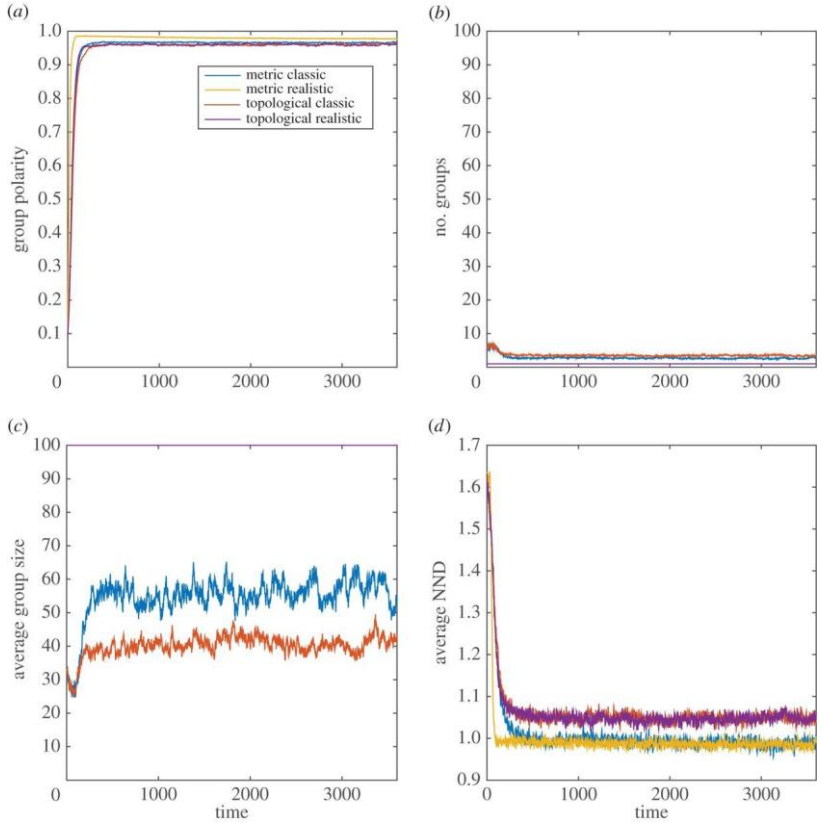

Figure 1.2 MM and TM outputs comparing the group properties: a) group polarity, b) number of groups, c) average group size and d) average nearest neighbor distance (NND) for the classic and realistic visual assumptions in the red-winged blackbird.

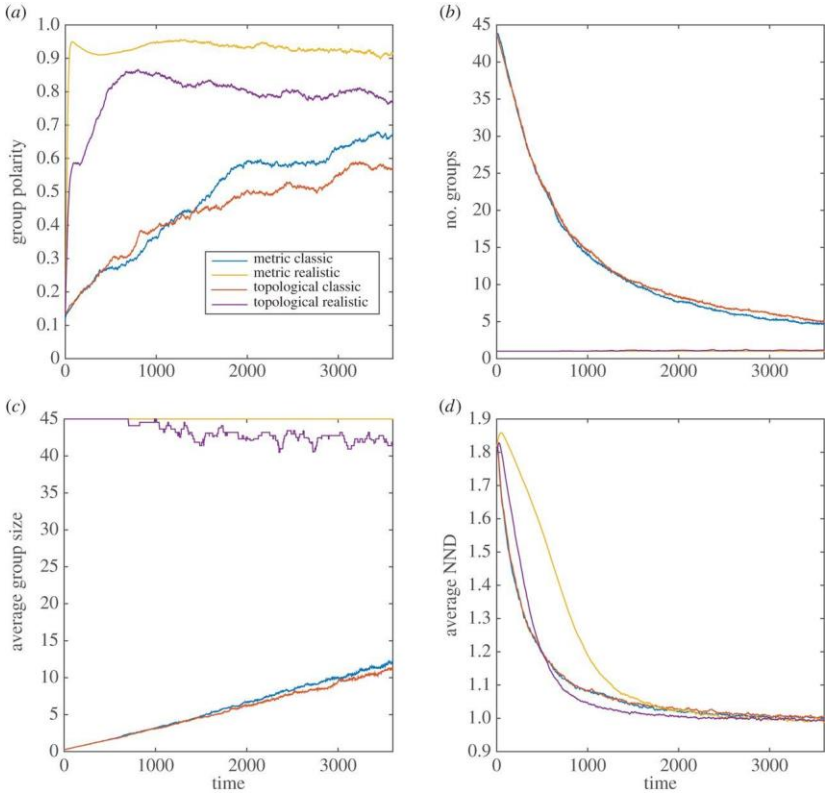

Figure 1.3 MM and TM outputs comparing the group properties: a) group polarity, b) number of groups, c) average group size and d) average nearest neighbor distance (NND) for the classic and realistic visual assumptions in the golden shiner.

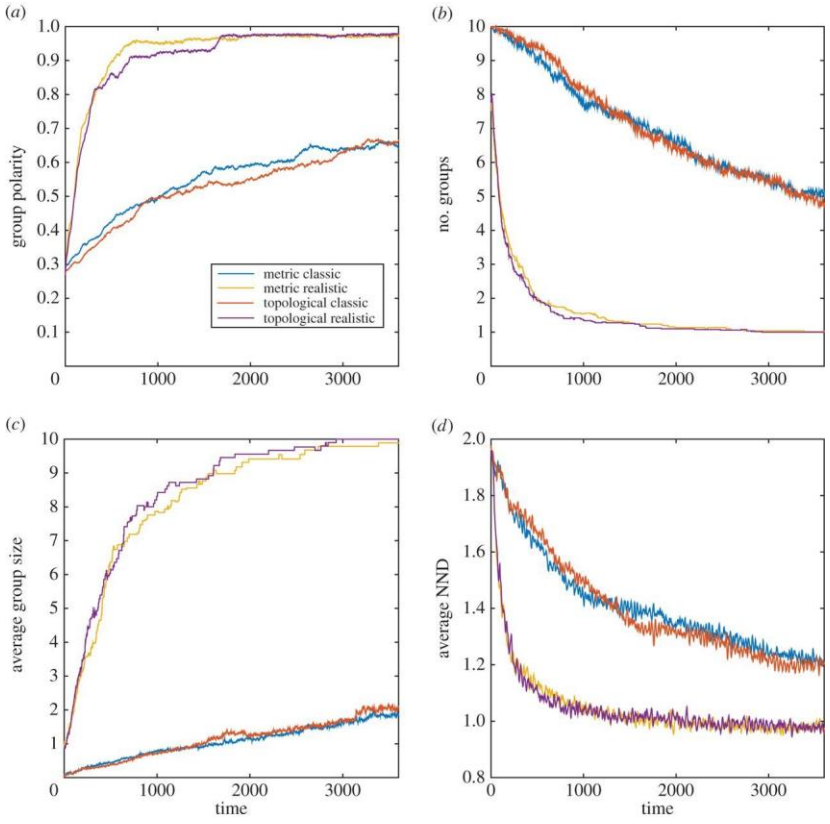

Figure 1.4 MM and TM outputs comparing the group properties: a) group polarity, b) number of groups, c) average group size and d) average nearest neighbor distance (NND) for the classic and realistic visual assumptions in the zebrafish.

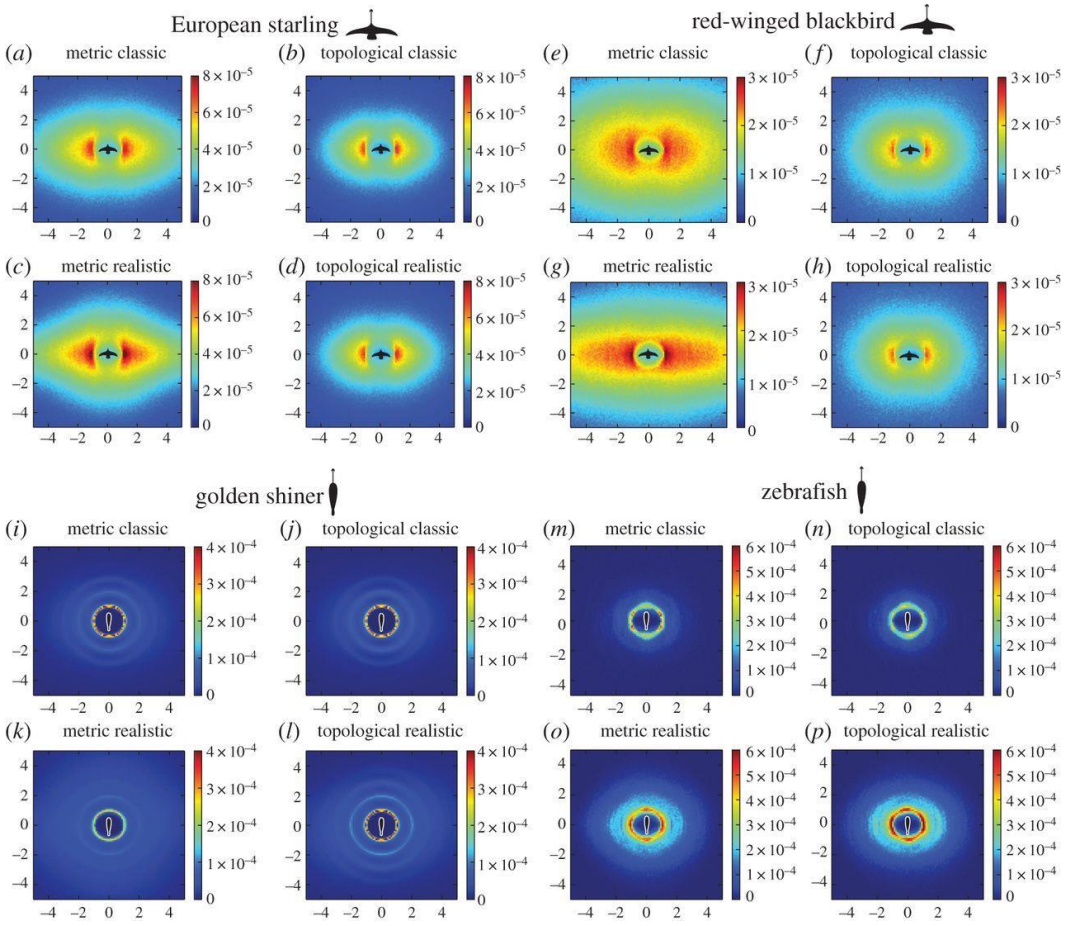

Figure 1.5 Spatial map illustrating the probability of neighbor presence surrounding an individual (i.e. warmer colors indicate high probability, cooler colors indicate low probability). Values detail the averages per each species represented throughout the entire stimulus duration (3600-time steps).

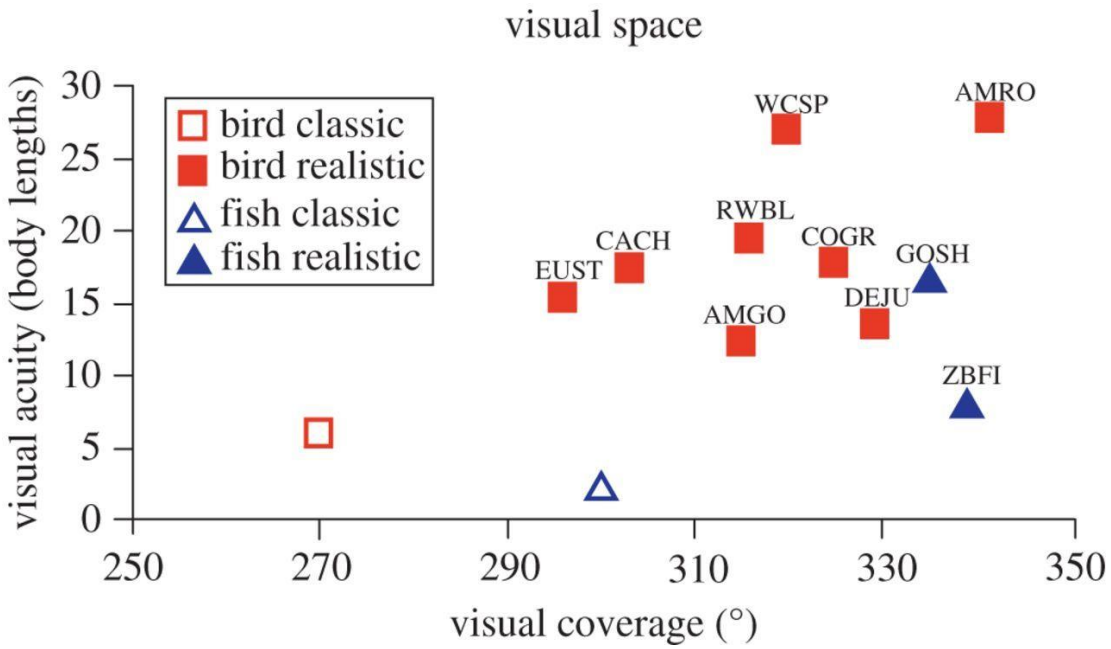

Figure 1.6 Overlap of the visual space of the visual coverage (measured ophthalmoscopically) and interaction distance (derived from the minimum visual acuity and converted into units of body length) comparing the classic parameters used for birds and fish and the realistic visual parameters of the animals used in this study (European starling (EUST), red-winged blackbird (RWBL), golden shiner (GOSH) and zebrafish (ZBFI). Additionally, we have included other realistic estimates of bird species for which both the visual field and visual acuity information has been measured (American goldfinch (AMGO), American robin (AMRO), Carolina chickadee (CACH), common grackle (COGR), dark-eyed junco (DEJU), and white-crowned sparrow (WCSP)).

1.7 References

Amorim, P. (2015). Modeling ant foraging: A chemotaxis approach with pheromones and trail formation. *J. Theor. Biol.* 385, 160–173. doi:10.1016/j.jtbi.2015.08.026.

Ballerini, M., Cabibbo, N., Candelier, R., Cavagna, a, Cisbani, E., Giardina, I., et al. (2008). Interaction ruling animal collective behavior depends on topological rather than metric distance: evidence from a field study. *Proc. Natl. Acad. Sci. U. S. A.* 105, 1232–1237. doi:10.1073/pnas.0711437105.

Ben-Shaul, Y. (2015). Extracting social information from chemosensory cues: Consideration of several scenarios and their functional implications. *Front. Neurosci.* 9, 1–15. doi:10.3389/fnins.2015.00439.

Burgess, J. W., and Shaw, E. (1981). Effects of acoustico-lateralis denervation in a facultative schooling fish: a nearest-neighbor matrix analysis. *Behav. Neural Biol.* 33, 488–497. doi:10.1016/S0163-1047(81)91869-0.

Butler, S. R., Fernandez-Juricic, E., and Fernández-Juricic, E. (2014). European starlings recognize the location of robotic conspecific attention. *Biol. Lett.* 10, 20140665. doi:10.1098/rsbl.2014.0665.

Catalano, A., Raymond, P., Goldman, D., and Wei, X. (2007). Zebrafish dou yan mutation causes patterning defects and extensive cell death in retina. *Dev. Dyn.* 236, 1295–1306. doi:10.1002/dvdy.21148.Zebrafish.

Cavagna, A., Cimarelli, A., Giardina, I., Parisi, G., Santagati, R., Stefanini, F., et al. (2010). Scale-free correlations in starling flocks. *Proc. Natl. Acad. Sci. U. S. A.* 107, 11865–11870. doi:10.1073/pnas.1005766107.

Clayton, N. S., and Krebs, J. R. (1994). Memory for spatial and object-specific cues in food-storing and non-storing birds. *J. Comp. Physiol. A* 174, 371–379. doi:10.1007/BF00240218.

Couzin, I. D., and Krause, J. (2003). Self-organization and collective behavior in vertebrates. *Adv. Study Behav.* 32, 1–75.

Couzin, I. D., Krause, J., James, R., Ruxton, G. D., and Franks, N. R. (2002). Collective memory and spatial sorting in animal groups. *J. Theor. Biol.* 218, 1–11. doi:10.1006/yjtbi.3065.

Dall, S. R. X., Giraldeau, L.-A., Olsson, O., McNamara, J. M., and Stephens, D. W. (2005). Information and its use by animals in evolutionary ecology. *Trends Ecol. Evol.* 20, 187–93. doi:10.1016/j.tree.2005.01.010.

Danchin, E., Giraldeau, L.-A., Valone, T. J., and Wagner, R. H. (2004). Public information: from nosy neighbors to cultural evolution. *Science.* 305, 487–91. doi:10.1126/science.1098254.

Delcourt, J., Denoël, M., Ylieff, M., and Poncin, P. (2013). Video multitracking of fish behaviour: A synthesis and future perspectives. *Fish.* 14, 186–204. doi:10.1111/j.1467-2979.2012.00462.x.

Dolan, T., and Fernández-Juricic, E. (2010). Retinal ganglion cell topography of five species of ground-foraging birds. *Brain. Behav. Evol.* 75, 111–21. doi:10.1159/000305025.

Emran, F., Rihel, J., Adolph, A. R., Wong, K. Y., Kraves, S., and Dowling, J. E. (2007). OFF ganglion cells cannot drive the optokinetic reflex in zebrafish. *Proc. Natl. Acad. Sci.* 104, 19126–31.

Fernández-Juricic, E. Unpublished data.

Fernández-Juricic, E., and Kowalski, V. (2011). Where does a flock end from an information perspective? A comparative experiment with live and robotic birds. *Behav. Ecol.* 22, 1304–1311. doi:10.1093/beheco/arr132.

Fischl, J., and Caccamise, D. F. (1985). Influence of habitat and season on foraging flock composition in the European Starling (*Sturnus vulgaris*). *Oecologia* 67, 532–539. doi:10.1007/BF00790025.

Flamarique, N. (2016). Diminished foraging performance of a mutant zebrafish with reduced population of ultraviolet cones. *Proc. R. Soc. B* 283.

Gao, J., Chen, Z., Cai, Y., and Xu, X. (2010). Enhancing the convergence efficiency of a self-propelled agent system via a weighted model. *Phys. Rev. E - Stat. Nonlinear, Soft Matter Phys.* 81, 1–7. doi:10.1103/PhysRevE.81.041918.

Gerlotto, F., Bertrand, S., Bez, N., and Gutierrez, M. (2006). Waves of agitation inside anchovy schools observed with multibeam sonar: a way to transmit information in response to predation. *ICES J. Mar. Sci.* 63, 1405–1417. doi:10.1016/j.icesjms.2006.04.023.

Giardina, I. (2008). Collective behavior in animal groups: theoretical models and empirical studies. *HFSP J.* 2, 205–219. doi:10.2976/1.2961038.

Gordon, D. M. (2014). The Ecology of Collective Behavior. *PLoS Biol.* 12, 1–4. doi:10.1371/journal.pbio.1001805.

Hall, S. J., Wardle, C. S., and MacLennan, D. N. (1986). Predator evasion in a fish school: test of a model for the fountain effect. *Mar. Biol.* 91, 143–148.

Harpaz, R., and Schneidman, E. (2014). Receptive-field like models accurately predict individual zebrafish behavior in a group. *J. Mol. Neurosci.* 53, S61–S61.

Hart, N. S. (2001). The visual ecology of avian photoreceptors. *Prog. Retin. Eye Res.* 20, 675–703. doi:10.1016/S1350-9462(01)00009-X.

Hemelrijk, C. K., and Hildenbrandt, H. (2011). Some causes of the variable shape of flocks of birds. *PLoS One* 6. doi:10.1371/journal.pone.0022479.

Hemelrijk, C. K., and Hildenbrandt, H. (2012). Schools of fish and flocks of birds: their shape and internal structure by self-organization. *Interface Focus* 2, 726–737. doi:10.1098/rsfs.2012.0025.

Hemelrijk, C. K., and Kunz, H. (2005). Density distribution and size sorting in fish schools: An individual-based model. *Behav. Ecol.* 16, 178–187. doi:10.1093/beheco/arh149.

Hildenbrandt, H., Carere, C., and Hemelrijk, C. K. (2010). Self-organized aerial displays of thousands of starlings: a model. *Behav. Ecol.* 21, 1349–1359. doi:10.1093/beheco/arq149.

Hogan, K. E., and Laskowski, K. L. (2013). Indirect information transfer: three-spined sticklebacks use visual alarm cues from frightened conspecifics about an unseen predator. *Ethology* 119, 999–1005. doi:10.1111/eth.12143.

Hughes, A. (1977). "The topography of vision in mammals of contrasting life style: comparative optics and retinal organization," in *The visual system in vertebrates* (New York: Springer), 613–756.

Huth, A., and Wissel, C. (1992). The simulation of the movement of fish schools. *J. Theor. Biol.* 156, 365–385. doi:10.1016/S0022-5193(05)80681-2.

Huth, A., and Wissel, C. (1994). The simulation of fish schools in comparison with experimental data. *Ecol. Modell.* 75–76, 135–146. doi:10.1016/0304-3800(94)90013-2.

Katz, Y., Tunstrom, K., Ioannou, C. C., Huepe, C., and Couzin, I. D. (2011). Inferring the structure and dynamics of interactions in schooling fish. *Proc. Natl. Acad. Sci.* 108, 18720–18725. doi:10.1073/pnas.1107583108.

King, A. J., and Cowlishaw, G. (2007). When to use social information: the advantage of large group size in individual decision making. *Biol. Lett.* 3, 137–9. doi:10.1098/rsbl.2007.0017.

Krause, J., and Ruxton, G. D. (2002). *Living in groups*. Oxford: Oxford University Press.

Kunz, H., and Hemelrijk, C. K. (2012). Simulations of the social organization of large schools of fish whose perception is obstructed. *Appl. Anim. Behav. Sci.* 138, 142–151. doi:10.1016/j.applanim.2012.02.002.

Lemasson, B. H., Anderson, J. J., and Goodwin, R. a. (2009). Collective motion in animal groups from a neurobiological perspective: The adaptive benefits of dynamic sensory loads and selective attention. *J. Theor. Biol.* 261, 501–510. doi:10.1016/j.jtbi.2009.08.013.

Litherland, L., and Collin, S. P. (2008). Comparative visual function in elasmobranchs: spatial arrangement and ecological correlates of photoreceptor and ganglion cell distributions. *Vis. Neurosci.* 25, 549–561. doi:10.1017/S0952523808080693.

Lopez, U., Gautrais, J., Couzin, I. D., and Theraulaz, G. (2012). From behavioural analyses to models of collective motion in fish schools. *Interface Focus* 2, 693–707. doi:10.1098/rsfs.2012.0033.

Martin, G. R. (1984). The visual fields of the tawny owl, *Strix aluco L*. *Vision Res.* 24, 1739–1751.

Martin, G. R. (1986). The eye of a passeriform bird, the European starling (*Sturnus vulgaris*): eye movement amplitude, visual fields and schematic optics. *J. Comp. Physiol. A* 159, 545–557.

Martin, G. R. (2007). Visual fields and their functions in birds. *J. Ornithol.* 148, 547–562. doi:10.1007/s10336-007-0213-6.

Martinho, A., Biro, D., Guilford, T., Gagliardo, A., and Kacelnik, A. (2015). Asymmetric visual input and route recapitulation in homing pigeons. *Proc. R. Soc. B* 282.

Miller, N., and Gerlai, R. (2012). From Schooling to Shoaling: Patterns of Collective Motion in Zebrafish (*Danio rerio*). *PLoS One* 7, e48865. doi:10.1371/journal.pone.0048865.

Nagy, M., Akos, Z., Biro, D., Vicsek, T., Ákos, Z., Biro, D., et al. (2010). Hierarchical group dynamics in pigeon flocks. *Nature* 464, 890–893. doi:10.1038/nature08891.

Newman, J. P., and Sayama, H. (2008). Effect of sensory blind zones on milling behavior in a dynamic self-propelled particle model. *Phys. Rev. E - Stat. Nonlinear, Soft Matter Phys.* 78, 1–5. doi:10.1103/PhysRevE.78.011913.

Niizato, T., and Gunji, Y. P. (2011). Metric-topological interaction model of collective behavior. *Ecol. Modell.* 222, 3041–3049. doi:10.1016/j.ecolmodel.2011.06.008.

Partridge, B. L. (1980). The effect of school size on the structure and dynamics of minnow schools. *Anim. Behav.* 28, 68–77. doi:10.1016/S0003-3472(80)80009-1.

Partridge, B. L., and Pitcher, T. J. (1980). The sensory basis of fish schools: Relative roles of lateral line and vision. *J. Comp. Physiol.* 135, 315–325. doi:10.1007/BF00657647.

Perna, A., Gregoire, G., and Mann, R. P. (2014). A note on the duality between interaction responses and mutual positions in flocking and schooling. *Mov. Ecol.* 2, 1–18. doi:10.1186/s40462-014-0022-5.

Pettigrew, J. D., and Manger, P. R. (2008). Retinal ganglion cell density of the black rhinoceros (*Diceros bicornis*): calculating visual resolution. *Vis. Neurosci.* 25, 215–20. doi:10.1017/S0952523808080498.

Pettit, B., Perna, A., Biro, D., and Sumpter, D. J. T. (2013). Interaction rules underlying group decisions in homing pigeons. *J. R. Soc. Interface* 10, 20130529. doi:10.1098/rsif.2013.0529.

Pita, D., Moore, B. A., Tyrrell, L. P., and Fernández-Juricic, E. (2015). Vision in two cyprinid fish: implications for collective behavior. *PeerJ* 3, e1113. doi:10.7717/peerj.1113.

Pitcher, T. J., and Parrish, J. K. (1993). "Functions of shoaling behaviour in teleosts," in *Behaviour of Teleost Fishes* (London: Chapman & Hall), 363–439.

Plaut, I., and Gordon, M. (1994). Swimming Metabolism of Wild-Type and Cloned Zebrafish *Brachydanio rerio*. *J. Exp. Biol.* 194, 209–23. doi:10.1016/S0300-9629(96)00284-8.

Polverino, G., Phamduy, P., and Porfiri, M. (2013). Fish and robots swimming together in a water tunnel: robot color and tail-beat frequency influence fish behavior. *PLoS One* 8, e77589. doi:10.1371/journal.pone.0077589.

Prior, H., Wiltschko, R., Stapput, K., Güntürkün, O., and Wiltschko, W. (2004). Visual lateralization and homing in pigeons. *Behav. Brain Res.* 154, 301–310. doi:10.1016/j.bbr.2004.02.018.

Pritchard, V., Lawrence, J., Butlin, R. K., and Krause, J. (2001). Shoal choice in zebrafish, *Danio rerio*: the influence of shoal size and activity. *Anim. Behav.* 62, 1085–1088. doi:10.1006/anbe.2001.1858.

Reynolds, C. W. (1987). Flocks, herds and schools: A distributed behavioral model. *ACM SIGGRAPH Comput. Graph.* 21, 25–34. doi:10.1145/37402.37406.

Romey, W. W. L., and Vidal, J. J. M. (2013). Sum of heterogeneous blind zones predict movements of simulated groups. *Ecol. Modell.* 258, 9–15. doi:10.1016/j.ecolmodel.2013.02.020.

Rosenthal, S. B., Twomey, C. R., Hartnett, A. T., Wu, H. S., and Couzin, I. D. (2015). Revealing the hidden networks of interaction in mobile animal groups allows prediction of complex behavioral contagion. *Proc. Natl. Acad. Sci.* 112, 4690–4695. doi:10.1073/pnas.1420068112.

Røskaft, E., and Rohwer, S. (1987). An experimental study of the function of the red epaulettes and the black body colour of male red-winged blackbirds. *Anim. Behav.* 35, 1070–1077. doi:10.1016/S0003-3472(87)80164-1.

Rowland, W. J. (1999). Studying visual cues in fish behavior: a review of ethological techniques. *Environ. Biol. Fishes* 56, 285–305.

Sarkar, A. (2003). *Development of Animal Behaviour*. New Delhi, India: Discovery Publishing House.

Saverino, C., and Gerlai, R. (2008). The social zebrafish: Behavioral responses to conspecific, heterospecific, and computer animated fish. *Behav. Brain Res.* 191, 77–87. doi:10.1016/j.bbr.2008.03.013.

Sherpa, T., Hunter, S. S., Frey, R. A., Robinson, B. D., and L., S. D. (2011). Retinal proliferation response in the buphthalmic zebrafish bugeye. *Exp. Eye Res.* 93, 424–436. doi:10.1016/j.exer.2011.06.001.Retinal.

Strandburg-Peshkin, A., Twomey, C. R., Bode, N. W. F., Kao, A. B., Katz, Y., Ioannou, C. C., et al. (2013). Visual sensory networks and effective information transfer in animal groups. *Curr. Biol.* 23, R709–R711. doi:10.1016/j.cub.2013.07.059.

Sumpter, D. (2010a). *Collective Animal Behavior*. Princeton, NJ: Princeton University Press.

Sumpter, D., Buhl, J., Biro, D., and Couzin, I. (2008). Information transfer in moving animal groups. *Theory Biosci.* 127, 177–86. doi:10.1007/s12064-008-0040-1.

Sumpter, D. J. T. (2006). The principles of collective animal behaviour. *Philos. Trans. R. Soc. Lond. B. Biol. Sci.* 361, 5–22. doi:10.1098/rstb.2005.1733.

Sumpter, D. J. T. (2010b). *Collective Animal Behavior*. Princeton, N.J.: Princeton University Press.

Suriyampola, P. S., Shelton, D. S., Shukla, R., Roy, T., Anuradha, B., and Martins, E. P. (2015). Zebrafish Social Behavior in the Wild. *Zebrafish*, 1–8. doi:10.1089/zeb.2015.1159.

Templeton, J. J., and Christensen-Dykema, J. M. (2008). A behavioral analysis of prey detection lateralization and unilateral transfer in European starlings (*Sturnus vulgaris*). *Behav. Processes* 79, 125–131. doi:10.1016/j.beproc.2008.06.003.

Thewissen, J., and Nummela, S. (2008). *Sensory Evolution on the Threshold: Adaptations in Secondarily Aquatic Vertebrates*. Berkeley and Los Angeles, California: University of California Press.

Tian, M., Chen, D., and Liu, W. Three-Dimensional agent-based model of fish collective behaviour using topological interaction.

Tunstrøm, K., Katz, Y., Ioannou, C. C., Huepe, C., Lutz, M. J., and Couzin, I. D. (2013). Collective States, Multistability and Transitional Behavior in Schooling Fish. *PLoS Comput. Biol.* 9. doi:10.1371/journal.pcbi.1002915.

Vicsek, T., Czirók, A., Ben-Jacob, E., Cohen, I., and Shochet, O. (1995). Novel type of phase transition in a system of self-driven particles. *Phys. Rev. Lett.* 75, 1226–1229.

Vicsek, T., and Zafeiris, A. (2012). Collective motion. *Phys. Rep.* 517, 71–140. doi:10.1016/j.physrep.2012.03.004.

Videler, J. J. (2005). *Avian Flight*. Oxford University Press.

Viscido, S. V., Parrish, J. K., and Grünbaum, D. (2005). The effect of population size and number of influential neighbors on the emergent properties of fish schools. *Ecol. Modell.* 183, 347–363. doi:10.1016/j.ecolmodel.2004.08.019.

Walls, G. L. (1942). *The vertebrate eye and its adaptive radiation*. Michigan: The Cranbook Institute of Science.

Wang, X. G., Zhu, C. P., Yin, C. Y., Hu, D. S., and Yan, Z. J. (2013). A modified Vicsek model for self-propelled agents with exponential neighbor weight and restricted visual field. *Phys. A Stat. Mech. its Appl.* 392, 2398–2405. doi:10.1016/j.physa.2013.01.022.

Warburton, K. (1997). "Social forces in animal congregations: interactive, motivational and sensory aspects," in *Animal Groups in Three Dimensions: How Species Aggregate*, ed. W. M. H. Julia K. Parrish (Cambridge University Press), 312–336.

Werner, E. E., Hall, D. J., and Werner, M. D. (1978). Littoral zone fish communities of two Florida lakes and a comparison with Michigan lakes. *Environ. Biol. Fishes* 3, 163–172. doi:10.1007/BF00691940.

Wood, A. J., and Ackland, G. J. (2007). Evolving the selfish herd: emergence of distinct aggregating strategies in an individual-based model. *Proc. Biol. Sci.* 274, 1637–1642. doi:10.1098/rspb.2007.0306.

Yasukawa, K., and Searcy, W. (1995). Red-winged Blackbird (*Agelaius phoeniceus*). *Birds North Am.*

CHAPTER 2. VISION IN TWO CYPRINID FISH: IMPLICATIONS FOR COLLECTIVE BEHAVIOR

Diana Pita[1], Bret A. Moore[1], Luke P. Tyrrell[1] & Esteban Fernández-Juricic[1]

[1]Department of Biological Sciences. Purdue University. 915 W. State Street. West Lafayette. IN 47907.USA

Citation:
A version of this chapter was originally published in PeerJ and is reproduced here with permission.

Pita, D., Moore, B. A., Tyrrell, L. P., and Fernández-Juricic, E. (2015). Vision in two cyprinid fish: implications for collective behavior. *PeerJ* 3, e1113. doi:10.7717/peerj.1113.

2.1 Abstract

Many species of fish rely on their visual systems to interact with conspecifics and these interactions can lead to collective behavior. Individual-based models have been used to predict collective interactions; however, these models generally make simplistic assumptions about the sensory systems that are applied without proper empirical testing to different species. This could limit our ability to predict (and test empirically) collective behavior in species with very different sensory requirements. In this study, we characterized components of the visual system in two species of cyprinid fish known to engage in visually dependent collective interactions (zebrafish *Danio rerio* and golden shiners *Notemigonus crysoleucas*) and derived quantitative predictions about the positioning of individuals within schools. We found that both species had relatively narrow binocular and blind fields and wide visual coverage. However, golden shiners had more visual coverage in the vertical plane (binocular field extending behind the head) and higher visual acuity than zebrafish. The centers of acute vision (*areae*) of both species projected in the fronto-dorsal region of the visual field, but those of the zebrafish projected more dorsally than those of the golden shiner. Based on this visual sensory information, we predicted that: (a) predator detection time could be increased by >1,000% in zebrafish and >100% in golden shiners with an increase in nearest neighbor distance, (b) zebrafish schools would have higher roughness value (surface area/volume ratio) than those of golden shiners, (c) and that nearest neighbor distance would vary from 8 to 20 cm to visually resolve conspecific striping patterns in both species. Overall, considering between-species differences in the sensory system of species exhibiting collective

behavior could change the predictions about the positioning of individuals in the group as well as the shape of the school, which can have implications for group cohesion. We suggest that more effort should be invested in assessing the role of the sensory system in shaping local interactions driving collective behavior.

2.2 Introduction

Animals in social groups often rely on the behavior of nearby conspecifics to obtain information about their environment (Dall et al., 2005). An individual's ability to perceive and assess conspecific cues, such as the change in position and orientation of neighbors (Couzin et al., 2002; Couzin & Krause, 2003), is mediated by the sensory system (Dall et al., 2005) and may facilitate group cohesion. In some species, the use of both vision and the lateral line together allow an individual to assess important cues during schooling interactions. For example, in saithe (*Pollachus virens*) the lateral line is used to assess changes in the speed and direction of neighbors, while the visual system provides cues about neighbor position (Partridge & Pitcher, 1980). However, depending on the ecological context, some sensory dimensions may provide more reliable information about the surrounding environment. For example, social fish in visually obscure waters (e.g., fast-flowing, high sediment) place greater emphasis on the use of their chemosensory or mechanosensory (i.e., lateral line) systems to detect conspecifics (Pitcher & Parrish, 1993). However, in species inhabiting clear waters with low turbidity and readily available downwelling light, visual cues are spatially and temporally more reliable (Heuschele et al., 2009; Hogan & Laskowski, 2013).

Local interactions between group mates drive the formation of largescale patterns of coordinated movement, referred to as collective behavior (Sumpter, 2010). In fish, a broad spectrum of collective behaviors has been characterized (Parrish, Viscido & Grünbaum, 2002). For example, fish that form groups to enhance foraging opportunities (i.e., shoals) are characterized by irregular neighbor separation and randomized individual alignment (i.e., low polarity) (Pitcher & Parrish, 1993). Whereas, in response to high predation risk, fish form more cohesive groups (i.e., schools), which tend to display fixed neighbor separation and ordered alignment (i.e., high polarity) (Pitcher & Parrish, 1993).

Although the behavioral mechanisms structuring these local interactions are still largely unknown (Lopez et al., 2012), individual-based models provide a useful way to predict collective

interactions (Parrish, Viscido & Grünbaum, 2002; Sumpter, 2010). However, these models often make multiple sensory assumptions. For example, some models assume that individuals have a specific degree of visual coverage (Aoki, 1980), defined as the extent of the binocular plus the lateral visual fields, excluding the blind area at the rear of the head (Martin, 2007). In these models, visual coverage is generally assumed to be around 300°, limited by a 60° posterior blind area (Wood & Ackland, 2007). However, this estimate is based solely on a single species of whiting (Hall, Wardle & MacLennan, 1986) and may not accurately reflect other fish. Other models assume that individuals can perceive social cues up to a certain distance, which defines the individual's social interaction range (Vicsek et al., 1995; Couzin et al., 2002). This interaction range is conventionally set to a radius of 0.5-2.0 body lengths (Barbaro et al., 2009; Katz et al., 2011) based upon empirical estimates solely from minnow schools (Partridge, 1980). Although these assumptions intend to consider some aspects of the sensory system, they do not necessarily reflect the configuration specific to the study species (Rountree & Sedberry, 2009; Romey & Vidal, 2013). This could be a major constraint in our ability to understand and model collective behavior, as recent evidence suggests that relaxing these sensory assumptions can influence model predictions (Lemasson, Anderson & Goodwin, 2009; Harpaz & Schneidman, 2014).

Our goal was to assess the visual system in two social species of cyprinids, the zebrafish (*Danio rerio*) and the golden shiner (*Notemigonus crysoleucas*) and discuss implications for their collective behavior. These species are excellent models because they both exhibit collective behavior and are thought to use vision as the primary modality during conspecific interactions (Miklosi & Andrew, 2006; Saverino & Gerlai, 2008; Polverino, Phamduy & Porfiri, 2013). We studied specific properties of the visual system that may be involved in the detection of conspecifics while animals are in schools: the visual field configuration (size of the binocular and lateral fields, and blind area), the density and distribution of retinal ganglion cells as well as eye size to estimate visual acuity, and the location of the center of acute vision.

The visual field configuration defines the visual coverage that an animal has around its head (Martin, 2007). Species with limited visual coverage (i.e., large blind areas) are expected to change their behavior (e.g., increase vigilance) to compensate for the lack of visual information in parts of their visual field (Guillemain, Martin & Fritz, 2002). Retinal ganglion cells relay information collected across the visual field to the visual centers of the brain (Pettigrew et al., 1988). Changes in the density of retinal ganglion cells are associated with changes in visual

resolution across the retina (Collin, 1999). For instance, regions of the retina with a localized high density of retinal ganglion cells (i.e., center of acute vision) provide higher visual resolution. These centers of acute vision generally project into a specific region of the visual space, which may require an individual to move its body and modify its position within the group to detect changes in the behavior of group mates (Butler & Fernández-Juricic, 2014). In addition, eye size and the overall density of retinal ganglion cells can be used to estimate the upper limits of overall visual acuity (Land & Nilsson, 2012), which establishes the distances at which animals are expected to resolve conspecifics. For example, animals with higher visual acuity would detect changes in the behavior of conspecifics from farther distances (Fernández-Juricic & Kowalski, 2011), which may have consequences for the spacing of individuals within a group.

The foraging ecology of a species has been suggested as one of the main drivers in the evolution of visual systems in vertebrates (Collin, 1999; Martin, 2014). Both the zebrafish and golden shiner are social cyprinids found in well-lit freshwater environments (Sigler, 1987; Spence et al., 2008). Both species, like many other cyprinids, are omnivorous visual feeders that forage on a variety of prey types located at the water surface (Sigler, 1987; Spence et al., 2008). Based on the foraging strategies of the golden shiner and zebrafish, it is likely that both species possess visual configurations allowing them to efficiently detect and localize dorsally located, passive prey. We predicted that in an effort to reduce their vulnerability to predators, both species would have a reduced blind area, but intermediate binocular fields due to their omnivorous diets (Sigler, 1987; Spence et al., 2008). In addition, these species are expected to have high acuity projecting to the surface of the water column to assist in the detection and capture of prey (Miyazaki, 2014). In fact, a previous study conducted on zebrafish characterized a ventro-temporal center of acute vision, which suggests adult zebrafish have high acuity in the region above the head (Mangrum, Dowling & Cohen, 2002), although this study did not estimate the specific projection into the visual field.

2.3 Methods

We used 5 adult wildtype zebrafish (AB genetic strain) and 12 adult golden shiners from two commercial vendors. The golden shiners were purchased from a local bait fishery (Lafayette, Indiana, USA), while the zebrafish were obtained from The Zebrafish International Resource Center (ZIRC, Eugene, Oregon, USA). The zebrafish used for retina extractions also had their visual field measured prior to retina removal. For the golden shiners, we used different subjects

for both the visual field measurements and retina extractions. Individuals were housed in separate aquaria under a 16-hour light: 8-hour dark cycle and supplied water via a flow-through filtration system. Fish were fed daily with a mixture of brine shrimp and commercially available dry foods (Tetramin ® Tropical Flakes). The Purdue Institutional Animal Care and Use Committee (1207000675) approved all experimental procedures.

2.3.1 Visual field configuration

A variety of different approaches, both direct and indirect have been used to measure the visual field configuration of fish (Watanuki et al., 2000; Bianco, Kampff & Engert, 2011). However, direct estimates are often more precise, as they consider the spatial extent of the retina and its projection into the visual space (Martin, 1984, 2007). For large species with large eyes that can tolerate supplemental ventilation and the placement of electrodes into the eye, the visual field can be measured with an electroretinogram on live animals (McComb & Kajiura, 2008; McComb, Tricas & Kajiura, 2009; Kajiura, 2010). However, for smaller species with small eyes, like the ones used in this study, ophthalmoscopic measurements are more appropriate (Collin & Shand, 2003). We measured the visual field configuration of 5 adult zebrafish and 9 adult golden shiners using an ophthalmoscopic reflex technique (Martin, 1984) and modified visual field apparatus developed for fish (Appendix B, Figure B1). This technique requires the direct observation of the eye with an ophthalmoscope (Keeler Professional; Keeler Ophthalmic Instruments, Broomall, Pennsylvania, USA) to detect the light reflected from the retina, so observations were measured immediately following euthanasia via rapid cooling through submersion in a 5 parts ice/1 part water mixture (Wilson, Bunte & Carty, 2009). The apparatus was configured such that 90° and 270° were directly in front and behind the animal, respectively, along the horizontal plane, while 0° and 180° represented the vertical plane above and below the animal. We recorded the visual field configuration across all angles around the head in 10° elevation increments. Our estimate of the visual field did not take into consideration variations due to eye movement, but considered the resting eye position, as previous studies suggest that the eyes assume a resting position postmortem (Martin, 1986). Additionally, the resting eye position is maintained in between convergent and divergent eye movements and is thought to remain stabilized by the vestibulo-ocular reflex as the animal swims (Easter & Johns, 1974; Schairer & Bennett, 1986).

Based on the combined measurements of both the left and right eye at each elevation, we

estimated the species' binocular, lateral and blind area sectors (Martin & Katzir, 1999). The binocular field was determined separately at each elevation as the overlap in vision between both eyes while the blind area represented regions devoid of vision. For the lateral area, we applied the following equation: (360 – (mean blind area + mean binocular field)/2) (Fernández-Juricic et al., 2008). Averages for each species were determined at each elevation with accuracy of ± 0.5°.

2.3.2 Retinal wholemounting

We extracted and wholemounted the retinas of 3 adult zebrafish and 3 adult golden shiners. Following euthanasia via rapid cooling (Wilson, Bunte & Carty, 2009), we submerged the head of the animal in Davidson's Fixative for 3-5 hours. While the eye remained attached to head by the optic nerve, we used spring scissors to remove the cornea, lens and vitreous humor. A dorsal cut was made to the retina before the eyecup was detached to ensure the correct orientation in later steps. We separated the retina from the eyecup by peeling away the sclera with forceps. The retina was then subjected to a (3%) bleaching solution until transparent to allow for the visualization of the ganglion cells. Following bleaching, 3-4 peripheral cuts were made to allow the retina to lie flat on a gelatinized glass slide. We followed the procedures described in (Ullman et al., 2012) to fix and stain the retina using a series of dehydrating and rehydrating steps in combination with 0.1% cresyl violet. In addition, we photographed images of the wholemounted retina and recorded area and perimeter measurements to account for retina shrinkage before and after staining using ImageJ (http://imagej.nih.gov/ij/). Average retina shrinkage values for the zebrafish and golden shiner were 0.07 ± 0.05 and 0.13 ± 0.07 respectively (mean ± SE).

Following staining, the retinas were viewed under an Olympus BX51 microscope. We traced the perimeter of the retinal periphery and optic nerve head with Stereo Investigator v.10 (MBF Bioscience, Williston, Vermont, USA) and then applied a sampling grid with a counting frame of 50 μm^2 x 50 μm^2 for a total of approximately 200 total sampling sites per retina. We then counted the total number of observed retinal ganglion cells at each of the sampling sites using ImageJ (http://imagej.nih.gov/ij/). Ganglion cells were distinguished from amacrine and glial cells according to previously established morphological characteristics (Hughes, 1977; Ehrlich, 1981; Collin & Pettigrew, 1988). We omitted counting sites where the retina appeared damaged or the cell visibility was poor. For the zebrafish, we counted 150 ± 54.9 sites per retina; while for the golden shiner we counted 112 ± 15.7 sites (mean ± SE). The Schaeffer coefficient of error for the

zebrafish and golden shiner was 0.006 ± 0.0015 and 0.003 ± 0.0002 respectively (Glaser & Wilson, 1998). Topographic maps were generating using the R program "one cell map V8 svg version.R" (Garza-Gisholt et al., 2014). This program constructs isodensity maps from regions of localized cell density within a defined retinal outline created with Adobe Illustrator.

2.3.3 Spatial resolving power

Retinal ganglion cells act as a bottleneck filter, summating the information from the other retinal cell types (i.e., bipolar cells, amacrine cells, photoreceptors) into a signal that is sent to the brain (Pettigrew et al., 1988). Considering the integral role that the ganglion cells play in relying visual information to higher processing centers, the anatomical estimates of spatial resolving power based on ganglion cell densities and eye size have been used extensively in the literature (Hughes, 1977; Collin & Pettigrew, 1989; Collin, 1999; Pettigrew & Manger, 2008). In addition, this anatomically derived measure of spatial resolving power has been shown to closely resemble behavioral estimates of visual acuity in species of fish, mammals and birds (Hughes, 1975, 1977; Pettigrew et al., 1988; Pettigrew & Manger, 2008; Temple, Manietta & Collin, 2013)

In fish, the lens provides the primary source of focusing power due to the large dissimilarity in the refractive index between the aquatic environment and the optical media (Bone & Moore, 2008). The lens diameter also provides an index of eye size and body length, as it has been shown to increase in diameter as the fish matures (Pankhurst, Pankhurst & Montgomery, 1993). Consequently, calculations of spatial resolving power in fish incorporate lens dimensions (Collin & Pettigrew, 1989) as opposed to similar estimates in other vertebrates where eye axial length is generally used (Hughes, 1977; Martin, 1986). We followed (Collin & Pettigrew, 1988, 1989) in the approach to estimate spatial resolving power using retinal ganglion cell density. For teleosts, the posterior nodal distance (PND) is calculated by multiplying 2.55 by the radius of the lens to estimate the area that an object would take up on the retina. Using the calculated PND, we then followed the equation from Pettigrew et al. (1988) and Williams & Coletta (1987) to estimate the retinal magnification factor, $RMF = \frac{2\pi * PND}{360}$ and anatomically derived spatial resolving power (SRP), where *D* is the density of retinal ganglion cells (cells/mm^2):

$$SRP = \frac{RMF}{2}\sqrt{\frac{2D}{\sqrt{3}}}$$

Using the estimated spatial resolving power of these cyprinid species, we calculate the extent of their ability to resolve objects in the environment. We followed the equation from (Tyrrell et al., 2013) to estimate the threshold distance (d) at which an object exhibiting maximum visual contrast can be resolved under optimal light conditions, where r is the radius of the object and α is the inverse of spatial resolving power:

$$d = \frac{r}{\tan\frac{\alpha}{2}}$$

With this equation, it is possible to estimate the threshold maximum distance that an animal can resolve an object across various regions of the visual field. However, these distances do not incorporate the sensitivity and distribution of the photoreceptors, which also are also responsible for contrast sensitivity under different light environments (Lythgoe & Partridge, 1989). For the purposes of this study, we used the peak spatial resolving power (i.e., area with maximum ganglion cell density) and the minimum spatial resolving power (i.e., area with minimum retinal ganglion cell density) to calculate the maximum distance at which the body of conspecific could be resolved for both species in different regions of the visual field. In addition, we also estimated the maximum resolvable distance for the species-specific conspicuous markings, as it has been suggested that social fish use characteristics of the conspecific phenotype, such as spots or stripes as reference marks to assess changes in neighbor movements when schooling (Guthrie & Muntz, 1993; Bone & Moore, 2008). Wildtype zebrafish possess alternating light and dark horizontal stripes along the sides of their bodies, which may be used as a cue to assess the separable distances of group mates when shoaling (Rosenthal & Ryan, 2005). Golden shiners contrastingly do not have conspicuous stripes like the zebrafish; however, they do possess defined cycloid scales, which have smooth edges that could allow animals to distinguish individual scales. Therefore, we calculated the maximum resolvable distance for the golden shiner scales, as in some species the reflective scales act as a visual cue during social interactions (Rowe & Denton, 1997). We measured photographs of the zebrafish wildtype striping pattern (four individuals) digitally using ImageJ (http://imagej.nih.gov/ij/) and estimated the length of one cycle to be the height of two alternating, horizontal stripes, one dark and one light, assuming that both stripes were equal in dimension.

Using similar procedures, we measured the average visible width of the cycloid scales of four golden shiners.

2.3.4 Position and projection of the center of acute vision into the environment

We followed the protocol of (Moore et al., 2012) to estimate the location of the center of acute vision on the flattened retina using Cartesian coordinates: -X, Y (dorsal nasal), X, Y (dorsal temporal), -X, -Y (ventral nasal), and X, -Y (ventral temporal). Coordinates were averaged across 3 individuals per species to determine the location of the center of acute vision along the four retinal axes (nasal, temporal, ventral and dorsal).

Additionally, using the monocular visual field of each eye and the ganglion cell topographic maps, we estimated the angular projection of the center of acute vision into the environment. Firstly, this required restoring the retina to its original shape because in the process of wholemounting we made several cuts to flatten it. The peripheral cuts of the topographic map were stitched together digitally using the R package, "Retistruct" (version 0.5.7) (Sterratt et al., 2013). The program uses a mathematical algorithm to digitally fit an object onto a spherical globe. The user provides the object of interest (i.e., retinal topographic map) and specifies the orientation in addition to other defining features of the retina, such as the optic disc (i.e., optic nerve head). We specified in the program the orientation of the dorsal cut applied to the retina during extraction. Following the reconstruction, we determined the angular position of the projection of the center of acute vision into the environment by reflecting the polar coordinates generated by the program into corresponding locations of each species' visual field. These coordinates utilize a colatitude and longitude system where 0° lies at the center. The nasal and dorsal poles are -90° and the temporal and ventral poles are +90°.

2.4 Results

2.4.1 Visual field configuration

In the horizontal plane of the head (90°-270°), the binocular field width of the zebrafish and golden shiner were 33 ± 3.54° and 31 ± 1.67°, respectively (Figure 2.1). The height of the binocular field extended well above and below the horizontal plane of the head in both species (Figure 2.1). In the zebrafish, the upper portion of the binocular field projected to a point right above the head, 0°

(Figure 2.1C). However, in the golden shiner, the height of the binocular field extended an additional 40° behind the head (Figure 2.1D), providing wider visual coverage in the vertical plane.

In the horizontal plane of the head, the zebrafish and golden shiner had a blind area of 21 ± 2.30° and 25 ± 1.20°, respectively. The size of the blind area limited the visual coverage (binocular plus lateral fields) in the horizontal plane to 339 ± 4.0° in the zebrafish and 335 ± 3.5° in the golden shiner. Considering all recorded elevations, the average visual coverage of these cyprinid species was: 336 ± 3.8° for the zebrafish, and 333 ± 3.5° for the golden shiner.

2.4.2 Retinal ganglion cell density and centers of acute vision

The density of retinal ganglion cells was not homogeneous across the retina (Figure 2.2). Both species had a high density of retinal ganglion cells in the ventro-temporal region of their retinae and the pattern of cell density increase was concentric (Figure 2.2). The characteristics of these areas of high retinal ganglion cell density (i.e., lack of morphological features associated with retinal invagination on the wholemounted retina, concentric increase in cell density) suggest that the centers of acute vision of both species are *areae* (i.e., enlargement of the retinal tissue due to the high density of photoreceptors and retinal ganglion cells; Walls, 1942). The zebrafish had a peak ganglion cell density of 36,224 ± 730 cells/mm^2, while the golden shiner a peak density of 14,380 ± 1272 cells/mm^2. In order to quantify the change in cell density across the retina, we utilized a concentric sampling approach to best reflect the characteristics of the *area* (Figure 2.3). The cell density difference between the center of acute vision (i.e., maximum density) and the retinal periphery (i.e., minimum density) was 18.29 ± 2.41% in the zebrafish and 17.55 ± 2.86% in the golden shiner on average (Figure 2.3A).

Based on the ventro-temporal location of the centers of acute vision (Figure 2.2), we can assume that both species possess high acuity vision in the fronto-dorsal region of their visual field (Figure 2.2). For the zebrafish, the center of the *area* projected to -32 ± 15°, -64± 10° (nasal, dorsal) of the visual field while the center of the *area* projected to -20 ± 8°, -9 ± 4° (nasal, dorsal) of the visual field in the shiner. However, the location of centers of acute vision on the retina was slightly different in both species (Figure 2.2). For the zebrafish, the center of the *area* was more ventrally shifted and located -0.10 ± 0.06 along the nasal-temporal axis and -0.21 ± 0.11 along the dorso-ventral axis. In the golden shiner, the center of the *area* was more temporally shifted and located

-0.01 ± 0.12 along the nasal-temporal axis and -0.17 ± 0.04 along the dorso-ventral axis. Consequently, the fronto-dorsal projection of the area varied between species.

2.4.3 Spatial resolving power and maximum resolvable distance

In terms of eye measurements, we recorded the average lens diameter (mm) of both species as 0.83 ± 0.03 for the zebrafish and 2.00 ± 00 for the golden shiner; the eye transverse diameter was 1.91 ± 0.04 and 4.53 ± 0.20; and the eye axial length was 1.35 ± 0.10 and 3.20 ± 0.23, respectively. Additionally, the average total body length (cm) was 4.17 ± 0.07 for the zebrafish, and 7.4 ± 0.06 for the golden shiner.

According to the peak density of retinal ganglion cells and lens size, the visual acuity of the zebrafish and golden shiner were estimated to be 1.89 ± 0.02 and 2.86 ± 0.12 (cycles/degree), respectively. With their highest acuity, provided by the center of acute vision, zebrafish could resolve the body a conspecific up to 75.80 cm (18 body lengths) away and the striping pattern up to 19.49 cm (5 body lengths) away; while golden shiners could resolve a conspecific up to 2.92 m (39 body lengths) away and the cycloid scales of a conspecific up to 19.66 cm (3 body lengths) away. In the peripheral region of the retina with the lowest cell density, visual acuity was estimated as 0.08 ± 0.06 cycles/degree for the zebrafish, and 1.18 ± 0.15 cycles/degree for the golden shiner. Based on this retinal periphery estimates, a zebrafish could resolve a conspecific and the striping pattern up to 32.08 cm (8 body lengths) and 8.25 cm (2 body lengths), respectively; while the golden shiner could resolve a conspecific and the cycloid scales up to 1.20 m (16 body lengths) and 8.11 cm (1 body length), with the periphery of the retina.

2.5 Discussion

Our results show that both cyprinid species share similar visual system properties: a wide degree of visual coverage and a ventro-temporally located center of acute vision projecting fronto-dorsally, which seems to be an *area*. However, there are some between species differences in the height of the binocular field, spatial resolving power, and the specific projection of the center of acute vision into the visual field. Additionally, our study is the first to estimate the spatial resolving power of adult zebrafish and golden shiners anatomically, using retinal ganglion cell densities. Although our estimate of the visual acuity in adult zebrafish (i.e., 1.89 cycles per degree) was higher

compared to behaviorally measured estimates using the optokinetic test (i.e., 0.6 cycles per degree) (Tappeiner et al., 2012; Cameron et al., 2013) this dissimilarity may be related to the additional filtering of information that occurs in the brain (Hughes, 1977; Pettigrew & Manger, 2008), and the fact that the optokinetic response relies on a specific subset of ganglion cells, and may not accurately reflect the total cell population (Pettigrew et al., 1988).

There has been limited visual field data collected on fish. Past studies have focused on predatory species belonging to the Batoidea, Serranidae and Lepisosteidae Families (Collin & Northcutt, 1995; Collin & Shand, 2003; McComb & Kajiura, 2008). Our study is the first to characterize the visual fields of two members of Cyprinidae, the largest Family of freshwater fish. In both cyprinid species, the binocular field widths are reduced in comparison to predatory species like the coral trout, painted comber, and blacktip grouper, which have binocular fields 36°, 40°, 54° wide respectively (Collin & Shand, 2003). The reduced binocular field widths of the zebrafish and golden shiner are likely associated with their foraging behavior focused on catching sessile and slow-moving prey. However, the lateral fields of both species are relatively wider than that of some members of the Lepisosteidae Family (137° in the horizontal plane; Collin & Northcutt, 1995), which encompass several predatory species (Schultz, 2004; Spence et al., 2008). Wide lateral fields in these two cyprinids may provide greater visual coverage to detect predators as well as conspecifics when schooling.

Variation in retinal topography has been associated with the foraging ecology and habitat structure (Collin & Pettigrew, 1988). Previous studies in other schooling species, such as the sardine (*Sardinops melanostictus* and *Etrumeus sadina*) and anchovy (*Engraulis japonicus*) found a ventral-temporal *area* projecting upward into the frontal visual field (Tamura & Wisby, 1963; Pankhurst, 1989; Miyazaki, 2014). The overall location of the *areae* is similar to that of the zebrafish and golden shiner, likely due to their similar foraging ecology (i.e., dorsally located prey). However, we found between-species differences in the projection of the *areae*, which may be related to their relative position in the water column. Zebrafish inhabit shallower waters than golden shiners, which may increase their susceptibility to aerial predators (Keast & Fox, 1992; Spence et al., 2008; Luca & Gerlai, 2012). Therefore, zebrafish may align their center of acute vision with the area of the environment where attacks from aerial predators are more likely, due to its more dorsal projection. It is possible that the selection pressure relative to aerial predators is not as pronounced in golden shiners because they are deeper in the water column.

2.5.1 Implications for collective behavior

Based on the characteristics of the visual field configuration and retinal topography reported in this study, we developed species-specific predictions relative to their collective behavior (i.e., positioning, orientation and spacing of individuals in a group) that can be tested empirically in the future.

Both species have a wide range of visual coverage limited by a posterior blind area, which may make them vulnerable to predator attacks. However, individuals may be able to increase their "collective" visual coverage by associating in groups where the vigilance can be shared among conspecifics (Rountree & Sedberry, 2009). In other words, an individual's blind area may be compensated for by the visual coverage of its surrounding neighbors, which have the capacity to provide cues to the individual about potential dangers. However, this degree of visual compensation would vary depending on the spatial arrangement of the group members. For example, in a school, where all of the members are facing the same direction, the individual blind areas are spatially located behind the school (Figure 2.4). Alternatively, in shoals, group members are not necessarily facing the same direction; therefore, the individual blind areas may project to different regions around the group. In some instances, a "collective" blind area (e.g., red area in Figure 2.4) is generated in which all of the individual blind areas overlap, and represents a blind zone that is shared between all of members of the group.

The size and location of the "collective" blind area could have implications for the group's ability to detect approaching predators (Rountree & Sedberry, 2009). As individuals space themselves out, the distance between the center of the school and the "collective" blind area increases, providing individuals with more time to detect and respond to potential predators approaching from behind (Figure 2.4), assuming equal predator attack speeds. Alternatively, as individuals become closer in the group, the distance to the "collective" blind area decreases, reducing the amount of time to respond to a predator attacking from behind (Figure 2.4).

Using the blind areas of both cyprinid species reported in this study, the average neighbor separation (Burgess & Shaw, 1981; Miller & Gerlai, 2012) and group sizes observed in the wild (Werner, Hall & Werner, 1978; Pritchard et al., 2001), we calculated the horizontal distance from the center of the school to the "collective" blind area following the equation presented in (Rountree & Sedberry, 2009). In addition, we used these calculated distance ranges to estimate the time that both species would have available to react to a predator originating from the starting point of the

"collective" blind zone (Figure 2.4). These estimates assume all individuals are the same size, are oriented in the same direction, and maintain the same nearest neighbor distance.

In the wild, zebrafish are known to form shoals consisting of 2-10 individuals (Pritchard et al., 2001) with nearest neighbor distances ranging from 0.5 to 5.5 cm (Miller & Gerlai, 2012). Based upon these behaviorally measured nearest neighbor distances, we would expect the distance to the "collective" blind area to range from 0.01 to 1.34 m behind the school (Figure 2.4). Golden shiners have been observed in schools up to 45 individuals with nearest neighbor distances ranging from 9 to 20 cm. Considering this neighbor separation distance, the distance to the "collective" blind area would range from 8.93 to 19.85 m behind the center of a golden shiner school (Figure 2.4). Considering these relationships, individuals may tradeoff having long interaction distances to increase predator detection with short interaction distances, to allow for the improved resolution of conspecific cues. In fact, studies on zebrafish seem to support this idea as, groups often decrease their neighbor separation immediately following predator exposure (Miller & Gerlai, 2007).

The freshwater garfish (*Xenentodon cancila*) is one of the most prevalent predators of zebrafish (Spence et al., 2008) and are known to rapidly pursue prey (Hossain et al., 2013). We calculated that the zebrafish could potentially increase the time available to react by 13,300% by widening the size of the school from of 0.01 m to its maximum 0.50 m by increasing in neighbor distance from 0.5 to 5.5 cm (0 to 1 body length), which is the range assumed by species in the wild and is also within the range to perceive conspecific cues (Miller & Gerlai, 2012). Largemouth bass (*Micropterus salmoides*) are common predators of golden shiners (Reid, Fox & Whillans, 1999) and by increasing the school width from 3.96 m to 8.80 m with an increase in neighbor distance from 9 to 20 cm (1 to 3 body lengths), golden shiners could potentially increase their reaction time to this predator by 122%. Similarly, the neighbor distances used in this calculation represents a range that would allow individuals to perceive conspicuous markings and has also been behaviorally measured in golden shiners (Burgess & Shaw, 1981). In active pursuit predators, like the billfish, which target large schools of prey, increasing the visual range behind the school may improve the survival of the individual group members, as it may allow members to detect rapid changes in the predator's movements (Hobson, 1979; Pitcher & Parrish, 1993). However, the predator detection benefits of increasing neighbor distance should be outweighed by the costs of reducing the benefits of dilution effects.

In both species, the centers of acute vision are directed towards the front-dorsal region of their visual field (Figure 2.2). When traveling in a school, zebrafish and golden shiners may prefer positions where they can align this high acuity region with conspecifics to enhance group cohesion. Zebrafish may preferentially respond to neighbors located 63° above the frontal plane of the body and 12° left and right of the sagittal plane of each eye; whereas for golden shiners, they may prefer positions where conspecifics are aligned 32° above the frontal plane of the body and 67° left and right of the sagittal plane for the left and right eye (Figure 2.5 C,D). There is evidence that information flows unidirectionally through fish groups such that individuals receive information and base their movement decisions from neighbors that are directly in front of them (Herbert-Read et al., 2011). Comparing these estimates with the literature, golden shiners have been shown to respond to changes in the directional movement of neighbors that are ahead of them rather than behind (Katz et al., 2011). Assuming that individuals use the center of acute vision to obtain social cues, and considering the between-species differences in the positioning of the *areae*, we can make predictions about the optimal position of individuals in a group from a visual sensory perspective (Figure 2.5). Taking into consideration the roughness of the school (surface area/volume ratio), we can predict the zebrafish will have a higher roughness value (i.e., more laterally compressed school; Figure 2.5C) than the golden shiner (i.e., more vertically compressed school; Figure 2.5D). Variations in roughness have been associated with access to oxygen and predator avoidance (Brierley & Cox, 2010). Unfortunately, there are no estimates of roughness for zebrafish and golden shiners in the literature.

Individuals often maintain a certain distance from group mates (i.e., nearest neighbor distance) (Krause & Ruxton, 2002) by using reference markings on the body (i.e., schooling marks, Bone & Moore, 2008). Based on our estimates of spatial resolving power, we calculated the maximum distance range that both cyprinid species would need to maintain in order to resolve visually these species-specific conspicuous markings, and thus remain attached to the group. In zebrafish, the centers of acute vision are capable of resolving the conspecific striping pattern up to 19.49 cm away using the fronto-dorsal region of their visual field, while the retinal periphery up to 8.25 cm away. Consequently, zebrafish would need to maintain a neighbor distance range of approximately 8-20 cm (~2-5 body lengths) (Figure 2.5A). Golden shiners could resolve the cycloid scales up to 19.66 cm away with their centers of acute vision that project to the fronto-dorsal region of the visual field and up to 8.11 cm with the retinal periphery. Therefore, golden

shiners would need to maintain a neighbor separation range of also 8-20 cm (~1-3 body lengths) (Figure 2.5B). However, this distance range assumes ideal, full spectrum light conditions, maximum contrast between the conspecific and the background, and does not account for variations in the optical clarity of the water environment; all these factors could potentially shorten this distance. However, considering that both species tend to inhabit shallow, relatively clear waters (i.e., depths up to 30 cm for the zebrafish and <55 cm for the golden shiner), there is likely to be a low degree of attenuation and consequently, a wide range of available wavelengths to perceive conspecifics. Therefore, the interaction ranges provided by our calculations should not be constrained by the depth of the water environment (Sigler, 1987; Krause, Godin & Brown, 1996; Spence et al., 2008). Comparing these estimates with the literature, lab experiments conducted on both species suggest that zebrafish maintain an average nearest neighbor separation of approximately 0.5-5.5 cm (~1 body length), and golden shiners of 9-20 cm (~1-3 body lengths) (Burgess & Shaw, 1981; Miller & Gerlai, 2012). Although our predicted distance ranges for the resolution of an entire conspecific are well above the behaviorally determined nearest neighbor distances of both species, our ranges based on the resolution of the conspicuous markings are more consistent with their natural behavior, supporting their role as a potential cue used during collective interactions. However, there are alternative explanations to the observed neighbor distances related to hydrodynamic efficiency (Hemelrijk & Hildenbrandt, 2012) and the use of vibrational cues to sense conspecifics via the lateral line (Partridge & Pitcher, 1980).

2.5.2 Concluding remarks

In the present study, we developed novel *quantitative* predictions for key parameters (position, spacing, orientation) underlying social interactions of zebrafish and golden shiners based on properties of their visual system. Therefore, an understanding of the species-specific features of the visual system allowed us to predict how individuals would position themselves in groups to optimize the transfer of visual social information. These predictions could be tested empirically in the future.

Most importantly, our findings contradict previous modeling assumptions, which assume that fish have a 60° blind zone and weigh information equally from multiple surrounding neighbors of a fixed distance. We found that the blind areas of both species were less than half the assumed width used in many models simulating fish. We also suggest that the maximum distance at which

individuals are able to perceive conspecific cues varies according to different regions of the visual field: 2-5 body lengths in the zebrafish and 1-3 body lengths in the golden shiner, with frontal areas providing the longest distances. Additionally, considering our estimate is in accordance with both species' behaviorally measured nearest neighbor distances (i.e., ~1 body length of the zebrafish and 1-3 body lengths for the golden shiner) (Burgess & Shaw, 1981; Miller & Gerlai, 2012), it is possible that these species are using cues about changes in conspecific movement through the resolution of the conspicuous markings. It should also be noted that our distance range estimates for the resolution of another conspecific (i.e., 8-18 body lengths for the zebrafish and 16-39 body lengths for the golden shiner) were much higher than the behaviorally determined interaction range (0.5-2.0 body lengths) typically used in individual-based models to specify when an individual becomes aware of another fish. Thus, making strict sensory assumptions in collective behavior models may misrepresent the basis of local interactions and emerging group structure. The overall implication is that the sensory dimensions of a given species are likely to influence the local interactions driving its collective behavior. We suggest that to better understand the mechanisms driving local interactions in groups, more effort should be invested in assessing how the sensory system may shape the spatial ability to gather information from group mates.

2.6 Figures

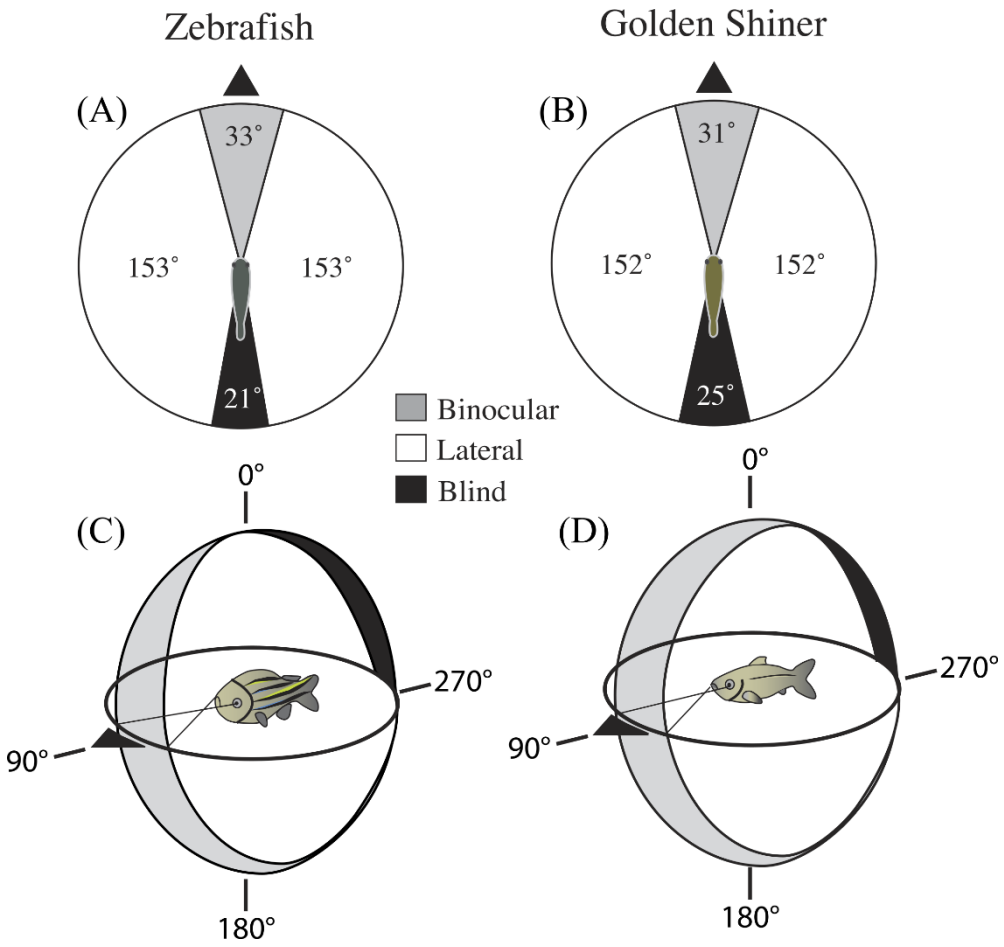

Figure 2.1 Visual field configuration of the (A) zebrafish and (B) golden shiner in the two-dimensional horizontal plane of the head (90-270°). Three-dimensional depiction of the zebrafish (C) and golden shiner (D) visual field across all elevations measured about the head. The black triangle points anterior to the body of the fish in the horizontal plane. Both depictions represent the visual field while the eyes are at rest.

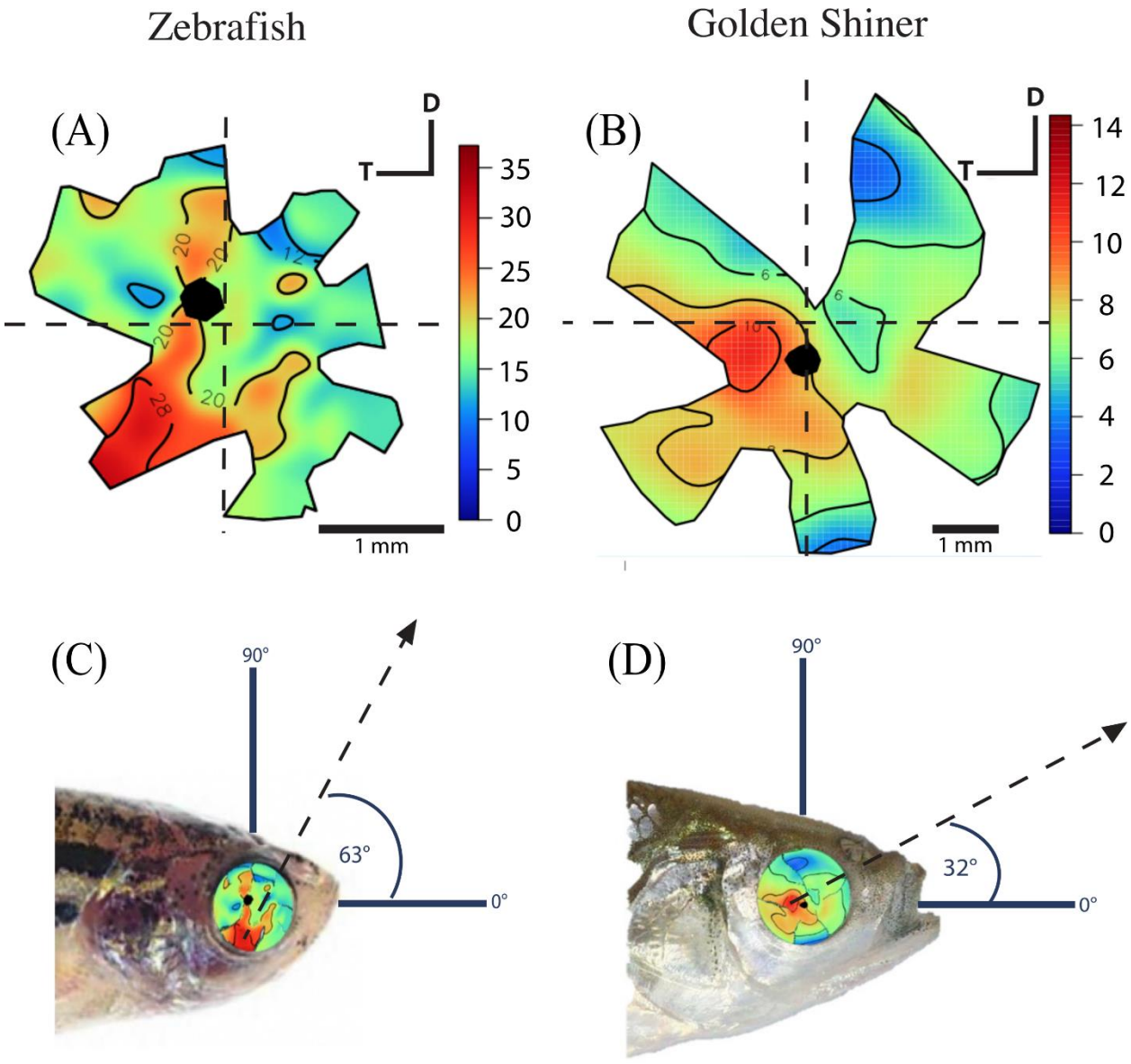

Figure 2.2 Retinal ganglion cell topography and projection of the center of acute vision. Ganglion cell topography across the retina of the (A) zebrafish and (B) golden shiner (cells/mm^2 x 10^3). Projection of the center of acute vision above the head of the (C) zebrafish and (D) golden shiner indicated with the dashed line and arrow. D, dorsal; T, temporal region.

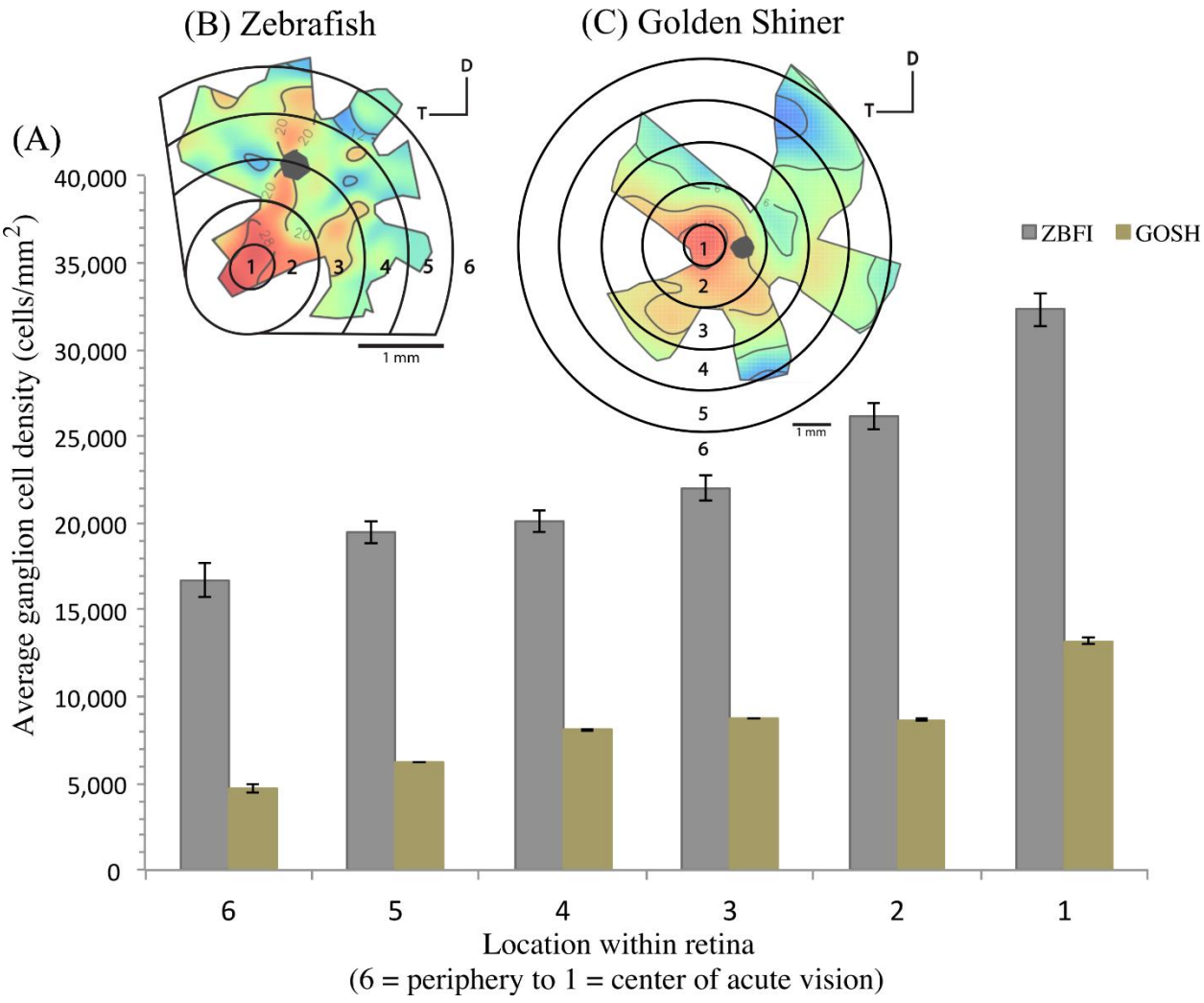

Figure 2.3 Variation in retinal ganglion cell density. (A) Graph depicting the variation in the retinal ganglion cell density across the retina within defined concentric regions from the periphery (6) to the center of acute vision (1). The bars represent the average retinal ganglion cell density ± SE in cells/mm^2 for the (B) zebrafish (ZBFI) and (C) golden shiner (GOSH).

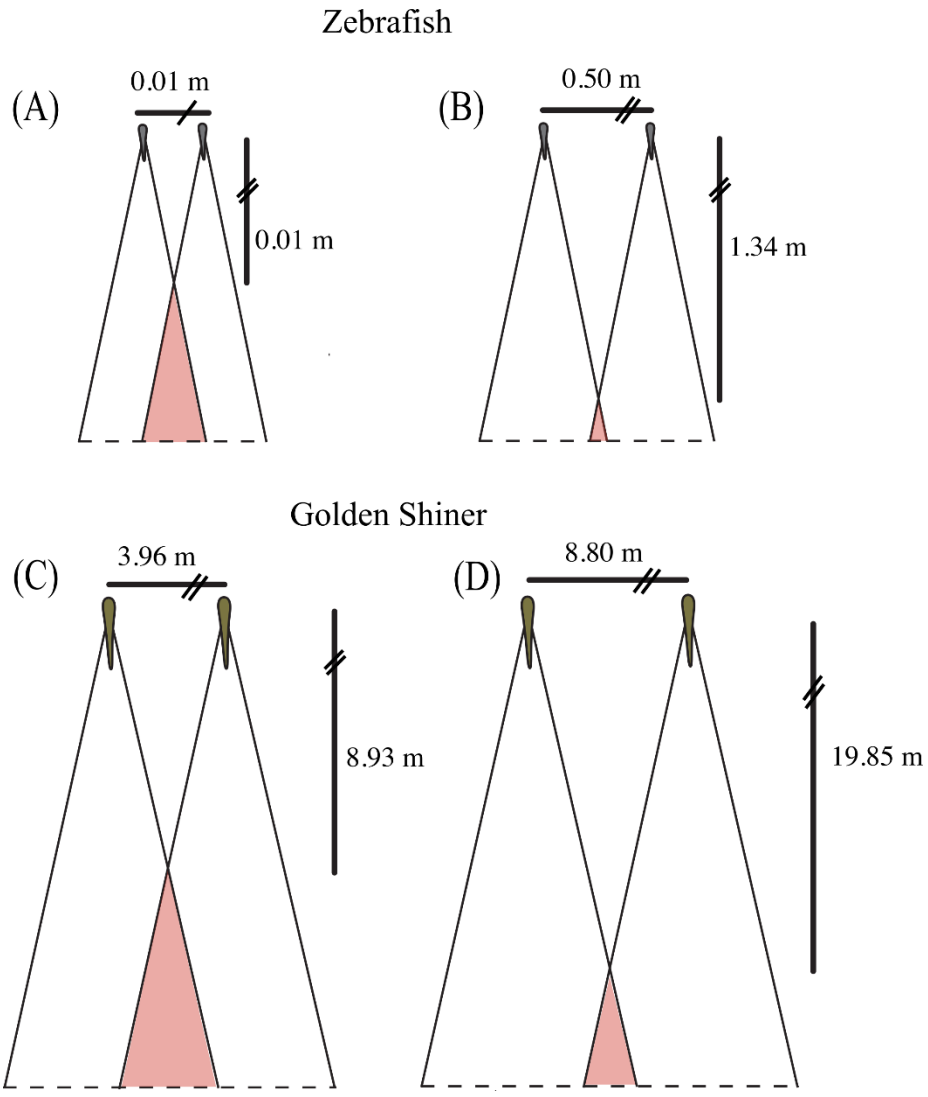

Figure 2.4 Collective blind area. Schematic representation of the "collective" blind area depicted in red for a hypothetical zebrafish (A, B) and golden shiner school (C, D) viewed from above. Although the width of the blind area does not vary within species, we provide the change in distance to the "collective blind area using the minimum (A, C) and maximum (B, D) limits of their assumed school widths (illustrated for simplicity with two fish) using the equation adopted from (Rountree & Sedberry, 2009).

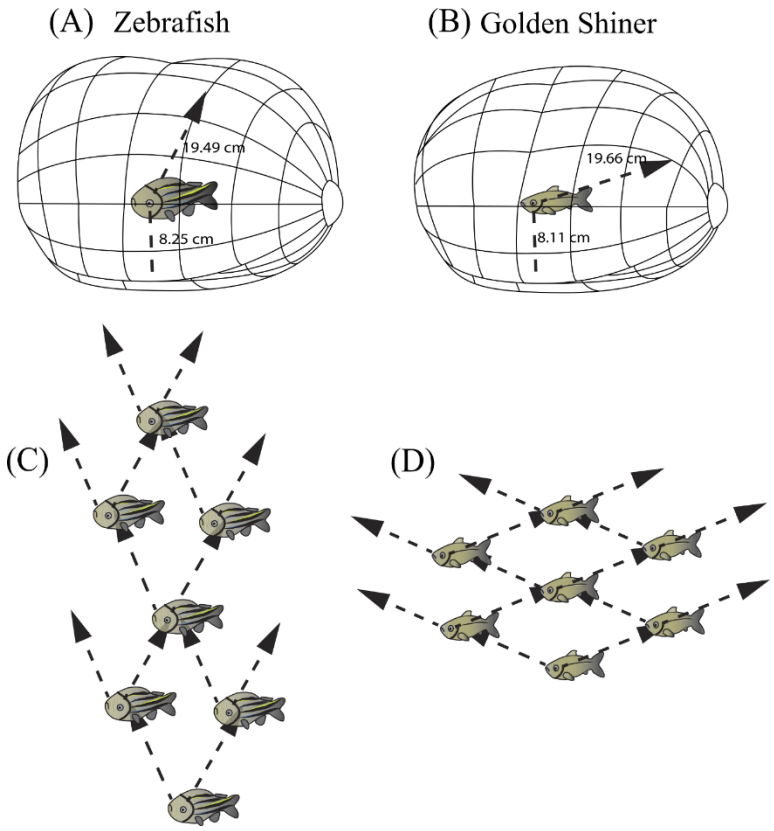

Figure 2.5 Resolvable distance range and three-dimensional school structure. Three-dimensional schematic of the resolvable distance range for the (A) zebrafish and (B) golden shiner based on the resolution of the conspecific conspicuous markings (i.e., zebrafish striping pattern and golden shiner scale width respectively). The arrow represents the projection of the center of acute vision into the visual field, figure adopted from (Tyrrell & Fernandez-Juricic, 2015). Additionally, we used the projection of the centers of acute vision in the (C) zebrafish and (D) golden shiner to generate their hypothetical school shapes, with individuals assuming positions where conspecifics may be resolved with the highest resolution.

2.7 References

Aoki I. 1980. An analysis of the schooling behavior of fish: Internal organization and process. In: *Bulletin of the Ocean Research Institute*. University of Tokyo, Japan,.

Barbaro A, Einarsson B, Birnir B, Sigurõsson S, Valdimarsson H, Pálsson ÓK, Sveinbjörnsson S, Sigurõsson Þ. 2009. Modelling and simulations of the migration of pelagic fish. *ICES Journal of Marine Science* 66:826–838.

Bianco IH, Kampff AR, Engert F. 2011. Prey Capture Behavior Evoked by Simple Visual Stimuli in Larval Zebrafish. *Frontiers in Systems Neuroscience* 5.

Bone Q, Moore R. 2008. Sensory Systems, and Communication. In: *Biology of Fishes*. New York: Taylor & Francis, 289–346.

Brierley AS, Cox MJ. 2010. Shapes of krill swarms and fish schools emerge as aggregation members avoid predators and access oxygen. *Current Biology* 20:1758–1762.

Burgess JW, Shaw E. 1981. Effects of acoustico-lateralis denervation in a facultative schooling fish: a nearest-neighbor matrix analysis. *Behavioral and neural biology* 33:488–497.

Butler SR, Fernández-Juricic E. 2014. European starlings recognize the location of robotic conspecific attention. *Biology Letters* 10.

Cameron DJ, Rassamdana F, Tam P, Dang K, Yanez C, Ghaemmaghami S, Dehkordi MI. 2013. The optokinetic response as a quantitative measure of visual acuity in zebrafish. *Journal of visualized experiments : JoVE*:1–6.

Collin SP. 1999. Behavioural ecology and retinal cell topography. In: *Adaptive Mechanisms in the Ecology of Vision*. Springer Netherlands, 509–535.

Collin SP, Northcutt GR. 1995. The Visual System of the Florida Garfish, *Lepisosteus platyrhincus* (Ginglymodi). *Brain, behavior and evolution* 45:34–43.

Collin SP, Pettigrew JD. 1988. Retinal ganglion cell topography in teleosts: a comparison between Nissl-stained material and retrograde labelling from the optic nerve. *The Journal of comparative neurology* 276:412–422.

Collin SP, Pettigrew JD. 1989. Quantitative Comparison of the Limits on Visual Spatial Resolution Set by the. Ganglion Cell Layer in Twelve Species of Reef Teleosts. *Brain, behavior and evolution* 34:184–192.

Collin SP, Shand J. 2003. Retinal Sampling and the Visual Field in Fishes. In: *Sensory Processing in Aquatic Environments*. 139–169.

Couzin ID, Krause J, James R, Ruxton GD, Franks NR. 2002. Collective memory and spatial sorting in animal groups. *Journal of Theoretical Biology* 218:1–11.

Couzin ID, Krause J. 2003. Self-organization and collective behavior in vertebrates. *Advances in the Study of Behavior* 32:1–75.

Dall SRX, Giraldeau L-A, Olsson O, McNamara JM, Stephens DW. 2005. Information and its use by animals in evolutionary ecology. *Trends in ecology & evolution* 20:187–93.

Easter SS, Johns PR. 1974. Horizontal compensatory eye movements in goldfish (*Carassius auratus*). *Journal of Comparative Physiology* 92:37–57.

Ehrlich D. 1981. Regional specialization of the chick retina as revealed by the size and density of neurons in the ganglion cell layer. *The Journal of comparative neurology* 195:643–657.

Fernández-Juricic E, Gall MD, Dolan T, Tisdale V, Martin GR. 2008. The visual fields of two ground-foraging birds, House Finches and House Sparrows, allow for simultaneous foraging and anti-predator vigilance. *Ibis* 150:779–787.

Fernández-Juricic E, Kowalski V. 2011. Where does a flock end from an information perspective? A comparative experiment with live and robotic birds. *Behavioral Ecology* 22:1304–1311.

Garza-Gisholt E, Hemmi JM, Hart NS, Collin SP. 2014. A comparison of spatial analysis methods for the construction of topographic maps of retinal cell density. *PLoS ONE* 9.

Glaser EM, Wilson PD. 1998. The coefficient of error of optical fractionator population size estimates: A computer simulation comparing three estimators. *Journal of Microscopy* 192:163–171.

Guillemain M, Martin GR, Fritz H. 2002. Feeding methods, visual fields and vigilance in dabbling ducks (Anatidae). *Functional Ecology* 16:522–529.

Guthrie DM, Muntz WRA. 1993. Role of vision in fish behaviour. In: Pitcher TJ ed. *Behaviour of Teleost Fishes*. London: Chapman & Hall, 89–128.

Hall SJ, Wardle CS, MacLennan DN. 1986. Predator evasion in a fish school: test of a model for the fountain effect. *Marine Biology* 91:143–148.

Harpaz R, Schneidman E. 2014. Receptive-field like models accurately predict individual zebrafish behavior in a group. *Journal of Molecular Neuroscience* 53:S61–S61.

Hemelrijk CK, Hildenbrandt H. 2012. Schools of fish and flocks of birds: their shape and internal structure by self-organization. *Interface Focus* 2:726–737.

Herbert-Read JE, Perna A, Mann RP, Schaerf TM, Sumpter DJT, Ward a. JW. 2011. Inferring the rules of interaction of shoaling fish. *Proceedings of the National Academy of Sciences* 108:18726–18731.

Heuschele J, Mannerla M, Gienapp P, Candolin U. 2009. Environment-dependent use of mate choice cues in sticklebacks. *Behavioral Ecology* 20:1223–1227.

Hobson ES. 1979. Interactions Between Piscivorous Fishes and Their Prey. *Predator-prey systems in fisheries management. Sport Fishing Institute, Washington DC*:231–241.

Hogan KE, Laskowski KL. 2013. Indirect information transfer: three-spined sticklebacks use visual alarm cues from frightened conspecifics about an unseen predator. *Ethology* 119:999–1005.

Hossain Y, Jewel AS, Rahman M, Haque ABMM, Elbaghdady HAM, Ohtomi J. 2013. Life-history traits of the freshwater garfish *Xenentodon cancila* (Hamilton 1822) (Belonidae) in the Ganges river, Northwestern Bangladesh. *Sains Malaysiana* 42:1207–1218.

Hughes A. 1975. A quantitative analysis of the cat retinal ganglion cell topography. *The Journal of comparative neurology* 163:107–128.

Hughes A. 1977. The topography of vision in mammals of contrasting life style: comparative optics and retinal organization. In: *The visual system in vertebrates*. New York: Springer, 613–756.

Kajiura SM. 2010. Pupil dilation and visual field in the piked dogfish, *Squalus acanthias*. *Environmental Biology of Fishes* 88:133–141.

Katz Y, Tunstrøm K, Ioannou CC, Huepe C, Couzin ID. 2011. Inferring the structure and dynamics of interactions in schooling fish. *Proceedings of the National Academy of Sciences* 108:18720–18725.

Keast A, Fox MG. 1992. Space use and feeding patterns of an offshore fish assemblage in a shallow mesotrophic lake. *Environmental Biology of Fishes* 34:159–170.

Krause J, Ruxton GD. 2002. *Living in groups*. Oxford University Press.

Land MF, Nilsson D-E. 2012. *Animal eyes*. Oxford University Press.

Lemasson BH, Anderson JJ, Goodwin R a. 2009. Collective motion in animal groups from a neurobiological perspective: The adaptive benefits of dynamic sensory loads and selective attention. *Journal of Theoretical Biology* 261:501–510.

Lopez U, Gautrais J, Couzin ID, Theraulaz G. 2012. From behavioural analyses to models of collective motion in fish schools. *Interface Focus* 2:693–707.

Luca RM, Gerlai R. 2012. In search of optimal fear inducing stimuli: differential behavioral responses to computer animated images in zebrafish. *Behavioural Brain Research* 226:66–76.

Lythgoe JN, Partridge JC. 1989. Visual pigments and the acquisition of visual information. *The Journal of experimental biology* 146:1–20.

Mangrum WI, Dowling JE, Cohen ED. 2002. A morphological classification of ganglion cells in the zebrafish retina. *Visual Neuroscience* 19:767–779.

Martin GR. 1984. The visual fields of the tawny owl, *Strix aluco L. Vision research* 24:1739–1751.

Martin GR. 1986. The eye of a passeriform bird, the European starling (*Sturnus vulgaris*): eye movement amplitude, visual fields and schematic optics. *Journal of Comparative Physiology A* 159:545–557.

Martin GR. 2007. Visual fields and their functions in birds. *Journal of Ornithology* 148:547–562.

Martin GR. 2014. The subtlety of simple eyes: the tuning of visual fields to perceptual challenges in birds. *Philosophical transactions of the Royal Society of London. Series B, Biological sciences* 369:20130040.

Martin GR, Katzir G. 1999. Visual fields in short-toed Eagles, *Circaetus gallicus* (Accipitridae), and the function of binocularity in birds. *Brain, Behavior and Evolution* 53:55–66.

McComb DM, Kajiura SM. 2008. Visual fields of four batoid fishes: a comparative study. *The Journal of Experimental Biology* 211:482–490.

McComb DM, Tricas TC, Kajiura SM. 2009. Enhanced visual fields in hammerhead sharks. *The Journal of experimental biology* 212:4010–4018.

Miklosi A, Andrew RJ. 2006. The Zebrafish as a Model for Behavioral Studies. *Zebrafish* 3:227–234.

Miller N, Gerlai R. 2007. Quantification of shoaling behaviour in zebrafish (*Danio rerio*). *Behavioural Brain Research* 184:157–166.

Miller N, Gerlai R. 2012. From Schooling to Shoaling: Patterns of Collective Motion in Zebrafish (*Danio rerio*). *PLoS ONE* 7:8–13.

Miyazaki T. 2014. Retinal ganglion cell topography in juvenile Pacific bluefin tuna *Thunnus orientalis* (Temminck and Schlegel). *Fish Physiology and Biochemistry* 40:23–32.

Moore B a, Kamilar JM, Collin SP, Bininda-Emonds ORP, Dominy NJ, Hall MI, Heesy CP, Johnsen S, Lisney TJ, Loew ER, Moritz G, Nava SS, Warrant E, Yopak KE, Fernández-Juricic E. 2012. A novel method for comparative analysis of retinal specialization traits from topographic maps. *Journal of vision* 12:13.

Pankhurst NW. 1989. The relationship of ocular morphology to feeding modes and activity periods in shallow marine teleosts from New Zealand. *Environmental Biology of Fishes* 26:201–211.

Pankhurst PM, Pankhurst NW, Montgomery JC. 1993. Comparison of behavioural and morphological measures of visual acuity during ontogeny in a teleost fish, *Forsterygion varium*, tripterygiidae (Forster, 1801). *Brain, behavior and evolution* 43:178–188.

Parrish JK, Viscido S V, Grünbaum D. 2002. Self-organized fish schools: an examination of emergent properties. *The biological bulletin* 202:296–305.

Partridge BL. 1980. The effect of school size on the structure and dynamics of minnow schools. *Animal Behaviour* 28:68–77.

Partridge B, Pitcher T. 1980. The Sensory Basis of Fish Schools: Relative Roles of Lateral Line and Vision. *Journal of Comparative Physiology* 135:315–325.

Pettigrew JD, Dreher B, Hopkins CS, McCall MJ, Brown M. 1988. Peak density and distribution of ganglion cells in the retinae of microchiropteran bats: implications for visual acuity. *Brain, behavior and evolution* 32:39–56.

Pettigrew JD, Manger PR. 2008. Retinal ganglion cell density of the black rhinoceros (*Diceros bicornis*): calculating visual resolution. *Visual neuroscience* 25:215–220.

Pitcher TJ, Parrish JK. 1993. Functions of shoaling behaviour in teleosts. In: *Behaviour of Teleost Fishes*. London: Chapman & Hall, 363–439.

Polverino G, Phamduy P, Porfiri M. 2013. Fish and robots swimming together in a water tunnel: robot color and tail-beat frequency influence fish behavior. *PloS one* 8:e77589.

Pritchard V, Lawrence J, Butlin RK, Krause J. 2001. Shoal choice in zebrafish, *Danio rerio*: the influence of shoal size and activity. *Animal Behaviour* 62:1085–1088.

Reid SM, Fox MG, Whillans TH. 1999. Influence of turbidity on piscivory in largemouth bass (*Micropterus salmoides*). *Canadian Journal of Fisheries and Aquatic Sciences* 56:1362–1369.

Romey WWL, Vidal JJM. 2013. Sum of heterogeneous blind zones predict movements of simulated groups. *Ecological Modelling* 258:9–15.

Rosenthal GG, Ryan MJ. 2005. Assortative preferences for stripes in danios. *Animal Behaviour* 70:1063–1066.

Rountree RA, Sedberry GR. 2009. A theoretical model of shoaling behavior based on a consideration of patterns of overlap among the visual fields of individual members. *Acta Ethologica* 12:61–70.

Rowe DM, Denton EJ. 1997. The physical basis of reflective communication between fish, with special reference to the horse mackerel, *Trachurus trachurus*. *Philosophical Transactions of the Royal Society B: Biological Sciences* 352:531–549.

Saverino C, Gerlai R. 2008. The social zebrafish: behavioral responses to conspecific, heterospecific, and computer animated fish. *Behavioural brain research* 191:77–87.

Schairer JO, Bennett M V. 1986. Changes in gain of the vestibulo-ocular reflex induced by sinusoidal visual stimulation in goldfish. *Brain research* 373:177–181.

Schultz K. 2004. *Ken Schultz's Field Guide to Freshwater Fish*. John Wiley & Sons.

Sigler WF. 1987. Golden Shiner. In: *Fishes of the Great Basin: A Natural History*. 188–190.

Spence R, Gerlach G, Lawrence C, Smith C. 2008. The behaviour and ecology of the zebrafish, *Danio rerio*. *Biological Reviews of the Cambridge Philosophical Society* 83:13–34.

Sterratt DC, Lyngholm D, Willshaw DJ, Thompson ID. 2013. Standard anatomical and visual space for the mouse retina: computational reconstruction and transformation of flattened retinae with the retistruct package. *PLoS Computational Biology* 9.

Sumpter D. 2010. *Collective Animal Behavior*. Princeton, NJ: Princeton University Press.

Tamura T, Wisby W. 1963. The visual sense of pelagic fishes especially the visual axis and accomodation. *Bulletin of Marine Science* 13:433–448.

Tappeiner C, Gerber S, Enzmann V, Balmer J, Jazwinska A, Tschopp M. 2012. Visual acuity and contrast sensitivity of adult zebrafish. *Frontiers in zoology* 9:10.

Temple SE, Manietta D, Collin SP. 2013. A comparison of behavioural (Landolt C) and anatomical estimates of visual acuity in archerfish (*Toxotes chatareus*). *Vision Research* 83:1–8.

Tyrrell LP, Moore BA, Loftis C, Fernández-Juricic E. 2013. Looking above the prairie: localized and upward acute vision in a native grassland bird. *Scientific reports* 3:3231.

Ullmann JFP, Moore B a, Temple SE, Fernández-Juricic E, Collin SP. 2012. The retinal wholemount technique: a window to understanding the brain and behaviour. *Brain, behavior and evolution* 79:26–44.

Vicsek T, Czirók A, Ben-Jacob E, Cohen I, Shochet O. 1995. Novel type of phase transition in a system of self-driven particles. 75:729–732.

Walls GL. 1942. *The vertebrate eye and its adaptive radiation*. Michigan: The Cranbook Institute of Science.

Watanuki N, Kawamura G, Kaneuchi S, Iwashita T. 2000. Role of vision in behavior, visual field, and visual acuity of cuttlefish *Sepia esculenta*. *Fisheries Science* 66:417–423.

Werner EE, Hall DJ, Werner MD. 1978. Littoral zone fish communities of two Florida lakes and a comparison with Michigan lakes. *Environmental Biology of Fishes* 3:163–172.

Williams DR, Coletta NJ. 1987. Cone spacing and the visual resolution limit. *Journal of the Optical Society of America A* 4:1514–1523.

Wilson JM, Bunte RM, Carty AJ. 2009. Evaluation of rapid cooling and tricaine methanesulfonate (MS222) as methods of euthanasia in zebrafish (*Danio rerio*). *Journal of the American Association for Laboratory Animal Science* 48:785–789.

Wood AJ, Ackland GJ. 2007. Evolving the selfish herd: emergence of distinct aggregating strategies in an individual-based model. *Proceedings. Biological sciences / The Royal Society* 274:1637–1642.

CHAPTER 3. ZEBRAFISH NEIGHBOR DISTANCE CHANGES RELATIVE TO CONSPECIFIC SIZE, POSITION IN THE WATER COLUMN, AND THE HORIZON: A VIDEO PLAYBACK EXPERIMENT

Diana Pita[1] & Esteban Fernández-Juricic[1]

[1]Department of Biological Sciences. Purdue University. 915 W. State Street. West Lafayette. IN 47907.USA

Citation:
A version of this chapter is currently published as a preprint in bioRxiv and is reproduced here with permission.

Pita, D., and Fernandez-Juricic, E. (2019). The visual social environment affects non-additively neighbor spacing and interaction time in zebrafish. *bioRxiv*, 511972. doi:10.1101/511972.

3.1 Abstract

Many fish form schools and maintain visual contact with their neighbors in a three-dimensional environment. In this study, we assessed whether zebrafish modified their spacing and interaction time in an additive or multiplicative way relative to multiple sources of social information using computer animations. We simultaneously manipulated: (a) the size of the virtual conspecific (as a proxy of social cue magnitude), (b) the position of the virtual conspecific in the water column (as a proxy of the level of perceived risk), and (c) the absence/presence of the visual horizon (as a proxy of depth perception). The size of the virtual conspecific and the presence of the visual horizon independently affected spacing behavior (zebrafish increased their separation distance when interacting with larger virtual conspecifics and when the visual horizon was present (i.e., depth perception enhanced)), but no manipulation independently affected interaction time. However, some of these factors interacted significantly, such that their effects on social behavior depended on each other. For instance, zebrafish increased their separation distance under high risk conditions when the virtual conspecific was larger, but this risk effect disappeared when the conspecific was the same size or smaller, likely to avoid aggression. Also, zebrafish increased their separation distance when depth perception was enhanced under low risk conditions, but the effect of depth perception disappeared under high risk conditions. Overall, the effects of certain dimensions of the visual social environment depended on the intensity of other dimensions,

ultimately tuning up or down different behavioral responses. We discuss the implications of these findings for the spatial organization of fish schools.

3.2 Introduction

Models of social behavior have long considered the spatial range over which a group is dispersed (Krause and Ruxton, 2002). This spatial range can affect the degree of separation between group mates (i.e., neighbor separation distance) and ultimately the transmission of social information within the group (Proctor et al., 2001, 2003) as animals use social cues to regulate their social interactions (Pritchard et al., 2001; Fernández-Juricic and Kacelnik, 2004; Abaid et al., 2012). Empirical studies have shown that longer neighbor distances constrain the flow of social information (Fernández-Juricic and Kacelnik, 2004; Fernández-Juricic and Kowalski, 2011; Pays et al., 2013) and modify the visual monitoring strategies of group members (Pays et al., 2009; Fernández-Juricic et al., 2011). The ability of an animal to acquire and evaluate the quality of social information available over distance could affect its decisions regarding its own position within the group to maintain social cohesion (Sumpter, 2010).

An important factor that can limit the transmission of social information is the perceptual ability of the receiver (Strandburg-Peshkin et al., 2013; Pita et al., 2016; Lavergne et al., 2019). In the case of visual information, visual acuity (i.e. ability to resolve two objects as separate entities) limits the spatial range over which an animal can resolve the details of an image, which can ultimately constrain its ability to interact with other group members (Pita et al., 2016). Group members experiencing such information constraints are expected to change their behavior to maintain the resolution of social information (Kimbell and Morrell, 2015). For instance, when social information becomes more difficult to gather, individuals can shorten their neighbor distances (Dawkins and Woodington, 1997), lengthen the duration of their interactions with group mates (Fernández-Juricic and Kacelnik, 2004; Fernández-Juricic et al., 2007), or use regions of the visual field with high visual acuity (i.e., centers of acute vision) (Butler and Fernandez-Juricic, 2014) to gather social information.

The availability of computer animations and robotic stimuli have allowed experimenters to manipulate social cues to assess their role in tuning social behavior (Gerlai, 2017; Bierbach et al., 2018; Kim et al., 2018). Several studies have manipulated single social cues at a time (Butail et al., 2013; Bartolini et al., 2016); however, we know less about the effects of *simultaneous*

manipulations of multiple social cues, and more specifically, how simultaneous manipulations affect the individual's ability to gather social information and respond to variations in its visual social environment (Larsch and Baier, 2018; Lemasson et al., 2018). This is particularly relevant because understanding how animals respond to variations in the social environment can allow us to identify the rules underlying social interactions (Herbert-Read, 2016). For instance, two different visual social cues (e.g., color and size) can act in an additive (i.e., the combined effect of color and size is equal to the sum of each effect taken individually) or multiplicative (i.e., the effect of color cues depends on the size cues) way. Furthermore, we can explore how these rules may be affected by environmental change, leading to the disruption of social interactions and changes in the spatial arrangement of groups. For example, increased water turbidity can reduce the transmission of visual information between fish, resulting in fewer social interactions and smaller group sizes (Chamberlain and Ioannou, 2019).

In this study, we assessed how zebrafish modified their social spacing behavior (i.e., distance between conspecifics while interacting) and social interaction time (i.e. time spent interacting with conspecifics) relative to three types of simultaneous changes in the visual social environment: (a) the size of the conspecific (as a proxy of the magnitude of the social cues), (b) the position of the conspecific in the water column (as a proxy of the levels of risk in the environment), and (c) the absence/presence of the visual horizon (as a proxy of depth perception). A detailed account of our predictions relative to interaction spacing and time is presented below. Additionally, we assessed whether the zebrafish would visually track our manipulations of the visual social environment. More specifically, we estimated the probability of zebrafish using their high vs. low acuity vision in the different social manipulations based on previous accounts of the position of different retinal landmarks (Pita et al. 2015). We had not developed specific hypotheses and predictions for the probability of using high vs. low acuity vision, so we considered this a post-hoc analysis.

We used zebrafish as our model species because they are highly social animals that depend on visual information during social interactions (Miklosi and Andrew, 2006; Saverino and Gerlai, 2008). We manipulated the visual social environment using computer animations following (Ingley et al., 2015; Balzarini et al., 2017). We only considered interactions with a single conspecific as a first attempt to identify some of the simplest rules underlying pairwise social

interactions. Future studies should consider how these rules scale up in larger groups (Lemasson et al., 2018).

3.2.1 Hypotheses and predictions

We first present predictions for single effects and then for their interactions.

An individual's ability to resolve social cues from a group mate (e.g., variations in coloration, body patterns, etc.) decreases with distance (Fernández-Juricic and Kowalski, 2011). To simulate changes in the magnitude of the social cues, we manipulated the size of the virtual conspecific. Zebrafish appear to use the diameter of the eye and the width of body stripes as social cues (Guthrie and Muntz, 1993; Bone and Moore, 2008), which scale directly with body size and may serve as a cue of perceived neighbor distance. We predicted that as the size of the conspecific decreased, individuals would move closer to the conspecific to enhance their ability to resolve the conspecific (Pita et al., 2015) and/or increase the amount of time spent interacting with the conspecific (Fernández-Juricic et al., 2004, 2007).

In zebrafish, the vertical position of the fish in the water column varies with the level of risk (Bishop et al., 2016; Oliveira et al., 2017). Zebrafish located at the bottom of the water column (i.e., low vertical spatial position) are associated with higher risk environments (e.g., predator presence) (Kalueff et al., 2013; Oliveira et al., 2017). We therefore predicted that when the conspecific was at the bottom of the water column, individuals would move closer to the conspecific and/or increase the duration of their interaction to obtain more information about a potential threat (Pham et al., 2012).

When animals assess the size of an object, they consider the visual angle or angular size (i.e., amount of space that the object takes up on the retina) (Douglas, 1996; Sperandio and Chouinard, 2015). However, distance can complicate this assessment, as objects that are far away have a reduced visual angle and consequently appear smaller than their actual size. To compensate for this, animals have evolved various mechanisms to improve depth perception (Howard, 2012; Nityananda and Read, 2017), ultimately allowing them to establish size constancy (i.e. ability to perceive the relative size of an object independent of its angular size) (Douglas et al., 1988; Zeil, 2000; Frech et al., 2012). One of the cues that facilitates depth perception is the presence of a *visual horizon*, which serves as a salient referential cue that can offer information about object orientation and distance (Layne et al., 1997; Caballero et al., 2015). In their natural habitats,

zebrafish have a visual horizon defined by a variety of environmental substrates (Zimmermann et al., 2018). We manipulated the presence/absence of a virtual visual horizon in our animations. We predicted that when the horizon was absent, individuals would move closer to the conspecific and/or increase the duration of the social interaction due to the lack of referential information and the need to better assess its relative size and location, compared to a situation in which the horizon was present.

One of the novel components of our study is the simultaneous manipulation of different factors to assess potential interaction effects. The conceptual frameworks we used allowed us to generate predictions for two-way interactions between pairs of the three factors considered (see also statistical analyses). First, we predicted a significant interaction between the size of the conspecific and the position of the conspecific in the water column, whereby individuals would increase their separation distance and reduce social interaction time particularly when exposed to a small conspecific at the bottom of the water column. We hypothesized that individuals may experience higher risk when joining a group composed of smaller conspecifics in a high-risk scenario because their larger size would make them more conspicuous to potential predators (Krause and Ruxton, 2002; Croft et al., 2006; Rodgers et al., 2015).

Second, we predicted a significant interaction effect between the size of the conspecific and the absence/presence of the visual horizon. When the horizon was absent, zebrafish would likely perceive conspecifics according to their absolute size due to the lack of referential information, leading to large and small conspecifics appearing as smaller or larger, respectively, than size-matched (i.e. intermediate) conspecifics. In these scenarios (small/large conspecifics with the horizon absent), we predicted zebrafish would increase their separation distance and reduce their interaction time to minimize the costs of interacting with differently sized group mates (Nakayama et al., 2009). For example, body size correlates with dominance in teleost fish and individuals of larger body size are more likely to win fighting contests (Arnott and Elwood, 2009), while individuals of smaller body size are more likely to pay a cost for fighting (Hoare et al., 2000). On the other hand, when the horizon was present, individuals should perceive conspecifics according to their relative size (i.e., a small conspecific would be perceived to be far away compared to a large conspecific) because of the enhanced ability to perceive depth.

Third, we predicted an interaction between the position of the conspecific in the water column and the absence/presence of the visual horizon, whereby individuals would move closer

to the conspecific and increase their interaction time particularly when the conspecific is at the bottom of the water column and the horizon is present. We hypothesized that the closer the conspecific is to the horizon, the more pronounced the enhanced depth perception benefits would be, and consequently the perception of a high-risk environment.

3.3 Methods

We used 10 adult zebrafish (5 male and 5 female zebrafish, wildtype AB genetic strain) acquired from The Zebrafish International Resource Center (ZIRC, Eugene, Oregon, USA). Our sample size per combination of factors (10 individuals) was similar to previous studies in zebrafish that manipulated some of the factors we studied (Abaid et al., 2012; Bartolini et al., 2016; Macrì et al., 2017; Ruberto et al., 2017). Before the experiment, zebrafish were housed together in a 12-gallon glass stock tank (51.4 cm L x 26.7 cm W x 32.1 cm H) maintained with a recirculating water filter (Aqueon Power Filter ®) and exposed to a 16-hour light: 8-hour dark cycle. Water quality checks were preformed daily (pH, temperature) and weekly (ammonia, nitrates, nitrites, chlorine) to ensure appropriate housing conditions. We fed zebrafish daily with commercial fish flakes (Tetramin ® Tropical Flakes).

Before the initiation of the experiment, zebrafish were transferred from their stock tank into individual 2.5-gallon tanks (30.5 cm L x 15.2 cm W x 20.3 cm H) with air stones to provide aeration. To reduce stress behaviors associated with exposure to a novel tank environment, each zebrafish was tested within its individual 2.5-gallon home tank. During treatment exposure, the home tank was placed directly against the screen of a computer monitor (Acer LCD monitor, model v176L) displaying the animated treatment video (Appendix C, Figure C1). The computer monitor had a resolution of 1280 x 1024 pixels and a refresh rate of 75 hertz.

Video animations have been used considerably in animal behavior (Rosenthal, 2002; Woo and Rieucau, 2008; Chouinard-Thuly et al., 2017). We followed (Ingley et al., 2015; Balzarini et al., 2017) by manipulating visual social cues using computer animations. We considered this technique to be an appropriate method because zebrafish have already been shown to be responsive to computer animations (Saverino and Gerlai, 2008; Stowers et al., 2017), reacting to animated conspecifics in the same way they do to live conspecifics (Qin et al., 2014; Gerlai, 2017). We utilized tank dimensions that fell within the dimensions used in previous studies testing zebrafish's response to animations (i.e., 50 x 25 x 30 cm (Qin et al., 2014) and 51 x 30 x 25 cm (Saverino and

Gerlai, 2008)). Therefore, we did not find it necessary to perform a validation study of our experimental setup.

We generated animations using the open source software anyfish (http://swordtail.tamu.edu/anyfish/), which allows the user to create realistic animated fish stimuli (Ingley et al., 2015). We used a photograph of an adult female wildtype zebrafish as a model for our animated stimulus. A female zebrafish was utilized because other studies have shown that males are less likely to engage in interactions with other males, but females are preferred by both sexes (Ruhl and McRobert, 2005). Following previous studies using computer animated zebrafish, we used one photographic image of a zebrafish, which remained constant across treatments (Saverino and Gerlai, 2008; Gerlai et al., 2009; Qin et al., 2014). By modifying the positions of the animated stimulus with user-defined key frames, we designed the virtual conspecific to swim back and forth, horizontally across the screen. The individual frames were then combined to generate a 60 frame per second video to simulate a conspecific swimming at approximately 5 cm per second which is the approximate speed maintained by zebrafish when schooling (Miller and Gerlai, 2012). The flicker rate of the animation was designed to simulate smooth continuous movement in the eyes of the zebrafish as the critical flicker fusion frequency of many fish are thought to be within the range of 14-67 Hz (Lythgoe, 1979).

We positioned top- and side-view cameras (JVC Everio GZ-MG330-HU camcorder) to record the behavior of the zebrafish throughout the trial (Appendix C, Figure C1). We temporally synchronized both camera views with a portable DVR (Night Owl, H264-4 channel DVR) with multiplexer, which brought together the different video inputs and allowed us to calibrate the position of the zebrafish and computer monitor in both the top and side camera views. We spatially synchronized both camera views by standardizing the dimension of the tank using a premeasured scale (length of the tank) in the top and side camera views with ImageJ (https://imagej.nih.gov/ij/). The synchronization of the cameras allowed us to determine the 3D position of the live zebrafish. The 15.24 cm sides and the 30.48 cm bottom of the tank were covered with opaque white tape and the experimental arena, consisting of a table that supported the tank and computer monitor were surrounded by opaque white curtains to reduce visual distractions during trials. Before each trial, there was a 10-min acclimation period followed by the 3-min treatment video that provided 1 min of continuous conspecific exposure. The first min of the treatment video displayed only the virtual environment followed by 1 min of the conspecific swimming within in the virtual environment,

while the last minute displayed again the virtual environment without the conspecific. Light levels at the surface of the water (mean ± SE; 1072 ± 1.35 lux) and temperature levels (mean ± SE; 74 ± 0.07 °F) remained constant throughout the experiment.

We exposed each zebrafish (4.5 ± 0.15 cm body length; mean ± SE) to a total of 12 treatments, represented by the combination of 3 categorical independent variables: size of the conspecific (3 levels: large, intermediate, small), the position of the conspecific in the water column (2 levels: top, bottom), and the absence/presence of a visual horizon (2 levels: absent, present). Each zebrafish was exposed to one treatment per day, allowing for approximately 24 hrs between each successive trial over the course of 12 days. Additionally, we randomized both the testing order of the zebrafish each day and the order of each zebrafish's treatment exposure.

Videos were coded manually and blind by an individual unaware of the experimental question or design. First, we used the program idTracker (http://www.idtracker.es/) to divide each video into frames (30 frames per second). Following this procedure, we used ImageJ (https://imagej.nih.gov/ij/) to measure the visual separation distance between the eye of the live zebrafish and the midpoint of the body of the animated conspecific. We chose to manually code the videos (Delcourt and Poncin, 2012) because other fully-automated tracking programs tend to only measure the distance between the center of the live fish and the computer screen, but we intended our measurements to be more sensory specific, as the distance over which visual information is acquired (distance between the eye of the zebrafish and virtual conspecific). An example of the movement trajectories we generated is in Appendix C (Figure C2). By using 3D measurements obtained from manual coding, we were able to calculate the position of the conspecific within the zebrafish's visual field following (Pita et al., 2015) to determine if the conspecific was aligned with high (i.e., center of acute vision) or low (i.e., retinal periphery) acuity retinal regions. High acuity retinal regions are expected to provide finer scale spatial information compared to low acuity retinal regions (Pettigrew et al., 1988). In the case of zebrafish, a previous study found that each eye has one center of acute vision (enlargement of the retinal tissue due to the higher density of cone photoreceptors/reginal ganglion cells or *area*) that projects fronto-dorsally surrounded by low acuity reguions (periphery of the retina) (Pita et al., 2015).

Measurements were taken during defined interaction periods. The beginning of an interaction period represented any approach made by the zebrafish towards the computer screen (Kalueff et al., 2013). In zebrafish, the turning angle represents a change in the directional heading

(Kalueff et al., 2013), and we used it to define the end of each interaction period. Specifically, we measured the separation distance of the zebrafish prior to the frame where the zebrafish altered its directional heading over 45° from its original angle of approach. One measurement was recorded during each interaction period, evaluating the separation distance (i.e., distance between the eye of the zebrafish and the virtual conspecific) and the interaction duration (i.e., difference between the start and end time of the interaction period). Additionally, we assessed whether the zebrafish was viewing the virtual conspecific with the center of acute vision or the retinal periphery. We had not developed specific predictions for the region of the visual field used, so we considered this as a post-hoc analysis.

We manipulated the size of the conspecific through a 2-fold increase (large conspecific = 8 cm) and 2-fold decrease (small conspecific = 2 cm) in size relative to a size-matched (intermediate conspecific = 4 cm) zebrafish. The eyes are an important cue involved in social recognition and the initiation of shoaling behavior (Landgraf et al., 2016), while the striping pattern is used as a reference mark to assess changes in conspecific movement when individuals are interacting in groups (Guthrie and Muntz, 1993; Bone and Moore, 2008). Because we kept the relative eye diameter and width of the lateral body stripes constant in each conspecific size manipulation, the net result was that the eyes and stripes could have been easier or more difficult to visually resolve in the large and small conspecifics, respectively.

We manipulated the position of our animation along the water column by making the virtual conspecific swim in either the upper portion of the tank (7.6 cm, low risk level) or lower portion of the tank (12.7 cm, high risk level), relative to the bottom of the tank. Previous studies have shown that under stress, zebrafish position themselves at the bottom of the water column (Egan et al., 2009; Kalueff et al., 2013).

In animals moving in two-dimensional and three-dimensional space and through manipulative approaches, it has been demonstrated that the presence of a visual horizon acts as a depth cue and can influence the visual perception of (and behavioral responses to) objects in the environment (Layne et al., 1997; Zeil, 2000; Caballero et al., 2015). The empirical evidence on the visual horizon effect also includes fish (Douglas, 1996). We therefore manipulated the presence/absence of the virtual horizon under the hypothesis that it would modify the perceived depth of the conspecific in the virtual environment, and ultimately affect the quality of information (i.e., higher with the presence of the visual horizon because the spatial reference could enhance

the perception of depth). Treatments with the horizon absent (low perceived depth) had a white background with the virtual conspecific swimming. Treatments with the horizon present (high perceived depth) had a virtual substrate, the default terrain of the anyfish program. When the virtual horizon was present, the conspecifics were 8 cm and 3 cm above the horizon in high and low risk treatments, respectively.

We also coded whether the zebrafish was using the center of acute vision (i.e., high acuity region of visual field) or retinal periphery (i.e., low acuity region of visual field) for each observation to establish if zebrafish may utilize high acuity regions of the visual field to increase their uptake of social information. We measured the position (angle in 3D space) of the conspecific relative to the eye of the zebrafish (Pita et al., 2015). The distance between the eye of the live zebrafish and the center of the virtual conspecific was calculated from 2D measurements of the top and side view camera recordings (Appendix C, Figure C1). To estimate where the center of acute vision projected in the visual space of our experimental arena, we calculated both the horizontal (angle relative to the horizontal plane of the zebrafish) and vertical (angle relative to the vertical plane of the zebrafish) positions of the eye of the zebrafish. We then evaluated the position of the conspecific relative to the projection of the zebrafish's center of acute vision utilizing a 95% confidence interval range based on the retinal topographic map of the density of retinal ganglion cells of this species (Pita et al., 2015). If the virtual conspecific was within the 95% confidence interval range, we recorded that the live zebrafish was visualizing it with its center of acute vision for that frame. If the virtual conspecific was outside the 95% confidence interval, we deemed it as being visualized by areas of the retina with low visual acuity at that time frame (e.g., retinal periphery). Although zebrafish can move their eyes, these movements act to provide image stabilization when swimming (Chen et al., 2014) or for prey localization when foraging (Bianco et al., 2011; Patterson et al., 2013). We assumed that any eye movements generated during the approach to the animation were used to maintain image stabilization of the conspecific within the zebrafish's visual field. Although zebrafish can move their eyes in certain contexts (Brockerhoff et al., 1997), the assumption of lack of eye movements has been used in social interaction studies in which fish are individually tracked relative to the position of neighbors (Strandburg-Peshkin et al., 2013; Rosenthal et al., 2015). Nevertheless, because of the possibility of some eye movements, we acknowledge that our results should be taken with care.

3.3.1 Statistical analysis

We ran general linear mixed models using a repeated measures design in SAS (version 9.4). The code and the data used are available in Appendix C. We tested the effects of the size of the conspecific, the position of the conspecific in the water column, and the absence/presence of the visual horizon on separation distance and interaction duration. Across trials, there were 10.66 ± 0.63 (mean ± SE) interaction behaviors analyzed per trial per individual. Each interaction behavior totaled approximately 23.9 ± 0.40 frames (mean ± SE). In addition to the main effects, we also analyzed two-way interaction effects (i.e. size of the conspecific x position of the conspecific in the water column, size of the conspecific x absence/presence of the visual horizon, and the position of the conspecific in the water column x absence/presence of the visual horizon) on separation distance and interaction duration. The original models included the three-way interaction (size of the conspecific x position of the conspecific in the water column x absence/presence of the visual horizon) as well as the sex of the live zebrafish, but did not turn out to be significant; so, we removed it to increase the power of the tests. We added to the final model the order in which individual zebrafish were exposed to the multiple treatment combinations as an independent factor (despite our randomizing order presentation) to control statistically for potential temporal effects. We defined the model in SAS PROC MIXED by setting each of the three main factors (size of the conspecific, position of the conspecific in the water column, absence/presence of the visual horizon) as within-subject factors relative to subject ID, which was defined as a random factor, following (Moser, 2004) (see Appendix C). This model allowed covariances to vary due to subject ID, size of the conspecific, position of the conspecific in the water column, and absence/presence of the visual horizon. We used an unstructured variance-covariance matrix, which is recommended by West et al. (2015) when dealing with multiple repeated-measures factors like in our case. We used the between-within method for estimating the degrees of freedom in the mixed models given the presence of three repeated measure factors. We checked for the normality of the residuals and the homogeneity of variance visually and we found extremely minor deviations that did not justify transforming the data. We used t-tests to assess post-hoc differences between levels of a given factor or interaction but did not control for multiple post-hoc comparisons because of the increased likelihood of Type II error (Nakagawa, 2004).

We also ran a generalized linear mixed model in SAS (version 9.4) to analyze whether the probability of using different regions of the visual field (i.e., center of acute vision vs. periphery)

varied in the different treatment conditions. In SAS PROC GLIMMIX, we defined the model in much the same way as described above for the general linear models. The main differences were that our dependent variable was binomial (center of acute vision, periphery) with a logit link function, and a first-order autoregressive covariance structure (Appendix C). For the purposes of this model, we set our dependent variable as 1, when the conspecific was viewed with the center of acute vision, and 0, when the conspecific was viewed with the retinal periphery.

3.4 Results

3.4.1 Separation distance

The size of the conspecific and the visual horizon affected zebrafish separation distance (Table 3.1). Zebrafish increased their separation distance as the virtual conspecific increased in size (Figure 3.1a). Zebrafish increased their separation distance when the horizon was present compared to when it was absent (Figure 3.1b). However, we did not detect a significant change in separation distance relative to the position of the conspecific in the water column (Table 3.1).

We also found two significant two-way interaction effects between the factors we manipulated (Table 3.1). First, the size of the conspecific interacted with its position in the water column, whereby separation distances were significantly longer when the conspecific was at the bottom rather than the top of the water column and its size was large (Figure 3.2a). However, no significant difference for separation distance was observed between the two positions in the water column when subjects were exposed to the intermediate and small conspecifics (Figure 3.2a).

Second, the position of the conspecific in the water column also interacted with the absence/presence of the visual horizon (Table 3.1), such that when the conspecific was at the top of the water column, the separation distance was longer when the horizon was present compared to when it was absent (Figure 3.2b). However, no significant difference in separation distance relative to the visual horizon was detected when the conspecific was at the bottom of the water column (Figure 3.2b).

3.4.2 Interaction duration

There were no significant effects of size of the conspecific, its position in the water column, and absence/presence of the visual horizon, as single factors, on the duration of the interaction between the zebrafish and the conspecific (Table 3.1). However, we found a significant interaction effect between the size of the conspecific and its position in the water column (Table 3.1), by which interaction duration was significantly higher when the conspecific was at the top rather than the bottom of the water column under the large conspecific treatment (Figure 3.3). However, we did not detect an effect of conspecific position in the water column on interaction duration with virtual conspecifics of intermediate or small sizes (Figure 3.3).

3.4.3 Probability of viewing the conspecific with different regions of the visual field

The probability of the zebrafish viewing the virtual conspecific with the center of acute vision was not significantly affected by any of our manipulated treatments or their interactions (Table 3.1). The implication is that during the social interactions, our subjects have similar probabilities of viewing the conspecific with either the center of acute vision or the retinal periphery.

3.5 Discussion

In a social pairwise scenario, zebrafish modified two aspects of their social behavior (spacing and interaction time) with changes to features of their social environment (size, position of the neighbor in the water column, and presence of a visual horizon). Zebrafish responded to our manipulations not just in an additive way (i.e., independent effects of each type of manipulation), but also in a multiplicative way (i.e., interaction effects between different types of manipulations). Zebrafish modulated their behavioral responses based on combinations of different visual social inputs such that their behavior towards one input depended on the levels of the second input. These interaction effects were more pronounced for spacing behavior than for interaction time.

Some of our original predictions for single independent effects were supported by our findings. First, there was an inverse relationship between the size of the virtual conspecific and separation distance (i.e., zebrafish moved closer to the virtual conspecific as its size decreased), which may allow for the improved resolution of social cues (i.e., eye and stripes) to maintain social cohesion (Bone and Moore, 2008). In fact, a previous study found that zebrafish prefer to associate

with size-matched or smaller conspecifics instead of large conspecifics (Fernandes et al., 2015; Bartolini et al., 2016). Second, when the virtual conspecific was displayed in combination with the visual horizon, zebrafish distanced themselves farther away probably because the referential information enhanced their ability to perceive depth and get a better estimate of neighbor distance (Layne et al., 1997; Caballero et al., 2015). However, the effects of the factors we manipulated cannot be interpreted in isolation because of the significant interaction effects we found.

The effect of conspecific position in the water column depended on the size of the virtual conspecific. Zebrafish maintained shorter separation distances when the large conspecific was at the top of the water column (i.e., low risk scenario) compared to the bottom of the water column (i.e., high risk scenario). On the other hand, for intermediate and small-sized conspecifics the position in the water column did not have a significant effect on separation distance. These results do not support our original predictions, although the water column effects with the large conspecific may be explained by size disparity and the potential for aggressive interactions. Fighting ability is positively correlated with body size (Li et al., 2018). In particular, smaller individuals suffer more costs when engaging in aggressive interactions with larger individuals (Arnott and Elwood, 2009). Additionally, in some fish species, low vertical spatial positions are associated with aggressive behavior (Nakayama et al., 2009). Our live zebrafish may have maintained a longer separation distance when large conspecifics occupied low positions in the water column in order to reduce the probability of a potentially costly aggressive interaction. Alternatively, the large conspecific could have been perceived as a predator; however, this is unlikely as we did not observe any antipredator associated behaviors (e.g., increased turning rate, jumping, erratic movement) (Kalueff et al., 2013). The lack of a significant change in separation distance with position of the water column for the small and intermediate conspecifics could be explained by an insufficient elicitation of antipredator avoidance behaviors. Although zebrafish typically maintain low positions in the water column under high risk of predation, this behavior is often coupled with other behaviors such as erratic movement, increased speed, freezing and increased opercular movement (Kalueff et al., 2013). We were not able to generate these behaviors in our virtual displays.

The effects of the visual horizon depended on the position of the conspecific in the water column. Specifically, we observed greater separation distances when the horizon was present rather than absent and the conspecific was at the top of the water column. This supports our

predictions that the visual horizon is likely providing additional depth information regarding the position of the conspecific but only in the low risk scenario. It is possible that in the high risk scenario (conspecific at the bottom of the tank), the putative enhancement in depth perception with the presence of the horizon is reduced as individuals maintain similar separation distances irrespective of the absence/presence of the horizon possibly to increase the perception of social information or improve survival through dilution effects (Krause and Ruxton 2002).

In terms of interaction time, we did not detect any significant independent effects of any of the three visual social inputs manipulated. Nevertheless, we did find a significant interaction effect between the size of the conspecific and its position in the water column. In contrast to our predictions, zebrafish spent less time interacting with the large conspecific when it was at the bottom rather than the top of the water column. Similar to the effect on separation distance, this finding may also be explained by size disparity and the motivation to avoid potentially costly aggressive interactions by decreasing the amount of time spent interacting with the conspecific when positioned at the bottom of the water column. An alternative explanation is related to the difficulty of maintaining social cohesion with large conspecifics. Swimming speed is limited by body size (Aivaz and Ruckstuhl, 2011) and small individuals may be at a disadvantage when they interact with larger conspecifics in high risk environments due to their inability to keep up with their evasive escape maneuvers (Peuhkuri, 1998). The potential for small individuals to get left behind by larger group members may decrease their motivation to interact, resulting in a decreased interaction duration with large conspecifics under situations of high risk (i.e., bottom of water column). The lack of a significant effect of position in the water column for intermediate or small conspecifics may also be related to the lack of additional risk-associated behaviors in the virtual conspecific.

We also found that none of our manipulations affected the portion of the visual field (high vs. low acuity) zebrafish used to view the conspecific. The implication is that zebrafish use their high and low acuity vision with relatively equal probability to track conspecifics. However, the ability of zebrafish to resolve a spatial grain is limited by the visual resolution of its eye. We used the spatial resolving power of zebrafish (Pita et al., 2015) to estimate whether individuals in our experiment would have been able to resolve the eyes and stripes of each of conspecific based on their observed average neighbor distances (see Appendix, Figure C3). We found that when interacting with size-matched (i.e. intermediate) and large conspecifics, individuals maintained a

separation distance that would have allowed them to resolve key social cues (i.e., eye and stripes) with both high and low acuity vision (Appendix, Figure C3). However, when interacting with small conspecifics, the separation distance they maintained would have only allowed them to resolve the eye and stripes with their high acuity vision but not with their low acuity vision (Appendix, Figure C3). However, we did not detect any behavioral response associated with this sensory constraint (i.e., increase in the probability of using the center of acute vision when viewing the small virtual conspecific). One potential explanation is that the information zebrafish get from viewing conspecifics with their center of acute vision is enough without the need to compensate for difficult viewing conditions. Alternatively, our sample size may have been limited to detect an effect.

Overall, it appears that the visual social environment affects zebrafish social interactions in complex ways. Many vertebrates (fish and birds) interact socially in three-dimensional space. Previous findings (Larsch and Baier, 2018; Lemasson et al., 2018) and ours suggest that the rules underlying these three-dimensional interactions are likely affected by multiple parameters acting simultaneously. In other words, the effects of some visual features of the social environment may depend on the intensity of other visual features tuning up or down different behavioral responses. We believe this is relevant because research on collective behavior sometimes tries to pin down simple rules (i.e., effects of single factors) governing between-individual interactions (Schellinck and White, 2011; Arganda et al., 2012; Pita et al., 2016). Although simplification is certainly necessary to understand complex behaviors, we suggest that considering the multiplicative effects of different features of the visual social environment can enhance our ability to predict social interactions in groups.

One of the implications of the dynamic nature of zebrafish social behavior is that it could influence the spatial configuration of fish schools depending on habitat complexity and water turbidity. For example, in a low-risk environment with an easily visible horizon, individuals may maintain long separation distances, which would lead to low density groups with low intra-specific competition (Krause and Ruxton, 2002). Low density fish schools that could detect predators more quickly because of greater group visibility (Rountree and Sedberry, 2009; Pita et al., 2015). In these low-density groups, the presence of a threat could be quickly transmitted across the group via social information, which could lead to rapid changes in the spatial configuration of the school ending in spatially tighter (e.g., higher density) schools. However, if the group is composed of

individuals with different sizes, there may be increased interaction costs particularly under high risk situations. These costs may alter the flow of social information and the structural dynamics of the group. More work along the lines of (Lemasson et al., 2018) should establish the relevance of the different sources of visual social information in triggering these structural changes as the number of group members increases (and their position in three-dimensional space changes) in environments with different levels of habitat complexity and visibility.

3.6 Tables and Figures

Table 3.1 Effects of the size of the virtual conspecific, the position of the virtual conspecific in the water column, and the absence/presence of the visual horizon: (a) separation distance, (b) interaction duration, and (c) the probability of viewing the conspecific with the center of acute vision (1) or the retinal periphery (0). Significant effects are marked in bold.

	F	**df**	**P**
Separation Distance			
Conspecific Size	17.88	2, 1054	< **0.001**
Position of Conspecific	0.06	1, 1054	0.8090
Visual Horizon	3.96	1, 1054	**0.047**
Trial order	0.02	1, 1054	0.893
Conspecific Size x Position of Conspecific	4.68	2, 1054	**0.010**
Conspecific Size x Visual Horizon	0.69	2, 1054	0.504
Position of Conspecific x Visual Horizon	11.03	1, 1054	< **0.001**
Interaction Duration			
Conspecific Size	0.04	2, 1054	0.958
Position of Conspecific	0.08	1, 1054	0.783
Visual Horizon	0.03	1, 1054	0.869
Trial order	0.02	1, 1054	0.902
Conspecific Size x Position of Conspecific	3.99	2, 1054	**0.019**
Conspecific Size x Visual Horizon	0.82	2, 1054	0.443
Position of Conspecific x Visual Horizon	0.01	1, 1054	0.928
Probability of using center of acute vision vs. retinal periphery			
Conspecific Size	0.12	2, 18	0.892
Position of Conspecific	2.61	1, 9	0.141
Visual Horizon	0.01	1, 9	0.925
Trial order	3.23	1, 1009	0.073
Conspecific Size x Position of Conspecific	1.63	1, 1009	0.196
Conspecific Size x Visual Horizon	0.87	1, 1009	0.418
Position of Conspecific x Visual Horizon	0.42	1, 1009	0.516

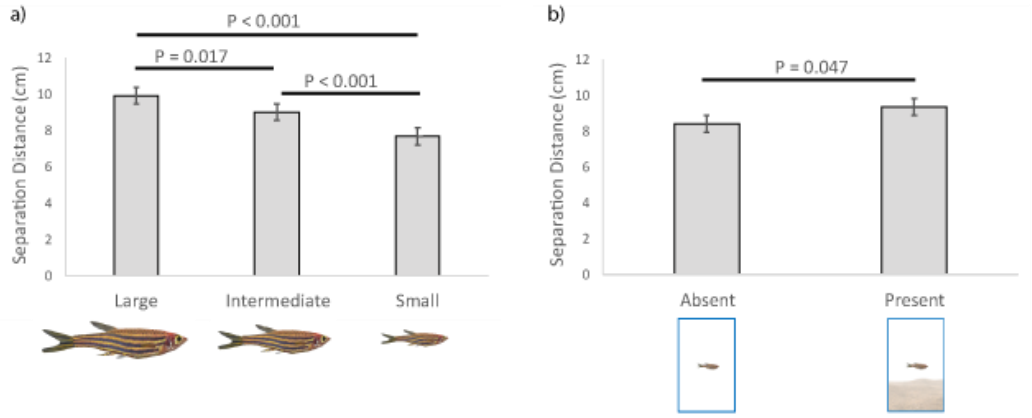

Figure 3.1 Variation in separation distance between the zebrafish and virtual conspecific (cm) relative to: (a) the size of the conspecific (large, intermediate, small), and (b) absence/presence of the visual horizon. Shown are means and SEs.

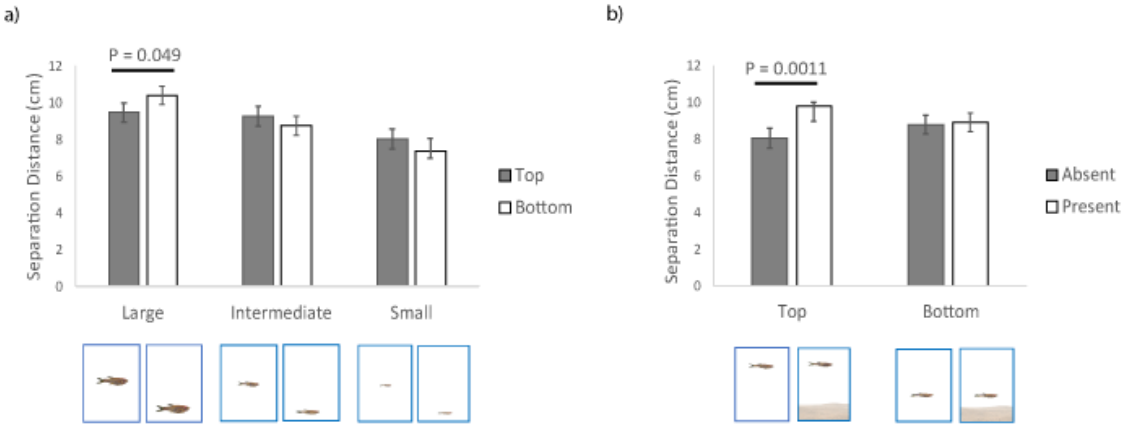

Figure 3.2 Variation in separation distance between the zebrafish and virtual conspecific (cm) relative to the simultaneous effect of: (a) size of the conspecific (large, intermediate, small) and position of the conspecific in the water column (top, bottom); and (b) position of the conspecific in the water column (top, bottom) and absence/presence of the visual horizon. Shown are means and SEs.

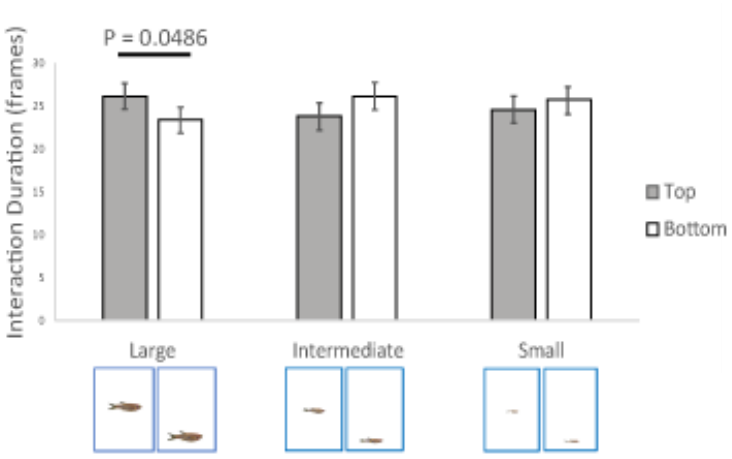

Figure 3.3 Duration (frames) of the interaction between the zebrafish and virtual conspecific relative to the size of the conspecific (large, intermediate, small) and position of the conspecific in the water column (top, bottom). Shown are means and SEs.

3.7 References

Abaid, N., Bartolini, T., Macrì, S., and Porfiri, M. (2012). Zebrafish responds differentially to a robotic fish of varying aspect ratio, tail beat frequency, noise, and color. *Behav. Brain Res.* 233, 545–553. doi:10.1016/j.bbr.2012.05.047.

Aivaz, A. N., and Ruckstuhl, K. E. (2011). Costs of behavioral synchrony as a potential driver behind size-assorted grouping. *Behav. Ecol.* 22, 1353–1363. doi:10.1093/beheco/arr141.

Arganda, S., Perez-Escudero, A., and de Polavieja, G. G. (2012). A common rule for decision making in animal collectives across species. *Proc. Natl. Acad. Sci.* 109, 20508–20513. doi:10.1073/pnas.1210664109.

Arnott, G., and Elwood, R. W. (2009). Assessment of fighting ability in animal contests. *Anim. Behav.* 77, 991–1004. doi:10.1016/j.anbehav.2009.02.010.

Balzarini, V., Taborsky, M., Villa, F., and Frommen, J. G. (2017). Computer animations of color markings reveal the function of visual threat signals in *Neolamprologus pulcher*. *Curr. Zool.* 63, 45–54. doi:10.1093/cz/zow086.

Bartolini, T., Mwaffo, V., Showler, A., Macrì, S., Butail, S., and Porfiri, M. (2016). Zebrafish response to 3D printed shoals of conspecifics: The effect of body size. *Bioinspiration and Biomimetics* 11. doi:10.1088/1748-3190/11/2/026003.

Bianco, I. H., Kampff, A. R., and Engert, F. (2011). Prey Capture Behavior Evoked by Simple Visual Stimuli in Larval Zebrafish. *Front. Syst. Neurosci.* 5, 1–13. doi:10.3389/fnsys.2011.00101.

Bierbach, D., Landgraf, T., Romanczuk, P., Lukas, J., Nguyen, H., Wolf, M., et al. (2018). Using a robotic fish to investigate individual differences in social responsiveness in the guppy. *R. Soc. Open Sci.* 5, 181026. doi:10.1098/rsos.181026.

Bishop, B. H., Spence-Chorman, N., and Gahtan, E. (2016). Three-dimensional motion tracking reveals a diving component to visual and auditory escape swims in zebrafish larvae. *J. Exp. Biol.* 219, 3981–3987. doi:10.1242/jeb.147124.

Bone, Q., and Moore, R. (2008). "Sensory Systems, and Communication," in *Biology of Fishes* (New York: Taylor & Francis), 289–346.

Brockerhoff, S. E., Hurley, J. B., Niemi, G. A., and Dowling, J. E. (1997). A new form of inherited red-blindness identified in zebrafish. *J. Neurosci.* 17, 4236–42. Available at: http://www.ncbi.nlm.nih.gov/pubmed/9151740.

Butail, S., Bartolini, T., and Porfiri, M. (2013). Collective response of zebrafish shoals to a free-swimming robotic fish. *PLoS One* 8, e76123. doi:10.1371/journal.pone.0076123.

Butler, S. R., and Fernandez-Juricic, E. (2014). European starlings recognize the location of robotic conspecific attention. *Biol. Lett.* 10, 20140665–20140665. doi:10.1098/rsbl.2014.0665.

Caballero, J., Mazo, C., Rodriguez-Pinto, I., and Theobald, J. C. (2015). A visual horizon affects steering responses during flight in fruit flies. *J. Exp. Biol.* 218, 2942–50. doi:10.1242/jeb.119313.

Chamberlain, A. C., and Ioannou, C. C. (2019). Turbidity increases risk perception but constrains collective behaviour during foraging by fish shoals. *Anim. Behav.* 156, 129–138. doi:10.1016/j.anbehav.2019.08.012.

Chen, C., Bockisch, C. J., Bertolini, G., Olasagasti, I., Neuhauss, S. C. F., Weber, K. P., et al. (2014). Velocity storage mechanism in zebrafish larvae. *J. Physiol.* 592, 203–214. doi:10.1113/jphysiol.2013.258640.

Chouinard-Thuly, L., Gierszewski, S., Rosenthal, G. G., Reader, S. M., Rieucau, G., Woo, K. L., et al. (2017). Technical and conceptual considerations for using animated stimuli in studies of animal behavior. *Curr. Zool.* 63, 5–19. doi:10.1093/cz/zow104.

Croft, D. P., Morrell, L. J., Wade, A. S., Piyapong, C., Ioannou, C. C., Dyer, J. R. G., et al. (2006). Predation risk as a driving force for sexual segregation: A cross population comparison. *Am. Nat.* 167, 867–878. doi:10.1086/504853.

Dawkins, M. S., and Woodington, A. (1997). Distance and the presentation of visual stimuli to birds. *Anim. Behav.* 54, 1019–1025. doi:10.1006/anbe.1997.0519.

Delcourt, J., and Poncin, P. (2012). Shoals and schools: Back to the heuristic definitions and quantitative references. *Rev. Fish Biol. Fish.* 22, 595–619. doi:10.1007/s11160-012-9260-z.

Douglas, R. H. (1996). Goldfish use the visual angle of a familiar landmark to locate a foodsource. *J. Fish Biol.* 49, 532–536. doi:10.1006/jfbi.1996.0179.

Douglas, R. H., Eva, J., and Guttridge, N. (1988). Size constancy in goldfish (*Carassius auratus*). *Behav. Brain Res.* 30, 37–42. doi:10.1016/0166-4328(88)90006-X.

Egan, R. J., Bergner, C. L., Hart, P. C., Cachat, J. M., Canavello, P. R., Elegante, M. F., et al. (2009). Understanding behavioral and physiological phenotypes of stress and anxiety in zebrafish. *Behav. Brain Res.* 205, 38–44. doi:10.1016/j.bbr.2009.06.022.

Fernandes, Y., Rampersad, M., Jia, J., and Gerlai, R. (2015). The effect of the number and size of animated conspecific images on shoaling responses of zebrafish. *Pharmacol. Biochem. Behav.* 139, 94–102. doi:10.1016/j.pbb.2015.01.011.

Fernández-Juricic, E., Beauchamp, G., and Bastain, B. (2007). Group-size and distance-to-neighbour effects on feeding and vigilance in brown-headed cowbirds. *Anim. Behav.* 73, 771–778. doi:10.1016/j.anbehav.2006.09.014.

Fernández-Juricic, E., Beauchamp, G., Treminio, R., and Hoover, M. (2011). Making heads turn: Association between head movements during vigilance and perceived predation risk in brown-headed cowbird flocks. *Anim. Behav.* 82, 573–577. doi:10.1016/j.anbehav.2011.06.014.

Fernández-Juricic, E., and Kacelnik, A. (2004). Information transfer and gain in flocks: The effects of quality and quantity of social information at different neighbour distances. *Behav. Ecol. Sociobiol.* 55, 502–511. doi:10.1007/s00265-003-0698-9.

Fernández-Juricic, E., and Kowalski, V. (2011). Where does a flock end from an information perspective? A comparative experiment with live and robotic birds. *Behav. Ecol.* 22, 1304–1311. doi:10.1093/beheco/arr132.

Fernández-Juricic, E., Siller, S., and Kacelnik, A. (2004). Flock density, social foraging, and scanning: an experiment with starlings. *Behav. Ecol.* 15, 371–379. doi:10.1093/beheco/arh017.

Frech, B., Vogtsberger, M., and Neumeyer, C. (2012). Visual discrimination of objects differing in spatial depth by goldfish. *J. Comp. Physiol. A Neuroethol. Sensory, Neural, Behav. Physiol.* 198, 53–60. doi:10.1007/s00359-011-0685-y.

Gerlai, R. (2017). Animated images in the analysis of zebrafish behavior. *Curr. Zool.* 63, 35–44. doi:10.1093/cz/zow077.

Gerlai, R., Fernandes, Y., and Pereira, T. (2009). Zebrafish (*Danio rerio*) responds to the animated image of a predator: Towards the development of an automated aversive task. *Behav. Brain Res.* 201, 318–324. doi:10.1016/j.bbr.2009.03.003.

Guthrie, D. M., and Muntz, W. R. A. (1993). "Role of vision in fish behaviour," in *Behaviour of Teleost Fishes*, ed. T. J. Pitcher (London: Chapman & Hall), 89–128.

Herbert-Read, J. E. (2016). Understanding how animal groups achieve coordinated movement. *J. Exp. Biol.* 219, 2971–2983. doi:https://doi.org/10.1242/jeb.129411.

Hoare, D. J., Krause, J., Peuhkuri, N., and Godin, J. G. (2000). Body size and shoaling in fish. *J. Fish Biol.* 57, 1351–1366. doi:10.1006/jfbi.2000.1446.

Howard, I. P. (2012). *Perceiving in Depth: (Vol. 3) Other Mechanisms of Depth Perception*. New York, NY: Oxford University Press doi:10.1093/acprof:oso/9780199764167.001.0001.

Ingley, S. J., Rahmani Asl, M., Wu, C., Cui, R., Gadelhak, M., Li, W., et al. (2015). anyFish 2.0: An open-source software platform to generate and share animated fish models to study behavior. *SoftwareX* 3–4, 13–21. doi:10.1016/j.softx.2015.10.001.

Kalueff, A. V, Gebhardt, M., Stewart, A. M., Cachat, J. M., Brimmer, M., Chawla, J. S., et al. (2013). Towards a comprehensive catalog of zebrafish behavior 1.0 and beyond. *Zebrafish* 10, 70–86. doi:10.1089/zeb.2012.0861.

Kim, C., Ruberto, T., Phamduy, P., and Porfiri, M. (2018). Closed-loop control of zebrafish behaviour in three dimensions using a robotic stimulus. *Sci. Rep.* 8, 1–15. doi:10.1038/s41598-017-19083-2.

Kimbell, H. S., and Morrell, L. J. (2015). Turbidity influences individual and group level responses to predation in guppies, *Poecilia reticulata*. *Anim. Behav.* 103, 179–185. doi:10.1016/j.anbehav.2015.02.027.

Krause, J., and Ruxton, G. D. (2002). *Living in groups*. Oxford: Oxford University Press.

Landgraf, T., Bierbach, D., Nguyen, H., Muggelberg, N., Romanczuk, P., and Krause, J. (2016). RoboFish: Increased acceptance of interactive robotic fish with realistic eyes and natural motion patterns by live Trinidadian guppies. *Bioinspiration and Biomimetics* 11. doi:10.1088/1748-3190/11/1/015001.

Larsch, J., and Baier, H. (2018). Biological Motion as an Innate Perceptual Mechanism Driving Social Affiliation. *Curr. Biol.* 28, 3523-3532.e4. doi:10.1016/j.cub.2018.09.014.

Lavergne, F. A., Wendehenne, H., Bäuerle, T., and Bechinger, C. (2019). Group formation and cohesion of active particles with visual perception – dependent motility. *Science (80).* 364, 70–74. doi:https://doi.org/10.1126/science.aau5347.

Layne, J., Land, M., and Zeil, J. (1997). Fiddler crabs use the visual horizon to distinguish predators from conspecifics: A review of the evidence. *J. Mar. Biol. Assoc. United Kingdom* 77, 43–54. doi:10.1017/S0025315400033774.

Lemasson, B., Tanner, C., Woodley, C., Threadgill, T., Qarqish, S., and Smith, D. (2018). Motion cues tune social influence in shoaling fish. *Sci. Rep.* 8, 1–10. doi:10.1038/s41598-018-27807-1.

Li, C. Y., Jones, R., and Earley, R. L. (2018). Contest decisions are governed by own size and opponent size category in mangrove rivulus fish, *Kryptolebias marmoratus*. *Anim. Behav.* 146, 97–103. doi:10.1016/j.anbehav.2018.09.020.

Lythgoe, J. N. (1979). *The Ecology of Vision*. Oxford: Clarendon Press.

Macrì, S., Neri, D., Ru, T., Mwaffo, V., and Butail, S. (2017). Three-dimensional scoring of zebrafish behavior unveils biological phenomena hidden by two-dimensional analyses. *Sci. Rep.* 7, 1–10. doi:10.1038/s41598-017-01990-z.

Miklosi, A., and Andrew, R. J. (2006). The Zebrafish as a Model for Behavioral Studies. *Zebrafish* 3, 227–234.

Miller, N., and Gerlai, R. (2012). From Schooling to Shoaling: Patterns of Collective Motion in Zebrafish (*Danio rerio*). *PLoS One* 7, e48865. doi:10.1371/journal.pone.0048865.

Moser, E. B. (2004). Repeated Measures Modeling With PROC MIXED. *Stat. Data Anal.* SUG 29, 1–19.

Nakagawa, S. (2004). A farewell to Bonferroni: the problems of low statistical power and publication bias. *Behav. Ecol.* 15, 1044–1045. doi:10.1093/beheco/arh107.

Nakayama, S., Ojanguren, A., and Fuiman, L. (2009). To fight, or not to fight: determinants and consequences of social behaviour in young red drum (*Sciaenops ocellatus*). *Behaviour* 146, 815–830. doi:10.1163/156853909X446226.

Nityananda, V., and Read, J. C. A. (2017). Stereopsis in animals: evolution, function and mechanisms. *J. Exp. Biol.* 220, 2502–2512. doi:10.1242/jeb.143883.

Oliveira, T. A., Idalencio, R., Kalichak, F., dos Santos Rosa, J. G., Koakoski, G., de Abreu, M. S., et al. (2017). Stress responses to conspecific visual cues of predation risk in zebrafish. *PeerJ* 5, e3739. doi:10.7717/peerj.3739.

Patterson, B. W., Abraham, A. O., Maciver, M. A., and Mclean, D. L. (2013). Visually guided gradation of prey capture movements in larval zebrafish. *J. Exp. Biol.* 216, 3071–3083. doi:10.1242/jeb.087742.

Pays, O., Beauchamp, G., Carter, A. J., and Goldizen, A. W. (2013). Foraging in groups allows collective predator detection in a mammal species without alarm calls. *Behav. Ecol.* 24, 1229–1236. doi:10.1093/beheco/art057.

Pays, O., Dubot, A. L., Jarman, P. J., Loisel, P., and Goldizen, A. W. (2009). Vigilance and its complex synchrony in the red-necked pademelon, Thylogale thetis. *Behav. Ecol.* 20, 22–29. doi:10.1093/beheco/arn110.

Pettigrew, J. D., Dreher, B., Hopkins, C. S., McCall, M. J., and Brown, M. (1988). Peak density of ganglion cells in the retinae of michiropteran bats: implications for visual acuity. *Brain. Behav. Evol.* 32, 39–56.

Peuhkuri, N. (1998). Shoal composition, body size and foraging in sticklebacks. *Behav. Ecol. Sociobiol.* 43, 333–337. doi:10.1007/s002650050499.

Pham, M., Raymond, J., Hester, J., Kyzar, E., Gaikwad, S., and Bruce, I. (2012). "Assessing Social Behavior Phenotypes in Adult Zebrafish: Shoaling, Social Preference, and Mirror Biting Tests," in *Zebrafish Protocols for Neurobehavioral Research*, eds. K. A. and S. A. (Humana Press, Totowa, NJ), 231–246.

Pita, D., Collignon, B., Halloy, J., and Fernández-Juricic, E. (2016). Collective behaviour in vertebrates: a sensory perspective. *R. Soc. Open Sci.* 3, 160377. doi:10.1098/rsos.160377.

Pita, D., and Fernandez-Juricic, E. (2019). The visual social environment affects non-additively neighbor spacing and interaction time in zebrafish. *bioRxiv*, 1–35. doi:10.1101/511972.

Pita, D., Moore, B. A., Tyrrell, L. P., and Fernández-Juricic, E. (2015). Vision in two cyprinid fish: implications for collective behavior. *PeerJ* 3, e1113. doi:10.7717/peerj.1113.

Pritchard, V., Lawrence, J., Butlin, R. K., and Krause, J. (2001). Shoal choice in zebrafish, *Danio rerio*: the influence of shoal size and activity. *Anim. Behav.* 62, 1085–1088. doi:10.1006/anbe.2001.1858.

Proctor, C. J., Broom, M., and Ruxton, G. D. (2001). Modelling antipredator vigilance and flight response in group foragers when warning signals are ambiguous. *J. Theor. Biol.* 211, 409–417. doi:10.1006/jtbi.2001.2353.

Proctor, C. J., Broom, M., and Ruxton, G. D. (2003). A communication-based spatial model of antipredator vigilance. *J. Theor. Biol.* 220, 123–137. doi:10.1006/jtbi.2003.3159.

Qin, M., Wong, A., Seguin, D., and Gerlai, R. (2014). Induction of Social Behavior in Zebrafish: Live Versus Computer Animated Fish as Stimuli. *Zebrafish* 11, 185–197. doi:10.1089/zeb.2013.0969.

Rodgers, G. M., Downing, B., and Morrell, L. J. (2015). Prey body size mediates the predation risk associated with being "odd." *Behav. Ecol.* 26, 242–246. doi:10.1093/beheco/aru185.

Rosenthal, G. G. (2002). Design considerations and techniques for constructing video stimuli. *Acta Ethol.* 3, 49–54. doi:10.1007/s102110000024.

Rosenthal, S. B., Twomey, C. R., Hartnett, A. T., Wu, H. S., and Couzin, I. D. (2015). Revealing the hidden networks of interaction in mobile animal groups allows prediction of complex behavioral contagion. *Proc. Natl. Acad. Sci.* 112, 4690–4695. doi:10.1073/pnas.1420068112.

Rountree, R. A., and Sedberry, G. R. (2009). A theoretical model of shoaling behavior based on a consideration of patterns of overlap among the visual fields of individual members. *Acta Ethol.* 12, 61–70. doi:10.1007/s10211-009-0057-6.

Ruberto, T., Polverino, G., and Porfiri, M. (2017). How different is a 3d-printed replica from a conspecific in the eyes of a zebrafish? *J. Exp. Anal. Behav.* 107, 279–293. doi:10.1002/jeab.247.

Ruhl, N., and McRobert, S. P. (2005). The effect of sex and shoal size on shoaling behaviour in Danio rerio. *J. Fish Biol.* 67, 1318–1326. doi:10.1111/j.0022-1112.2005.00826.x.

Saverino, C., and Gerlai, R. (2008). The social zebrafish: Behavioral responses to conspecific, heterospecific, and computer animated fish. *Behav. Brain Res.* 191, 77–87. doi:10.1016/j.bbr.2008.03.013.

Schellinck, J., and White, T. (2011). A review of attraction and repulsion models of aggregation: Methods, findings and a discussion of model validation. *Ecol. Modell.* 222, 1897–1911. doi:10.1016/j.ecolmodel.2011.03.013.

Sperandio, I., and Chouinard, P. A. (2015). The Mechanisms of Size Constancy. *Multisens. Res.* 28, 253–283. doi:10.1163/22134808-00002483.

Stowers, J. R., Hofbauer, M., Bastien, R., Griessner, J., Higgins, P., Farooqui, S., et al. (2017). Virtual reality for freely moving animals. *Nat. Methods* 14, 995–1002. doi:10.1038/nmeth.4399.

Strandburg-Peshkin, A., Twomey, C. R., Bode, N. W. F., Kao, A. B., Katz, Y., Ioannou, C. C., et al. (2013). Visual sensory networks and effective information transfer in animal groups. *Curr. Biol.* 23, R709–R711. doi:10.1016/j.cub.2013.07.059.

Sumpter, D. J. T. (2010). *Collective Animal Behavior*. Princeton, N.J.: Princeton University Press.

West, B. T., Welch, K. B., Galecki, A. T., and Gillespie, B. W. (2015). *Linear mixed models: a practical guide using statistical software*. Boca Raton : CRC Press, Taylor & Francis Group.

Woo, K. L., and Rieucau, G. (2008). Considerations in video playback design: Using optic flow analysis to examine motion characteristics of live and computer-generated animation sequences. *Behav. Processes* 78, 455–463. doi:10.1016/j.beproc.2008.03.003.

Zeil, J. (2000). Depth cues, behavioural context, and natural illumination: some potential limitations of video playback techniques. *Acta Ethol.* 3, 39–48. doi:10.1007/s102110000021.

Zimmermann, M. J. Y., Nevala, N. E., Yoshimatsu, T., Osorio, D., Nilsson, D.-E., Berens, P., et al. (2018). Zebrafish Differentially Process Color across Visual Space to Match Natural Scenes. *Curr. Biol.* 28, 2018-2032.e5. doi:10.1016/j.cub.2018.04.075.

CHAPTER 4. THE ROLE OF VISUAL CONTRAST ON SOCIAL BEHAVIOR

4.1 Abstract

Effective communication relies on the receiver being able to perceive information transmitted by the signaler. In many visually-oriented aquatic organisms, visual contrast is an important component of social communication, allowing individuals to acquire information regarding perceived differences in luminance (i.e., achromatic contrast) or color (i.e., chromatic contrast). In this study we explored the role of visual contrast on zebrafish social behavior using a playback experiment to manipulate the perception of conspecific information. We found that chromatic and achromatic contrast interact simultaneously to affect zebrafish behavior, resulting in changes to separation distance and interaction time. Achromatic contrast appears to enhance the perception of conspecific cues, but only when the chromatic dimension is consistent with reality. Additionally, the simultaneous reduction in chromatic and achromatic contrast appears to place limitations on cue perception with distance. Overall, the effects of chromatic and achromatic contrast interact in complex ways, which could reflect evolutionary adaptations to facilitate social communication in their environment.

4.2 Introduction

Physiological color change is an adaptation used by many species in response to environmental stimuli (Nilsson Sköld et al., 2013). Physiological color change is under neuroendocrine control and results in the local movement of pigment organelles within the skin to induce color change (Nilsson Sköld et al., 2013; Duarte et al., 2017). In many situations, physiological color changes can be tuned to the situation. For some animals, this may include reducing predation risk (Stuart-Fox et al., 2008; Stevens et al., 2014), increasing mating success (Kodric-brown, 1998; Rehberg-Besler et al., 2015; Hiermes et al., 2016) or deescalating agonistic interactions (O'Connor et al., 1999; Höglund et al., 2000; Ligon, 2014). The dynamic feature of physiological color change also serves as a particularly honest and informative source of social information (Ligon and McGraw, 2016; Heathcote et al., 2018). Physiological color change has the potential to be conspicuous or

cryptic depending on several factors such as, the characteristics of the visual background, environmental lighting and visual perception of the receiver (Marshall and Johnsen, 2011; Nilsson Sköld et al., 2013). In a social context, natural selection is likely to favor the evolution of conspicuous signals (Endler, 1992). However, aquatic environments can vary dramatically in their spectral properties, which can limit visual signal detectability. For example, factors such as water depth, turbidity, and dissolved organic matter all have the potential to influence the perception of social information by altering conspecific visual contrast (Loew and Zhang, 2006; Wilkins et al., 2016).

Visual contrast, the ability to distinguish an object from the visual background can be further classified in terms of chromatic and achromatic contrast. Chromatic contrast represents variation in wavelength (i.e. spectral color) (Kelber et al., 2003) and is thought to be more reliable in identifying objects under variable light conditions. This is because the chromatic composition of illumination is relatively stable across fluctuating light environments (Osorio et al., 1999; Marshall, 2000). On the other hand, achromatic contrast represents signal intensity (i.e. brightness), is thought to improve pattern discrimination, and is particularly reliable for the long-distance detection of small stimuli (Osorio et al., 1999; Schaefer et al., 2006).

In this study, we evaluated the constraints that visual contrast might impose on social behavior. To accomplish this, we utilized zebrafish (*Danio rerio*), a social species of freshwater fish that is capable of physiological color change (Singh and Nüsslein-Volhard, 2015) and is found across a wide range of aquatic habitats (Engeszer et al., 2007; Sundin et al., 2019). In a playback experiment, we exposed zebrafish to animated conspecifics in a virtual environment. Specifically, we sought to evaluate the effects of visual contrast through: 1) manipulation of the aquatic environment to alter the visual contrast of the conspecific against the virtual background and 2) manipulation of the spectral properties of the conspecific to alter the visual contrast of the stripes, a potential social cue.

4.2.1 Manipulating spectral properties of the aquatic environment

Zebrafish can be found across a wide range of aquatic environments under variable illumination (Engeszer et al., 2007; Suriyampola et al., 2015; Sundin et al., 2019). Chromatic information is likely to be more reliable during social interactions due to its stability across changing light environments (Osorio et al., 1999; Marshall, 2000). Evidence supports this as zebrafish are known

to display transient alterations to their chromatic coloration (Hutter et al., 2012). Specifically, during the morning hours when spawning occurs, both sexes develop a prominent yellow hue (Hutter et al., 2012). Additionally, male zebrafish that are more intensely colored tend to engage in more courtship behaviors compared to less vibrant yellow males (Hutter et al., 2012). In this situation, a higher chromatic signal may convey the signaler's mating receptivity. Xanthophores, cells made up of light absorbing carotenoid pigment, are largely responsible for the perceptible yellow hue displayed by zebrafish during times of spawning (Fujii, 2000; Price et al., 2008). In addition to skin pigmentation, carotenoids also play a role in immune function as an antioxidant (Maoka, 2020). As a result, there is thought to be a tradeoff in carotenoid allocation such that diseased individuals (e.g., high parasite load) have fewer carotenoid reserves for skin pigmentation, resulting in reduced chromatic signal production (Houde and Torio, 1992; Lozano et al., 1994; Clotfelter et al., 2007). Therefore, in addition to signaling mating receptivity, a higher chromatic signal may serve as an honest indicator of individual health status. As a result, a higher chromatic signal may provide increased motivation for social interaction. Experimental evidence seems to support this as zebrafish prefer to interact with yellow animated conspecifics over the typical wildtype phenotype (Saverino and Gerlai, 2008). It is likely that the higher the chromatic contrast of the body, the more attractive the zebrafish will appear to conspecifics, increasing the motivation for social interaction. Therefore, it is predicted that manipulation of the animated background to alter the chromatic contrast of the conspecific body will have a greater effect on the behavioral response compared to changes in achromatic contrast. Specifically, as the chromatic contrast of the body increases, zebrafish will decrease their separation distance and increase their interaction duration with the animated conspecific because of increased attraction.

4.2.2 Manipulating spectral properties of the conspecific

The wildtype zebrafish phenotype is the result of a combination of different cell types under neuroendocrine control (Oshima and Kasai, 2002; Singh and Nüsslein-Volhard, 2015). For instance, the dark stripes along the lateral aspect of the body contain a large proportion of melanophores which respond to neural and hormonal cues. Melanophores are composed of pigment-containing melanosomes that either concentrate at the center of the melanophore (i.e., low intensity signal, decreased pigmentation) or disperse within the cytoplasm (i.e., high intensity signal, increased pigmentation). Catecholamine neurotransmitters (e.g. norepinephrine) released

during times of acute stress, can induce changes in stripe luminance by stimulating melanosome concentration (Singh and Nüsslein-Volhard, 2015). Due to these changes in pigment dispersal, melanophores are likely to have greater variability along the achromatic visual dimension. A higher achromatic signal may improve the perception of the horizontal stripes during social interactions, as achromatic vision is thought to facilitate the discrimination of spatial patterns, especially at a distance (Osorio et al., 1999). Recent evidence seems to support this theory as many social species are thought to utilize contrasting achromatic stripes for communication (Negro et al., 2020). Specifically, it is thought that achromatic striping patterns are more efficient in conveying changes in conspecific movement compared to monochromatic phenotypes (Negro et al., 2020). In fact, zebrafish prefer to interact with conspecifics and heterospecifics displaying more salient horizontal stripes (Engeszer et al., 2008). Additionally, zebrafish are able to maintain longer separation distances when conspecific stripes are highly resolvable. (Pita and Fernandez-Juricic, 2019). Stripes with higher achromatic contrast may improve the acquisition of social information, especially at a distance. Therefore, it is predicted that changes in the achromatic contrast of the stripes will have a greater effect on the behavioral response compared to changes in chromatic contrast. Specifically, as the achromatic contrast of the stripes increases, zebrafish will be able to maintain longer separation distances and reduce their interaction duration during social interactions.

4.3 Methods

11 adult wildtype zebrafish (5 males and 6 females) were used for the experiment. The zebrafish were obtained from a local vendor (Lafayette, Indiana, USA). For the duration of the testing period, the zebrafish were housed in individual 2.5-gallon aquaria (51.4 cm L x 26.7 cm W x 32.1 cm H) with aeration supplied via air stones. The photoperiod was maintained on a 16-hour light: 8-hour dark cycle and the water temperature was set between 22-26 °C. Water quality assessments were performed daily (pH, temperature) and weekly (ammonia, nitrates, nitrites, chlorine) to ensure acceptable levels. The zebrafish were fed daily with commercial fish flakes (Tetramin ® Tropical Flakes). The Purdue Institutional Animal Care and Use Committee (1207000675) approved all experimental procedures.

The zebrafish were exposed to 2 experiments, represented by a total of 18 treatments with one treatment exposure per day. The first experiment involved manipulation of the visual contrast

of the animated background, represented by 2 independent categorical variables: chromatic contrast and achromatic contrast, each with 3 levels (low, medium, and high). The second experiment involved manipulating the visual contrast of the conspecific stripes. This experiment was represented by 2 independent categorical variables: chromatic contrast and achromatic contrast, each with 3 levels (low, medium, and high). One individual died during the testing period and was removed from the analysis. The order of treatment exposure as well as the testing order was randomized each day. The testing period occurred between the hours of 7 AM and 12 PM.

Treatment exposure occurred within the zebrafish's individual 2.5-gallon tank. The testing environment consisted of the computer monitor and tank stand on top of a small table. For each testing period, the tank was placed against the screen of a computer monitor (Acer LCD monitor, model v176L) and aligned with pre-defined markers to ensure consistent position across treatments. The monitor had an appropriate resolution (1280 x 1024 pixels) and refresh rate (75 hertz) for simulating smooth continuous movement based on known critical flicker fusion frequencies for fish (Lythgoe, 1979). An adjustable overhead light source (Deluxe Sunlight 1300 lm Floor Lamp, model #72-0890) provided even illumination of the testing environment. White curtains surrounded the testing environment while the short sides and bottom of each individual tank were covered with white opaque tape to reduce visual distractions.

Prior to treatment exposure, the zebrafish were habituated to the testing environment for 10 minutes. Following habituation, the treatment video was presented, represented by a homogenous animated background, displayed for 1 minute followed by presentation of the animated conspecific for 1 minute. The animated conspecific appeared to swim back and forth, along the horizontal plane, rotating 180 degrees when it reached the edge of the screen to change direction. The experimental zebrafish was recorded with two video cameras (JVC Everio GZ-MG330-HU camcorder) orthogonal to each another in order to provide top and side views. A portable DVR (Night Owl, H264-4 channel DVR) with multiplexer was used to temporally synchronize the top and side views into one video for behavioral analysis. Behaviors were only coded during the 1-minute period when the animated conspecific was being displayed.

4.3.1 Perceptual modeling

We estimated the saliency of zebrafish social cues (i.e. body and stripes) from the perspective of the zebrafish visual system. To accomplish this, we utilized a perceptual model that estimates the chromatic and achromatic distance of an object to the visual background (Vorobyev and Osorio, 1998). The object and background are represented in visual space characterized in units of just noticeable difference (JNDs). An object with a JND less than 1 is considered indistinguishable from the visual background while a JND above 3 is considered easily distinguishable (Siddiqi et al., 2004). Evidence in support of this model has been justified through behavioral experiments evaluating the visual perception of a variety of species (Champ et al., 2016; Fleishman et al., 2016; Escobar-Camacho et al., 2019).

We utilized the receptor-noise limited model described by (Vorobyev and Osorio, 1998) to model chromatic and achromatic contrast perception using the R package: Pavo 1.0 (Maia et al., 2013). This model incorporates several physiological parameters to estimate contrast perception specific to the species of interest by determining the degree to which the photoreceptors are stimulated by emitted colors. Specifically, the model utilizes: 1) the reflectance of the object of interest 2) the reflection of the background of interest 3) the ambient environmental light and 4) species-specific visual parameters: relative cone photoreceptor densities and wavelength sensitivities. In this experiment, we utilized parameters specific to the tetrachromatic zebrafish visual system. We estimated chromatic and achromatic contrast using a weber fraction of 0.1 for receptor noise and the sensmodel(), vismodel() and coldist() functions in Pavo 1.0 (Maia et al., 2013). Photoreceptor sensitivity curves were constructed using published adult zebrafish lambda max values along with parameters for calculating visual pigment templates (Govardovskii et al., 2000). We also utilized the relative photoreceptor densities of adult zebrafish (Allison et al., 2010). To estimate achromatic contrast perception, we followed previous methods utilized for fish which sum the MWS and LWS cones (Chiao, Wickiser, Allen, Genter, & Hanlon, 2009; Newport et al., 2017; Siebeck, Wallis, Litherland, Ganeshina, & Vorobyev, 2014). Due to size constrains of the zebrafish eye, we were unable to accurately measure the light transmission of the ocular media. Instead we used the published ocular transmission spectra from another cyprinid, the goldfish (*Carassius auratus*) (Hawryshyn et al., 1985). Irradiance from the light casted from the computer screen and an overhead lamp were measured using an Ocean Optics JAZ spectrometer (Ocean

Optics Inc. Dunedin, Florida, USA) and incorporated into the irradiance calculations for ambient light.

We exposed zebrafish to 9 different animated colors to evaluate the study predictions. Animated colors were generated using the RGB additive color model which incorporates proportions of red, green and blue to represent color on an animated device. The reflectance of each animated color was measured with a StellarNet spectrometer (StellarNet Inc. Tampa, Florida, USA) by holding the reflectance probe 90° to the surface of the computer monitor. Reflectance measurements were recorded from 300-700 nm in 1 nm increments and reflectance measurements of a white and dark standard were used to calculate the percent reflectance (Appendix D, Figure D1). The just noticeable differences (JNDs) were estimated, and specific RGB colors were selected to produce a set of 9 chromatic and achromatic treatments represented in categories of "low", "medium" and "high" contrast. The selected colors varied equidistantly in their perceptual saliency (see Appendix D, Figure D2). The 9 RGB animated colors were modeled separately in a background and stripe manipulation experiment. In total 18 treatment videos were generated.

4.3.2 Animation generation

Animated videos were generated using the program anyfish (http://swordtail.tamu.edu/anyfish), an open-source program that allows for the generation of realistic animated fish for video playback experiments (Ingley et al., 2015). Zebrafish are receptive to animated stimuli and appear to display an equivalent shoaling response when presented with either animated or live conspecifics (Woo and Rieucau, 2011; Qin et al., 2014; Gerlai, 2017). Additionally, using an animated conspecific allows repeatable aspects of chromatic and achromatic contrast to be adjusted easily with high precision. Zebrafish are tetrachromatic with visual sensitivity ranging into the ultraviolet spectrum. Our animations did not incorporate an ultraviolet component. Although reflectance measurements conducted on wildtype zebrafish body regions revealed that the phenotypic patterning does not reflect significant ultraviolet wavelengths (Appendix D, Figure D3). Animation design followed similar procedures described in (Pita and Fernandez-Juricic, 2019) where an animated conspecific was modeled from an image of a female zebrafish. A female model was utilized to reduce interaction biases, as females are preferred by both sexes while male zebrafish display a reduced preference for interacting with other males (Ruhl and McRobert, 2005). Animation design began with generating a morphometric file to model the zebrafish body shape in 3D. Then, a texture file

of the zebrafish phenotype was transformed to fit the 3D shape of the zebrafish model. Lastly, the motion of the animated zebrafish was defined by manually adjusting the position of the model within the virtual environment to simulate a of 5 cm per second swimming speed. Final rendering of each frame of the animation was assembled using adobe premiere pro. To create each treatment video, either the background or zebrafish image was modified in adobe illustrator to reflect each of the 9 RGB animated color treatments.

4.3.3 Behavior coding

Zebrafish behaviors were analyzed using the program idTracker (http://www.idtracker.es/). Videos were reviewed each frame (30 frames per second) for defined interaction behaviors. We assume that any movement towards the computer monitor is indicative of some level of attraction, either to obtain more information or to engage in further interaction with the conspecific (Kalueff et al., 2013). Therefore, the onset of an interaction represented any forward movement of the zebrafish towards the computer monitor when the animated conspecific was displayed (Pita and Fernandez-Juricic, 2019). Additionally, we assume that when an individual updates its information regarding the conspecific, it makes a movement decision by adjusting its turning angle (Kalueff et al., 2013). Therefore, the end of the interaction was defined when the zebrafish altered its directional heading over 45° from its original angle of approach. This method of defining interactions enhanced our information gathering ability as it allowed us to isolate more nuanced behaviors with higher precision compared to other methods which broadly assess the amount of time individuals spend in certain zones of the testing tank, which are often set arbitrarily and not based on perceptual constraints (Engeszer et al., 2004; Rosenthal and Ryan, 2005; Abril-De-Abreu et al., 2015; Bartolini et al., 2016). For each interaction, the separation distance and interaction duration were recorded. The separation distance represented the distance between the eye of the zebrafish and the center of the virtual conspecific, measured with ImageJ (https://imagej.net/Fiji) at the last frame of the isolated interaction. The interaction duration represented the difference in frames between the beginning and end of the interaction period. Videos were coded blindly regarding treatment identity.

4.3.4 Statistical analysis

We analyzed the data using general linear mixed models in R (v. 4.0.2) with the packages lme4 and afex. For both the background and conspecific manipulation experiment, we evaluated the dependent variables: separation distance and interaction duration relative to within-subject factors: chromatic and achromatic contrast. Both within-subject factors were categorical with 3 levels: low, medium and high. In addition to the main effects, we also analyzed the two-way interaction between chromatic and achromatic contrast. Subject ID was defined as a random factor. We utilized the uncorrelated random intercepts and random slopes model to fit the random structure of the data. We also included sex as an independent fixed factor however, it was not significant, so we removed it to increase the power of the tests. The data were log transformed to satisfy model assumptions for normality of the residuals and homogeneity of variance. Please see Appendix D R code.

4.4 Results

4.4.1 Background contrast

There were no significant main effects of background chromatic or achromatic contrast on separation distance or interaction duration. However, there was an interaction between the chromatic and achromatic contrast of the conspecific against the virtual background regarding separation distance and interaction duration (Table 4.1). Zebrafish maintained shorter separation distances when interacting with conspecifics against backgrounds with medium chromatic contrast when the achromatic contrast was low (Figure 4.1). Zebrafish also spent more time interacting with conspecifics when they were displayed against backgrounds with medium chromatic contrast when the achromatic contrast was high (Figure 4.2).

4.4.2 Stripe contrast

There were no significant main effects of conspecific chromatic or achromatic contrast on separation distance or interaction duration. However, there was a significant interaction between the chromatic and achromatic contrast of the conspecific (i.e. contrast of the stripes against the body) regarding separation distance and interaction duration (Table 4.1). Zebrafish maintained

shorter separation distances when interacting with conspecifics that displayed stripes with low achromatic contrast as opposed to medium achromatic contrast when the chromatic contrast was low (Figure 4.3). There was also a significant interaction regarding interaction duration, but the pairwise comparisons were not significant.

4.5 Discussion

Our results illustrate the complex role of chromatic and achromatic information on social behavior. In partial support of our predictions, zebrafish were sensitive to contrast manipulation of the virtual environment and animated conspecific. However, contrary to our predictions, we found that chromatic and achromatic contrast interacted significantly to affect behavior. Additionally, the relationship regarding this interaction varied depending on the experiment. Specifically, in the background manipulation experiment, changes in achromatic contrast were detectable, but only at levels of medium chromatic contrast. On the other hand, in the conspecific manipulation experiment, changes in achromatic contrast were only detectable at levels of low chromatic contrast. These results, although complex may be explained by a several different relationships.

In the background manipulation experiment, both significant interactions occurred at levels of medium chromatic contrast. To interpret this effect, we further characterized the specific chromatic properties of each treatment level by estimating its spectral category (i.e., hue) in color space (Figure 4.4). We also estimated the hue of several body regions (i.e., dark stripes, light stripes, dorsal, medial and lateral areas) from recently euthanized zebrafish (Figure 4.4). By estimating and plotting the hue, we could isolate wavelength specific information regarding our treatments and compare them to reality. We thought this information was relevant due to experimental evidence suggesting zebrafish have potential biases for certain colors, which may also serve a biological significance (Avdesh et al., 2012; Oliveira et al., 2015). We found that there were appreciable differences in hue between treatments and between zebrafish body regions (Figure 4.4). It also appeared that the chromatic treatment levels (low, medium, high) represented different areas of spherical color space. Treatments with high chromatic contrast resulted in more short-wavelength stimulation while treatments with low chromatic contrast were closer to the achromatic center. On the other hand, levels of medium chromatic contrast seemed to cover a broader range in color space, overlapping areas represented by the high and low chromatic treatments. Lastly,

the zebrafish body regions appeared to represent areas of the sphere with greater long-wavelength and medium-wavelength stimulation, depending on the body region.

Low and medium chromatic treatments appear to more closely match reality due to their proximity in color space to real zebrafish body regions (Figure 4.4). This closer match to reality may explain why zebrafish were only responsive to contrast manipulation at levels of medium chromatic contrast. While a lack of an effect seen at levels of low chromatic contrast may be explained by an insufficient amount of chromatic stimulation necessary to make an informed social decision. For example, there is evidence that female zebrafish are unable to discriminate individuals on the basis of sex when the ambient lighting was altered to reduce the visual contrast of conspecifics (Hutter et al., 2011). On the other hand, zebrafish may avoid interacting with conspecifics below a certain level of chromatic contrast due to potential disease risks associated with individuals displaying low chromatic contrast (Houde and Torio, 1992).

We also offer interpretations for differences in behavior that depended on the level of achromatic contrast when the chromatic contrast was at a medium level. Specifically, zebrafish maintained longer separation distances when the achromatic contrast of the conspecific against the virtual background was high and decreased their interaction duration when the achromatic contrast was low. Increasing achromatic contrast improves signal detection with distance (Osorio et al., 1999; Schaefer et al., 2006), which explains why zebrafish may be able to maintain longer separation distances at higher levels of achromatic contrast. Moreover, maintaining longer separation distances in the group is advantageous for predator avoidance as the farther apart individuals are spaced, the faster the group can collectively detect and respond to approaching predators (Rountree and Sedberry, 2009). Alternatively, higher levels of achromatic contrast may signal aggression. For example, princess cichlids are known to increase the darkness (i.e., achromatic contrast) of their facial stripe in order to alert conspecifics of dominance and aggressive intent (Bachmann et al., 2017). Similarly, guppies displaying black irises engaged in more aggressive behaviors compared to guppies with silver irises (Heathcote et al., 2018).

At levels of medium chromatic contrast when achromatic contrast was low, zebrafish decreased the amount of time spent acquiring social information which contradicts our prediction that lowering achromatic contrast would reduce the intensity of the visual signal, promoting an increased interaction time to enhance the uptake of information. However, we found the opposite result with zebrafish spending less time interacting with conspecifics as the achromatic contrast

decreased. One explanation is that zebrafish are instead responding to the biological realism of social cues. For example, if we consider the location of the low achromatic treatment in color space regarding hue, we can see that it occupies an area closer to real zebrafish body regions (Figure 4.4). As a result of this closer match to reality, zebrafish may be able to assess and acquire social information more rapidly compared to treatments with less biological realism (i.e., medium and high achromatic treatments).

In the conspecific manipulation experiment, there was also an interaction between chromatic and achromatic contrast such that zebrafish decreased their separation distance when the achromatic contrast of the stripes were low compared to medium at levels of low chromatic contrast. Considering that the stripes make up a relatively small area of the body and therefore, a smaller portion of the retina, zebrafish may have to maintain closer separation distances to compensate for the reduction in visual contrast in combination with the reduction in spatial resolution of the stripes. This size-dependent relationship with visual contrast is known as contrast sensitivity and illustrates the idea that smaller objects become more difficult to detect at a distance compared to larger objects when the visual contrast is reduced (O'Carroll and Wiederman, 2014).

Zebrafish appear sensitive to changes in chromatic and achromatic contrast and display different behaviors depending on the region of the body that is subject to these contrast effects. Not surprisingly, the effects of chromatic and achromatic contrast interact in complex ways, which could reflect evolutionary adaptations to their environment as well as their capacity for physiological color change under different situations. In many visually-oriented aquatic organisms, the visual system is tuned to optimize the spectral characteristics of the environment (Endler, 1992). Ideally, clear environments with even illumination should facilitate a long visual range to observe conspecific information (Lythgoe, 1968, 1979). As a result, zebrafish should maintain longer separation distances, leading to lower density groups which may reduce resource competition and enhance predator detection (Krause and Ruxton, 2002; Rountree and Sedberry, 2009). However, zebrafish are found across a broad range of aquatic environments subject to dynamic changes in turbidity, depth, vegetative cover and anthropogenic disturbance, which can influence the propagation of visual social information (Engeszer et al., 2004; Suriyampola et al., 2015; Sundin et al., 2019; Shelton et al., 2020). For example, increased dissolved organic matter reduces light intensity, especially for shorter wavelengths and may result in individuals maintaining closer separation distances to perceive achromatic cues (i.e., striping pattern) (Davies-Colley and Vant,

1987; Kelley et al., 2012). As a result, zebrafish groups may become denser, which may provide individuals at the center of the group increased protection from predators at the cost of reduced oxygen availability (Domenici et al., 2013). Alternatively, zebrafish may utilize signals that optimize longer wavelengths to improve conspecific visibility at the consequence of increasing conspicuousness to visual predators (Kelley et al., 2012; Bressman et al., 2019). Similarly, environments with less vegetation can increase predation risk (Orrock et al., 2013), resulting in the formation of large group sizes to enhance antipredator effects, such as the dilution effect which increases as a function of group size (Krause and Ruxton, 2002). On the other hand, increased vegetation provides refuge from predators and shifts the aquatic light spectrum towards medium wavelengths (Lythgoe and Partridge, 1989; Endler, 1993). As a result of this relaxed predation pressure, group sizes may become smaller and zebrafish may be able to display more diversity in their chromatic signals (Bhat et al., 2015). Further research should aim to characterize the spectral characteristics of the zebrafish natural environment to identify some of the evolutionary pressures involved in the transmittance and perception of social signals.

4.6 Tables and Figures

Table 4.1 Effects of background and stripe contrast on the separation distance and interaction duration of the zebrafish with the animated conspecific. Significant effects marked in bold.

	F	df	P
Separation Distance			
Background Chromatic	0.107	2, 13	0.899
Background Achromatic	2.102	2, 12	0.164
Background Chromatic x Achromatic	11.045	4, 1607	**7.73×10^{-9}**
Stripe Chromatic	0.178	2, 10	0.839
Stripe Achromatic	1.329	2, 11	0.305
Stripe Chromatic x Achromatic	2.594	4, 1761	**0.0349**
Interaction Duration			
Background Chromatic	0.627	2, 12	0.551
Background Achromatic	0.230	2, 12	0.798
Background Chromatic x Achromatic	3.030	4, 1346	**0.017**
Stripe Chromatic	0.494	2, 11	0.624
Stripe Achromatic	0.064	2, 9	0.938
Stripe Chromatic x Achromatic	3.130	4, 1636	**0.041**
Log Separation Distance			
Background Chromatic	0.577	2, 13	0.576
Background Achromatic	2.113	2, 12	0.162
Background Chromatic x Achromatic	10.898	4, 1605	**1.07×10^{-8}**
Stripe Chromatic	0.200	2, 11	0.822
Stripe Achromatic	2.052	2, 10	0.179
Stripe Chromatic x Achromatic	2.437	4, 1724	**0.045**
Log Interaction Duration			
Background Chromatic	0.530	2, 12	0.601
Background Achromatic	0.461	2, 11	0.643
Background Chromatic x Achromatic	3.997	4, 1228	**0.003**
Stripe Chromatic	0.283	2, 11	0.759
Stripe Achromatic	0.109	2, 9	0.898
Stripe Chromatic x Achromatic	2.107	4, 1625	0.078

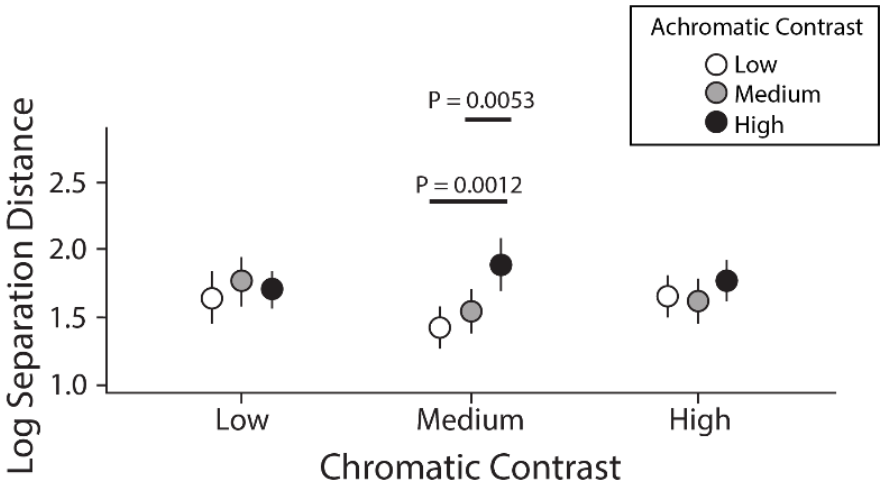

Figure 4.1 Separation distance (cm) between the zebrafish and animated conspecific in response to manipulation of the virtual background to alter chromatic and achromatic contrast of the conspecific. Results have been log transformed.

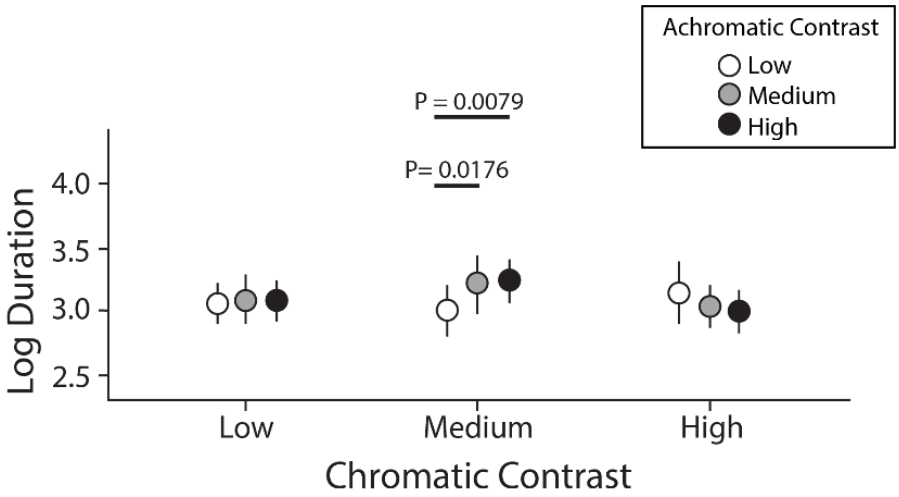

Figure 4.2 Duration (frames) of the interaction duration between the zebrafish and animated conspecific in response to manipulation of the virtual background to alter chromatic and achromatic contrast of the conspecific. Results have been log transformed.

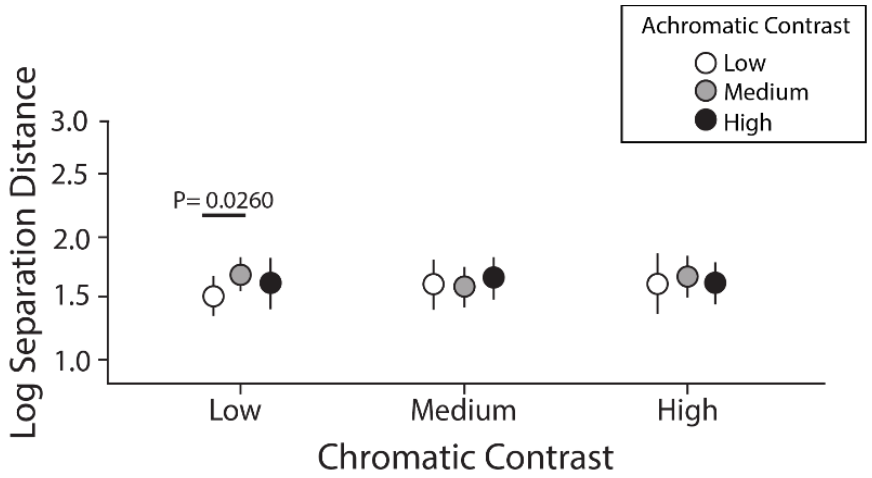

Figure 4.3 Separation distance (cm) between the zebrafish and animated conspecific in response to manipulation of animated conspecific to alter chromatic and achromatic contrast of the stripes. Results have been log transformed.

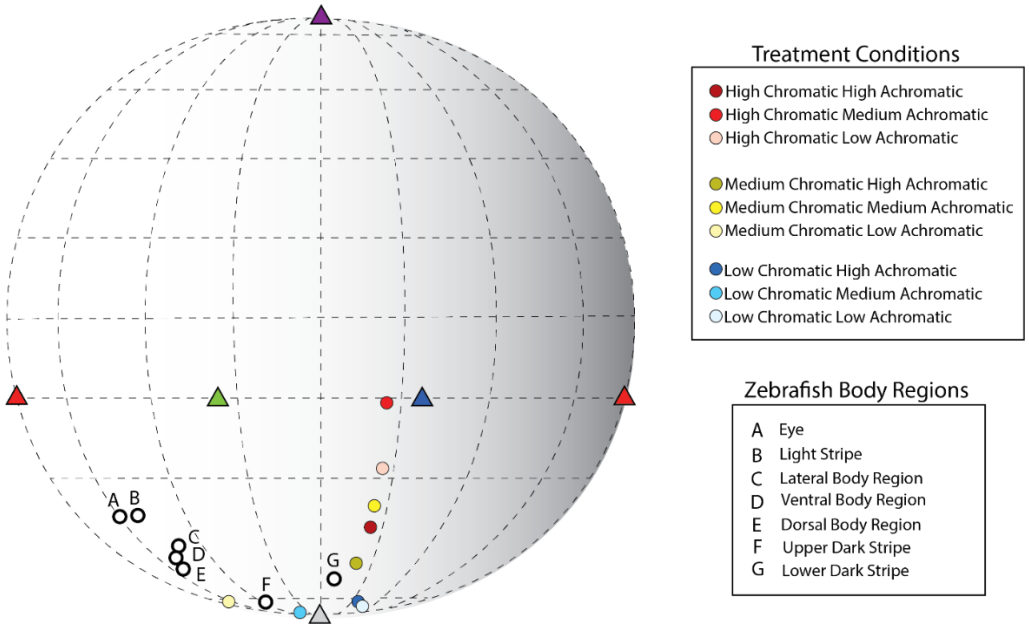

Figure 4.4 Spherical plot representing the animated treatments and zebrafish body regions in terms of their individual spectral characteristics (i.e., hue) in color space. Colored triangles represent each of the four cone photoreceptors: (UVS:LWS:MWS:SWS = purple:red:green:blue). The achromatic center is depicted with a grey triangle.

4.7 References

Abril-De-Abreu, R., Cruz, J., and Oliveira, R. F. (2015). Social Eavesdropping in Zebrafish: Tuning of Attention to Social Interactions. *Sci. Rep.* 5, 1–14. doi:10.1038/srep12678.

Allison, W. T., Barthel, L. K., Skebo, K. M., Takechi, M., Kawamura, S., and Raymond, P. a. (2010). Ontogeny of cone photoreceptor mosaics in zebrafish. *J. Comp. Neurol.* 518, 4182–4195. doi:10.1002/cne.22447.

Avdesh, A., Martin-Iverson, M. T., Mondal, A., Chen, M., Askraba, S., Morgan, N., et al. (2012). Evaluation of color preference in zebrafish for learning and memory. *J. Alzheimer's Dis.* 28, 459–469. doi:10.3233/JAD-2011-110704.

Bachmann, J. C., Cortesi, F., Hall, M. D., Marshall, N. J., Salzburger, W., and Gante, H. F. (2017). Real-time social selection maintains honesty of a dynamic visual signal in cooperative fish. *Evol. Lett.* 1, 269–278. doi:10.1002/evl3.24.

Bartolini, T., Mwaffo, V., Showler, A., Macrì, S., Butail, S., and Porfiri, M. (2016). Zebrafish response to 3D printed shoals of conspecifics: The effect of body size. *Bioinspiration and Biomimetics* 11. doi:10.1088/1748-3190/11/2/026003.

Bhat, A., Greulich, M. M., and Martins, E. P. (2015). Behavioral plasticity in response to environmental manipulation among zebrafish (*Danio rerio*) populations. *PLoS One* 10, 1–13. doi:10.1371/journal.pone.0125097.

Bressman, N. R., Love, J. W., King, T. W., Horne, C. G., and Ashley-Ross, M. A. (2019). Emersion and Terrestrial Locomotion of the Northern Snakehead (*Channa argus*) on Multiple Substrates. *Integr. Org. Biol.* 1. doi:10.1093/iob/obz026.

Champ, C. M., Vorobyev, M., and Marshall, N. J. (2016). Colour thresholds in a coral reef fish. *R. Soc. Open Sci.* 3. doi:10.1098/rsos.160399.

Clotfelter, E. D., Ardia, D. R., and McGraw, K. J. (2007). Red fish, blue fish: Trade-offs between pigmentation and immunity in *Betta splendens*. *Behav. Ecol.* 18, 1139–1145. doi:10.1093/beheco/arm090.

Davies-Colley, R. J., and Vant, W. N. (1987). Absorption of light by yellow substance in freshwater lakes. *Limnol. Oceanogr.* 32, 416–425. doi:10.4319/lo.1987.32.2.0416.

Domenici, P., Herbert, N. A., Lefrançois, C., Steffensen, J. F., and McKenzie, D. J. (2013). "The Effect of Hypoxia on Fish Swimming Performance and Behaviour," in *Swimming Physiology of Fish* (Berlin, Heidelberg: Springer Berlin Heidelberg), 129–159. doi:10.1007/978-3-642-31049-2_6.

Duarte, R. C., Flores, A. A. V., and Stevens, M. (2017). Camouflage through colour change: Mechanisms, adaptive value and ecological significance. *Philos. Trans. R. Soc. B Biol. Sci.* 372. doi:10.1098/rstb.2016.0342.

Endler, J. A. (1992). Signals, Signal Conditions, and the Direction of Evolution. *Am. Nat.* 139, S125–S153. doi:10.1086/285308.

Endler, J. A. (1993). The color of light in forests and its implications. *Ecol. Monogr.* 63, 1–27. doi:10.2307/2937121.

Engeszer, R. E., Patterson, L. B., Rao, A. A., and Parichy, D. M. (2007). Zebrafish in The Wild: A Review of Natural History And New Notes from The Field. *Zebrafish* 4, 21–40. doi:10.1089/zeb.2006.9997.

Engeszer, R. E., Ryan, M. J., and Parichy, D. M. (2004). Learned Social Preference in Zebrafish. *Curr. Biol.* 14, 881–884.

Engeszer, R. E., Wang, G., Ryan, M. J., and Parichy, D. M. (2008). Sex-specific perceptual spaces for a vertebrate basal social aggregative behavior. *Proc. Natl. Acad. Sci. U. S. A.* 105, 929–933. doi:10.1073/pnas.0708778105.

Escobar-Camacho, D., Taylor, M. A., Cheney, K. L., Green, N. F., Justin Marshall, N., and Carleton, K. L. (2019). Color discrimination thresholds in a cichlid fish: *Metriaclima benetos*. *J. Exp. Biol.* 222. doi:10.1242/jeb.201160.

Fleishman, L. J., Perez, C. W., Yeo, A. I., Cummings, K. J., Dick, S., and Almonte, E. (2016). Perceptual distance between colored stimuli in the lizard *Anolis sagrei*: comparing visual system models to empirical results. *Behav. Ecol. Sociobiol.* 70, 541–555. doi:10.1007/s00265-016-2072-8.

Fujii, R. (2000). The regulation of motile activity in fish chromatophores. *Pigment Cell Res.* 13, 300–319. doi:10.1034/j.1600-0749.2000.130502.x.

Gerlai, R. (2017). Animated images in the analysis of zebrafish behavior. *Curr. Zool.* 63, 35–44. doi:10.1093/cz/zow077.

Govardovskii, V. I., Fyhrquist, N., Reuter, T., Kuzmin, D. G., and Donner, K. (2000). In search of the visual pigment template. *Vis. Neurosci.* 17, 509–528. doi:10.1017/S0952523800174036.

Hawryshyn, C. W., Chou, B. R., and Beauchamp, R. D. (1985). Ultraviolet transmission by the ocular media of goldfish: implications for ultraviolet photosensitivity in fishes. *Can. J. Zool.* 63, 1244–1251. doi:10.1139/z85-186.

Heathcote, R. J. P., Darden, S. K., Troscianko, J., Lawson, M. R. M., Brown, A. M., Laker, P. R., et al. (2018). Dynamic eye colour as an honest signal of aggression. *Curr. Biol.* 28, R652–R653. doi:10.1016/j.cub.2018.04.078.

Hiermes, M., Rick, I. P., Mehlis, M., and Bakker, T. C. M. (2016). The dynamics of color signals in male threespine sticklebacks *Gasterosteus aculeatus*. *Curr. Zool.* 62, 23–31. doi:10.1093/cz/zov009.

Höglund, E., Balm, P. H. M., and Winberg, S. (2000). Skin darkening, a potential social signal in subordinate Arctic charr (*Salvelinus alpinus*): The regulatory role of brain monoamines and pro-opiomelanocortin-derived peptides. *J. Exp. Biol.* 203, 1711–1721.

Houde, A. E., and Torio, A. J. (1992). Effect of parasitic infection on male color pattern and female choice in guppies. *Behav. Ecol.* 3, 346–351. doi:10.1093/beheco/3.4.346.

Hutter, S., Hettyey, A., Penn, D. J., and Zala, S. M. (2012). Ephemeral Sexual Dichromatism in Zebrafish (*Danio rerio*). *Ethology* 118, 1208–1218. doi:10.1111/eth.12027.

Hutter, S., Zala, S. M., and Penn, D. J. (2011). Sex recognition in zebrafish (*Danio rerio*). *J. Ethol.* 29, 55–61. doi:10.1007/s10164-010-0221-5.

Ingley, S. J., Rahmani Asl, M., Wu, C., Cui, R., Gadelhak, M., Li, W., et al. (2015). anyFish 2.0: An open-source software platform to generate and share animated fish models to study behavior. *SoftwareX* 3–4, 13–21. doi:10.1016/j.softx.2015.10.001.

Kalueff, A. V, Gebhardt, M., Stewart, A. M., Cachat, J. M., Brimmer, M., Chawla, J. S., et al. (2013). Towards a comprehensive catalog of zebrafish behavior 1.0 and beyond. *Zebrafish* 10, 70–86. doi:10.1089/zeb.2012.0861.

Kelber, A., Vorobyev, M., and Osorio, D. (2003). Animal colour vision - Behavioural tests and physiological concepts. *Biol. Rev. Camb. Philos. Soc.* 78, 81–118. doi:10.1017/S1464793102005985.

Kelley, J. L., Phillips, B., Cummins, G. H., and Shand, J. (2012). Changes in the visual environment affect colour signal brightness and shoaling behaviour in a freshwater fish. *Anim. Behav.* 83, 783–791. doi:10.1016/j.anbehav.2011.12.028.

Kodric-brown, A. (1998). Sexual Dichromatism and Temporary Color Changes in the Reproduction of Fishes. *Am Zool*. 38,70-81. doi:10.1093/icb/38.1.70.

Krause, J., and Ruxton, G. D. (2002). *Living in groups*. Oxford: Oxford University Press.

Ligon, R. A. (2014). Defeated chameleons darken dynamically during dyadic disputes to decrease danger from dominants. *Behav. Ecol. Sociobiol.* 68, 1007–1017. doi:10.1007/s00265-014-1713-z.

Ligon, R. A., and McGraw, K. J. (2016). Social costs enforce honesty of a dynamic signal of motivation. *Proc. R. Soc. B Biol. Sci.* 283. doi:10.1098/rspb.2016.1873.

Loew, E. R., and Zhang, H. (2006). “Propagation of Visual Signals in the Aquatic Environment: An Interactive Windows-based Model,” in *Communication in Fishes*, eds. F. Ladich, S. P. Collin, P. Moller, and B. G. Kapoor (Enfield, NH: Science Publishers), 281–302.

Lozano, G. A., Ave, P., and Jbi, C. H. A. (1994). Carotenoids, Parasites, and Sexual Selection. *Oikos* 70, 309–311.

Lythgoe, J. N. (1968). Visual pigments and visual range underwater. *Vision Res.* 8, 997–1012. doi:10.1016/0042-6989(68)90073-4.

Lythgoe, J. N. (1979). *The Ecology of Vision*. Oxford: Clarendon Press.

Lythgoe, J. N., and Partridge, J. C. (1989). Visual pigments and the acquisition of visual information. *J. Exp. Biol.* 146, 1–20.

Maia, R., Eliason, C. M., Bitton, P. P., Doucet, S. M., and Shawkey, M. D. (2013). pavo: An R package for the analysis, visualization and organization of spectral data. *Methods Ecol. Evol.* 4, 906–913. doi:10.1111/2041-210X.12069.

Maoka, T. (2020). Carotenoids as natural functional pigments. *J. Nat. Med.* 74, 1–16. doi:10.1007/s11418-019-01364-x.

Marshall, J., and Johnsen, S. (2011). “Camouflage in marine fish,” in *Animal Camouflage: Mechanisms and Function*, eds. M. Stevens and S. Merilaita (Cambridge: Cambridge University Press), 186–211. doi:10.1017/CBO9780511852053.011.

Marshall, N. J. (2000). Communication and camouflage with the same “bright” colours in reef fishes. *Philos. Trans. R. Soc. B Biol. Sci.* 355, 1243–1248. doi:10.1098/rstb.2000.0676.

Negro, J. J., Doña, J., Blázquez, M. C., Rodríguez, A., Herbert-Read, J. E., and Brooke, M. de L. (2020). Contrasting stripes are a widespread feature of group living in birds, mammals and fishes. *Proc. R. Soc. B Biol. Sci.* 287, 20202021. doi:10.1098/rspb.2020.2021.

Nilsson Sköld, H., Aspengren, S., and Wallin, M. (2013). Rapid color change in fish and amphibians - function, regulation, and emerging applications. *Pigment Cell Melanoma Res.* 26, 29–38. doi:10.1111/pcmr.12040.

O’Carroll, D. C., and Wiederman, S. D. (2014). Contrast sensitivity and the detection of moving patterns and features. *Philos. Trans. R. Soc. B Biol. Sci.* 369. doi:10.1098/rstb.2013.0043.

O’Connor, K. I., Metcalfe, N. B., and Taylor, A. C. (1999). Does darkening signal submission in territorial contests between juvenile Atlantic salmon, *Salmo salar*? *Anim. Behav.* 58, 1269–1276. doi:10.1006/anbe.1999.1260.

Oliveira, J., Silveira, M., Chacon, D., and Luchiari, A. (2015). The zebrafish world of colors and shapes: Preference and discrimination. *Zebrafish* 12, 166–173. doi:10.1089/zeb.2014.1019.

Orrock, J. L., Preisser, E. L., Grabowski, J. H., and Trussell, G. C. (2013). The cost of safety: Refuges increase the impact of predation risk in aquatic systems. *Ecology* 94, 573–579. doi:10.1890/12-0502.1.

Oshima, N., and Kasai, A. (2002). Iridophores Involved in Generation of Skin Color in the Zebrafish, *Brachydanio rerio*. *Forma*, 91–101.

Osorio, D., Mikló, A., and Gonda, Z. (1999). Visual ecology and perception of coloration patterns by domestic chicks. *Evol. Ecol.* 13, 673–689. doi:10.1023/A:1011059715610.

Pita, D., and Fernandez-Juricic, E. (2019). The visual social environment affects non-additively neighbor spacing and interaction time in zebrafish. *bioRxiv*, 511972. doi:10.1101/511972.

Price, A. C., Weadick, C. J., Shim, J., and Rodd, F. H. (2008). Pigments, Patterns, and Fish Behavior. *Zebrafish* 5, 297–307. doi:10.1089/zeb.2008.0551.

Qin, M., Wong, A., Seguin, D., and Gerlai, R. (2014). Induction of Social Behavior in Zebrafish: Live Versus Computer Animated Fish as Stimuli. *Zebrafish* 11, 185–197. doi:10.1089/zeb.2013.0969.

Rehberg-Besler, N., Mennill, D. J., and Doucet, S. M. (2015). Dynamic sexual dichromatism produces a sex signal in an explosively breeding Neotropical toad: A model presentation experiment. *Behav. Processes* 121, 74–79. doi:10.1016/j.beproc.2015.09.013.

Rosenthal, G. G., and Ryan, M. J. (2005). Assortative preferences for stripes in danios. *Anim. Behav.* 70, 1063–1066. doi:10.1016/j.anbehav.2005.02.005.

Rountree, R. A., and Sedberry, G. R. (2009). A theoretical model of shoaling behavior based on a consideration of patterns of overlap among the visual fields of individual members. *Acta Ethol.* 12, 61–70. doi:10.1007/s10211-009-0057-6.

Ruhl, N., and McRobert, S. P. (2005). The effect of sex and shoal size on shoaling behaviour in *Danio rerio*. *J. Fish Biol.* 67, 1318–1326. doi:10.1111/j.0022-1112.2005.00826.x.

Saverino, C., and Gerlai, R. (2008). The social zebrafish: Behavioral responses to conspecific, heterospecific, and computer animated fish. *Behav. Brain Res.* 191, 77–87. doi:10.1016/j.bbr.2008.03.013.

Schaefer, H. M., Levey, D. J., Schaefer, V., and Avery, M. L. (2006). The role of chromatic and achromatic signals for fruit detection by birds. *Behav. Ecol.* 17, 784–789. doi:10.1093/beheco/arl011.

Shelton, D. S., Shelton, S. G., Daniel, D. K., Raja, M., Bhat, A., Tanguay, R. L., et al. (2020). Collective Behavior in Wild Zebrafish. *Zebrafish* 17, 243–252. doi:10.1089/zeb.2019.1851.

Siddiqi, A., Cronin, T. W., Loew, E. R., Vorobyev, M., and Summers, K. (2004). Interspecific and intraspecific views of color signals in the strawberry poison frog Dendrobates pumilio. *J. Exp. Biol.* 207, 2471–2485. doi:10.1242/jeb.01047.

Singh, A. P., and Nüsslein-Volhard, C. (2015). Zebrafish stripes as a model for vertebrate colour pattern formation. *Curr. Biol.* 25, R81–R92. doi:10.1016/j.cub.2014.11.013.

Stevens, M., Lown, A. E., and Denton, A. M. (2014). Rockpool gobies change colour for camouflage. *PLoS One* 9. doi:10.1371/journal.pone.0110325.

Stuart-Fox, D., Moussalli, A., and Whiting, M. J. (2008). Predator-specific camouflage in chameleons. *Biol. Lett.* 4, 326–329. doi:10.1098/rsbl.2008.0173.

Sundin, J., Morgan, R., Finnøen, M. H., Dey, A., Sarkar, K., and Jutfelt, F. (2019). On the Observation of Wild Zebrafish (*Danio rerio*) in India. *Zebrafish* 16, 546–553. doi:10.1089/zeb.2019.1778.

Suriyampola, P. S., Shelton, D. S., Shukla, R., Roy, T., Anuradha, B., and Martins, E. P. (2015). Zebrafish Social Behavior in the Wild. *Zebrafish*, 1–8. doi:10.1089/zeb.2015.1159.

Vorobyev, M., and Osorio, D. (1998). Receptor noise as a determinant of colour thresholds. *Proc. Biol. Sci.* 265, 351–358. doi:10.1098/rspb.1998.0302.

Wilkins, L., Marshall, N. J., Johnsen, S., and Osorio, D. (2016). Modelling fish colour constancy, and the implications for vision and signalling in water. *J. Exp. Biol.*, jeb.139147-. doi:10.1242/jeb.139147.

Woo, K. L., and Rieucau, G. (2011). From dummies to animations : a review of computer-animated stimuli used in animal behavior studies. 1671–1685. doi:10.1007/s00265-011-1226-y.

DISCUSSION

Through further examination of the role of the sensory system in structuring social interactions I have identified several key findings. Chapter 1 highlighted the important role that the visual system plays in structuring collective interactions. Not only are collective behavior models sensitive to modifications of the visual assumptions, it also appears that incorporating more biologically realistic assumptions may enhance their predictive value. This is important because misrepresenting the perception of various species can greatly underestimate the propagation of social information in the group, leading to inaccurate predictions regarding collective behavior.

Chapter 2 revealed important insights regarding the zebrafish's capacity to acquire and resolve social information. Zebrafish appear to benefit from a wide degree of visual coverage, allowing them to detect and respond to conspecifics in the environment. The zebrafish's small posterior blind area likely enhances predator detection, especially in the group setting where individuals can pool their visual coverage with conspecifics (Rountree and Sedberry, 2009). In a low-risk environment, the reduced demand for social information may allow for greater flexibility in individual positioning, leading to the formation of groups with low polarity and flexible shape. However, in high-risk environments, the increased demand for social information may result in groups with more rigid structure and higher polarity as individuals align themselves with neighbors using their centers of acute vision to enhance the resolution of social information.

Ideally, individuals in the group should detect predators early so they have a chance to escape or display avoidance maneuvers (Treherne and Foster, 1981). To accomplish this, individuals should maximize their neighbor separation distance and orient themselves in different directions in order to increase the group's collective visual coverage when the perceived risk in the environment is low. However, the maximum neighbor separation distance assumed by zebrafish may be limited by cue perception. Zebrafish appear to maintain a neighbor separation distance which facilitates the resolution of the stripes, a potential social cue. Maintaining resolution of the stripes likely facilitates the rapid transmission of social information regarding changes in neighbor movement (Negro et al., 2020). However, once a predator has been detected, maximizing neighbor separation distance is likely to be less advantageous in avoiding capture. Instead individuals may reduce their separation distance to enhance cohesion making it difficult for

predators to isolate any one individual from the group (i.e., confusion effect) (Krause and Ruxton, 2002).

Chapter 3 also revealed interesting tradeoffs regarding conspecific size disparity. Tradeoffs associated with interacting with large or small conspecific can affect social behavior in various ways. Large conspecifics are likely to have a competitive advantage in terms of fighting ability, resource acquisition and energy efficiency (Hoare et al., 2000). On the other hand, interacting with small conspecifics can increase an individual's predation risk due to the oddity effect where larger individuals offer a more profitable benefit to predators (Stephens and Krebs, 1986). As a result, certain situations may reduce the motivation for social interaction. We found that when interacting with large conspecifics, signals of potential aggression may result in individuals maintaining farther separation distances to avoid escalation. Additionally, incorporating environmental complexity through depth seems to supplement the perception of conspecific information while an increased perception of risk in the environment increases the motivation to obtain social information.

Chapter 4 emphasized the complexity of zebrafish visual signals and the potential wealth of information encoded in visual contrast. Not surprisingly, zebrafish social behavior is affected by different aspects of chromatic and achromatic contrast. Achromatic contrast appears to enhance the perception of conspecifics, but only when the chromatic dimension is close to reality. On the other hand, low levels of chromatic and achromatic contrast place limitations on cue perception with distance. Fluctuating changes in the visual properties of the aquatic environment are likely to greatly influence the propagation of social information (Lythgoe, 1979; Lythgoe and Partridge, 1989). For example, an environment with high turbidity can greatly impact visibility, reducing overall levels of illumination as well as shifting in the spectral properties of the environment to longer wavelengths (Lythgoe, 1979). As a result, zebrafish may need to maintain shorter separation distances, increase the achromatic contrast of their stripes or increase the long-wavelength signal of their body in order to enhance conspecific perception. It appears that for zebrafish, as in many other fish species, optimizing visual contrast is a constant battle between increasing saliency to enhance social communication and decreasing saliency to reduce predator detection.

The work in this dissertation provides unique insights regarding the potential factors involved in the formation and persistence of collective behavior. Ultimately, collective behavior is unlikely to be the result of fixed interaction rules. At the local level, individuals utilize various

dimensions to perceive social information. However, it appears that individuals also consider the context in which social information is received and this appears to influence their social interaction rules. Along similar lines, jackdaws (*Corvus monedula*) operate by topological-based rules in low risk environments, but then transition to metric-based rules in high risk environments (Ling et al., 2019). Like zebrafish, it is possible that in certain contexts, such as high-risk, individuals may place higher demands on acquiring social information, which may result in individuals placing greater reliance on certain visual dimensions that are likely to yield the most information. However, in low risk environments, individuals may reduce their demands for social information and instead prioritize acquiring personal information, which may shift visual demands to the surrounding environment. By learning more about the sensory demands on different species and their environment, we can expand our knowledge of the mechanisms guiding the formation of collective behavior.

4.8 Future Directions

This work provides the foundation to examine other exciting questions in collective behavior research. This dissertation focused mostly on characterizing the local interactions that occur between two individuals. However, future work should explore interactions at a larger scale, evaluating behavior at the group level. Advanced tracking software (Delcourt et al., 2013) can be used to test model predictions from chapter 1 as well as yield important insights about the structure of zebrafish groups and whether they follow the untested sensory-based grouping configurations as discussed in chapter 2.

It is also important to recognize that this work focused on examining the role of one modality, vision, in structuring social interactions. Realistically, multiple sensory modalities yield important information about the environment and conspecifics (Ladich et al., 2006). In fact, individuals often tradeoff the use of different modalities when information from one modality is reduced or unreliable (Partan, 2017). For example, in fish, the use of both vision and the lateral line are thought to play a role in structuring social interactions (Partridge and Pitcher, 1980). However, the aquatic environment is subject to variations in turbidity which can result in individuals placing a higher reliance on the lateral line when visibility is poor (Pitcher and Parrish, 1993). Further work should consider the role of higher order neural processing in structuring collective behavior. Some work has introduced the idea that individuals may have limits to their

social information processing (Lemasson et al., 2009). As a result, individuals may weigh conspecific information unequally when making behavioral decisions. Some models have attempted to incorporate this idea by placing limits on the number of conspecifics that an individual can obtain social information from (Ballerini et al., 2008). However, more work is needed to evaluate the role of higher order neural processing to determine its effects on collective behavior.

Further use of animated stimuli and manipulation of the visual social environment is likely to be another area of research with great potential. This work and others have shown that zebrafish are responsive to animated conspecific stimuli (Saverino and Gerlai, 2008; Qin et al., 2014; Gerlai, 2017). Incorporating more subtle behaviors to animated conspecifics is becoming increasingly possible and likely to yield new insights about social behavior. For example, one can examine the influence of agnostic interactions on social behavior by altering fin movements or changing swimming patterns to display aggressive or submissive behavior. Additionally, one can explore the effect of further modification to the virtual environment using virtual reality software which immerses the individual into a photorealistic world with conspecifics that respond to the individual's movements in real-time (Stowers et al., 2017).

This work also introduced the idea that zebrafish are responsive to changes in the visual contrast of conspecifics, but only when it is realistic to the natural phenotype. More work should explore the zebrafish's capacity for physiological color change in order to capture the spectrum of chromatic and achromatic changes that are capable of this species. Perhaps utilizing therapeutic or anesthetic agents could facilitate a way to measure the body reflectance from live zebrafish under various behavioral states (Hankison and Palmer, 2016).

The sensory drive hypothesis suggests that the environment plays a vital role in structuring the sensory system and that social signals evolve to optimize receiver perception (Endler, 1992; Cummings and Endler, 2018). Considering the diversity of the zebrafish natural environment, it is likely that the visual system must adapt to changes in the visual environment between sites. One of the assumptions of this work is that social communication is occurring in well-lit, full-spectrum, clear water. This is not always the reality for wild zebrafish which are exposed to daily and seasonal changes in the spectral properties of the aquatic environment as a result of changes in water depth, turbidity, vegetative cover and anthropogenic disturbance (Engeszer et al., 2007; Spence et al., 2008; Suriyampola et al., 2015; Sundin et al., 2019). As a result, it is very possible that the visual capabilities of the commercial wildtype zebrafish are vastly different from their wild

counterparts. Characterizing the visual adaptations of wild zebrafish could be the next exciting research frontier for this ubiquitous model organism.

References:

Ballerini, M., Cabibbo, N., Candelier, R., Cavagna, a, Cisbani, E., Giardina, I., et al. (2008). Interaction ruling animal collective behavior depends on topological rather than metric distance: evidence from a field study. *Proc. Natl. Acad. Sci. U. S. A.* 105, 1232–1237. doi:10.1073/pnas.0711437105.

Cummings, M. E., and Endler, J. A. (2018). 25 Years of Sensory Drive: the evidence and its watery bias. *Curr. Zool.* doi:10.1093/cz/zoy043.

Delcourt, J., Denoël, M., Ylieff, M., and Poncin, P. (2013). Video multitracking of fish behaviour: A synthesis and future perspectives. *Fish Fish.* 14, 186–204. doi:10.1111/j.1467-2979.2012.00462.x.

Endler, J. A. (1992). Signals, Signal Conditions, and the Direction of Evolution. *Am. Nat.* 139, S125–S153. doi:10.1086/285308.

Engeszer, R. E., Patterson, L. B., Rao, A. A., and Parichy, D. M. (2007). Zebrafish in The Wild: A Review of Natural History And New Notes from The Field. *Zebrafish* 4, 21–40. doi:10.1089/zeb.2006.9997.

Gerlai, R. (2017). Animated images in the analysis of zebrafish behavior. *Curr. Zool.* 63, 35–44. doi:10.1093/cz/zow077.

Hankison, S. J., and Palmer, M. S. (2016). Assays to Detect UV-reflecting Structures and Determine their Importance in Mate Preference using the Sailfin Molly (*Poecilia latipinna*). *J. Vis. Exp.*, 1–5. doi:10.3791/54453.

Hoare, D. J., Krause, J., Peuhkuri, N., and Godin, J. G. (2000). Body size and shoaling in fish. *J. Fish Biol.* 57, 1351–1366. doi:10.1006/jfbi.2000.1446.

Krause, J., and Ruxton, G. D. (2002). *Living in groups*. Oxford: Oxford University Press.

Ladich, F., Collin, S. P., Moller, P., and Kapoor, B. G. eds. (2006). *Communication in Fishes*. Enfield, NH: Science Publishers.

Lemasson, B. H., Anderson, J. J., and Goodwin, R. a. (2009). Collective motion in animal groups from a neurobiological perspective: The adaptive benefits of dynamic sensory loads and selective attention. *J. Theor. Biol.* 261, 501–510. doi:10.1016/j.jtbi.2009.08.013.

Ling, H., McIvor, G., Vaughan, R., Thornton, A., and Ouellette, N. (2019). Local interactions and their group-level consequences in flocking birds. *Proc. R. Soc. B Biol. Sci.*, 1–10.

Lythgoe, J. N. (1979). *The Ecology of Vision*. Oxford: Clarendon Press.

Lythgoe, J. N., and Partridge, J. C. (1989). Visual pigments and the acquisition of visual information. *J. Exp. Biol.* 146, 1–20.

Negro, J. J., Doña, J., Blázquez, M. C., Rodríguez, A., Herbert-Read, J. E., and Brooke, M. de L. (2020). Contrasting stripes are a widespread feature of group living in birds, mammals and fishes. *Proc. R. Soc. B Biol. Sci.* 287, 20202021. doi:10.1098/rspb.2020.2021.

Partan, S. R. (2017). Multimodal shifts in noise: switching channels to communicate through rapid environmental change. *Anim. Behav.* 124, 325–337. doi:10.1016/j.anbehav.2016.08.003.

Partridge, B., and Pitcher, T. (1980). The Sensory Basis of Fish Schools: Relative Roles of Lateral Line and Vision. *J. Comp. Physiol.* 135, 315–325.

Pitcher, T. J., and Parrish, J. K. (1993). "Functions of shoaling behaviour in teleosts," in *Behaviour of Teleost Fishes* (London: Chapman & Hall), 363–439.

Qin, M., Wong, A., Seguin, D., and Gerlai, R. (2014). Induction of Social Behavior in Zebrafish: Live Versus Computer Animated Fish as Stimuli. *Zebrafish* 11, 185–197. doi:10.1089/zeb.2013.0969.

Rountree, R. A., and Sedberry, G. R. (2009). A theoretical model of shoaling behavior based on a consideration of patterns of overlap among the visual fields of individual members. *Acta Ethol.* 12, 61–70. doi:10.1007/s10211-009-0057-6.

Saverino, C., and Gerlai, R. (2008). The social zebrafish: Behavioral responses to conspecific, heterospecific, and computer animated fish. *Behav. Brain Res.* 191, 77–87. doi:10.1016/j.bbr.2008.03.013.

Spence, R., Gerlach, G., Lawrence, C., and Smith, C. (2008). The behaviour and ecology of the zebrafish, *Danio rerio*. *Biol. Rev. Camb. Philos. Soc.* 83, 13–34.

Stephens, D., and Krebs, J. (1986). *Foraging Theory*. Princeton, N.J.: Princeton University Press.

Stowers, J. R., Hofbauer, M., Bastien, R., Griessner, J., Higgins, P., Farooqui, S., et al. (2017). Virtual reality for freely moving animals. *Nat. Methods* 14, 995–1002. doi:10.1038/nmeth.4399.

Sundin, J., Morgan, R., Finnøen, M. H., Dey, A., Sarkar, K., and Jutfelt, F. (2019). On the Observation of Wild Zebrafish (*Danio rerio*) in India. *Zebrafish* 16, 546–553. doi:10.1089/zeb.2019.1778.

Suriyampola, P. S., Shelton, D. S., Shukla, R., Roy, T., Anuradha, B., and Martins, E. P. (2015). Zebrafish Social Behavior in the Wild. *Zebrafish*, 1–8. doi:10.1089/zeb.2015.1159.

Treherne, J. E., and Foster, W. A. (1981). Group transmission of predator avoidance behaviour in a marine insect: The trafalgar effect. *Anim. Behav.* 29, 911–917. doi:10.1016/S0003-3472(81)80028-0.

APPENDIX A

Section 1: Estimation of species parameters: maximum turning angle, interaction distance and projection of the center of acute vision.

Estimation of species turning angle

Species turning angles were measured using the video analysis software, Tracker (http://physlets.org/tracker/). Using recorded videos of live species groups, we randomly selected a total of six individuals and measured their maximum turning angle per second. The measurements of each of these six individuals were then averaged across the group and were then used to represent each species respectively (
Table A1b).

Estimation of species interaction distances

We define each species interaction distance as the maximum resolvable distance that an individual was capable of perceiving visual social cues (i.e., head height for birds and body height for fish). We used these features as, in birds, the head region has been shown to provide reliable cues to assess conspecifics during social interactions (Butler et al., 2014), while in fish, visibility of the body is also likely to provide important information thought to influence social interactions (Croft et al., 2005).

First, we used the following equation to determine the retinal magnification factor (RMF) (Pettigrew et al., 1988), which represents the amount of space that an object takes up on the retina, where PND represents the posterior nodal distance, represented as 0.6 multiplied by the axial length of the eye for birds (Hughes, 1977), and 2.55 multiplied by the radius of the lens for fish (Collin and Pettigrew, 1988):

$$\mathrm{RMF} = \frac{2\pi \text{ x } \mathrm{PND}}{360}$$

After the RMF was determined, we calculated the spatial resolving power to estimate each species' ability to resolve conspecific features (i.e., head height for birds, body height for fish), using the minimum retinal ganglion cell density (cells/mm^2) across the retina (D) (Williams and Coletta, 1987). We used the minimum as opposed to the maximum retinal ganglion cell density because this value represented the minimum threshold limit allowing an individual to perceive social cues across all regions of its visual field, and not just localized regions of high visual acuity (i.e., center of acute vision). Although, it should be mentioned that the visual acuity achieved with the center of acute vision is much higher than the estimate used in this modeling exercise.

$$\mathrm{SRP} = \frac{\mathrm{RMF}}{2}\sqrt{\frac{2\mathrm{D}}{\sqrt{3}}}$$

The maximum resolvable visual distance (d) was then calculated using the equation where r represents the radius of the object (i.e., head height for birds and body height for fish) while α represents the inverse of spatial resolving power (SRP) (Tyrrell et al., 2013). This distance estimate assumes maximum visual contrast between the object and the background. The final resolvable distance estimate was then converted into units of body length, specific to each species and applied to both models (Table A1a).

$$d = \frac{r}{\tan\frac{\alpha}{2}}$$

Section 2: Results of the modeling exercises

Results for both the metric and topological model outputs comparing the group properties: group polarity (i.e., degree of alignment of all individuals in the population), number of groups, average group size (e.g., average number of individuals per each group) and average nearest neighbor distance (NND) for the classic and realistic sensory assumptions. Table 1 depicts the results upon final group stabilization. Additionally, Figure A1 illustrates the peak probability of neighbor presence used to assess group stability. Across all species, the realistic sensory assumptions result in fewer groups composed of a greater number of individuals compared to the classic sensory assumptions upon stabilization (Table A1). For some species (i.e., golden shiner and zebrafish) the realistic sensory assumptions produce populations with higher polarity and slightly shorter nearest neighbor distances upon stabilization (Table A1c,d). However, across all species, the realistic sensory assumptions produced a faster onset to group stabilization for all measured parameters.

Table A1. Results comparing the classic and realistic visual assumptions for the a. European starling, b. red-winged blackbird, c. golden shiner and d. zebrafish. Values indicate the grouping parameters (i.e., group polarity across the population, number of groups, average group size and average nearest neighbor distance (NND)) that resulted from each model (i.e., metric (MM) and topological (TM) upon stabilization (± SD).

a. European Starling

	Classic (MM)	Realistic (MM)	Classic (TM)	Realistic (TM)
Group Polarity	0.97 ± 0.01	0.97 ± 0.005	0.96 ± 0.02	0.96 ± 0.03
Number of Groups	2.16 ± 1.07	1 ± 0	2.64 ± 1.08	1.14 ± 0.35
Average Group Size	17.41 ± 8.71	30 ± 0	13.63 ± 5.82	28.26 ± 4.62
Average NND	1.14 ± 0.12	1.13 ± 0.11	1.18 ± 0.14	1.17 ± 0.11

b. Red-winged Blackbird

	Classic (MM)	Realistic (MM)	Classic (TM)	Realistic (TM)
Group Polarity	0.97 ± 0.006	0.97 ± 0.005	0.96 ± 0.010	0.96 ± 0.010
Number of Groups	2.76 ± 1.15	1 ± 0	3.50 ± 1.29	1 ± 0
Average Group Size	54.35 ± 23.45	100 ± 0	42.61 ± 20.21	100 ± 0
Average NND	1.00 ± 0.055	0.99 ± 0.046	1.05 ± 0.057	1.05 ± 0.073

c. Golden Shiner

	Classic (MM)	Realistic (MM)	Classic (TM)	Realistic (TM)
Group Polarity	0.67 ± 0.19	0.91 ± 0.056	0.57 ± 0.24	0.77 ± 0.25
Number of Groups	4.64 ± 1.35	1 ± 0	5.02 ± 1.72	1.14 ± 0.35
Average Group Size	12.37 ± 4.58	45 ± 0	11.22 ± 5.51	41.85 ± 7.88
Average NND	1.00 ± 0.025	0.98 ± 0.052	1.00 ± 0.024	0.99 ± 0.014

d. Zebrafish

	Classic (MM)	Realistic (MM)	Classic (TM)	Realistic (TM)
Group Polarity	0.64 ± 0.66	0.97 ± 0.01	0.66 ± 0.24	0.98 ± 0.01
Number of Groups	5.1 ± 1.62	1.0 ± 0.14	4.8 ± 1.85	1.0 ± 0
Average Group Size	1.9 ± 0.97	9.9 ± 0.77	2.1 ± 1.3	10.0 ± 0
Average NND	1.2 ± 0.17	0.97 ± 0.10	1.2 ± 1.6	0.96 ± 0.06

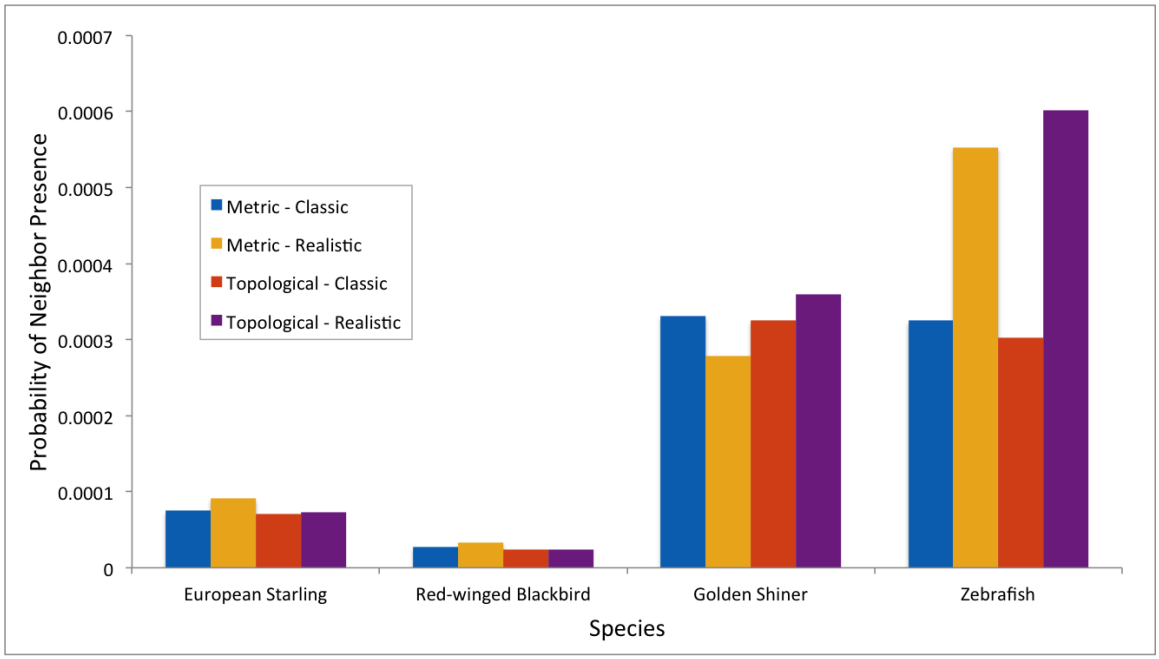

Figure A1. Graph depicting the peak probability of neighbor presence for all species using both the metric and topological versions of the model.

Section 3: Comparison of visual parameters with empirical findings

We estimated the projection of the center of acute vision (i.e., visual axis) in the horizontal plane for species in which the angle of the nearest neighbor's position (i.e., bearing angle) has been measured (Figure 2). European starlings have a 90° bearing angle (Ballerini et al., 2008) and their center of acute vision projects 60° from their directional heading (Butler et al., 2014) (Figure A2a). However, in the golden shiner, the bearing angle and projection of the center of acute vision are 60° (Katz et al., 2011) and 67° degrees (Pita et al., 2015) from their directional heading respectively (Figure A2b).

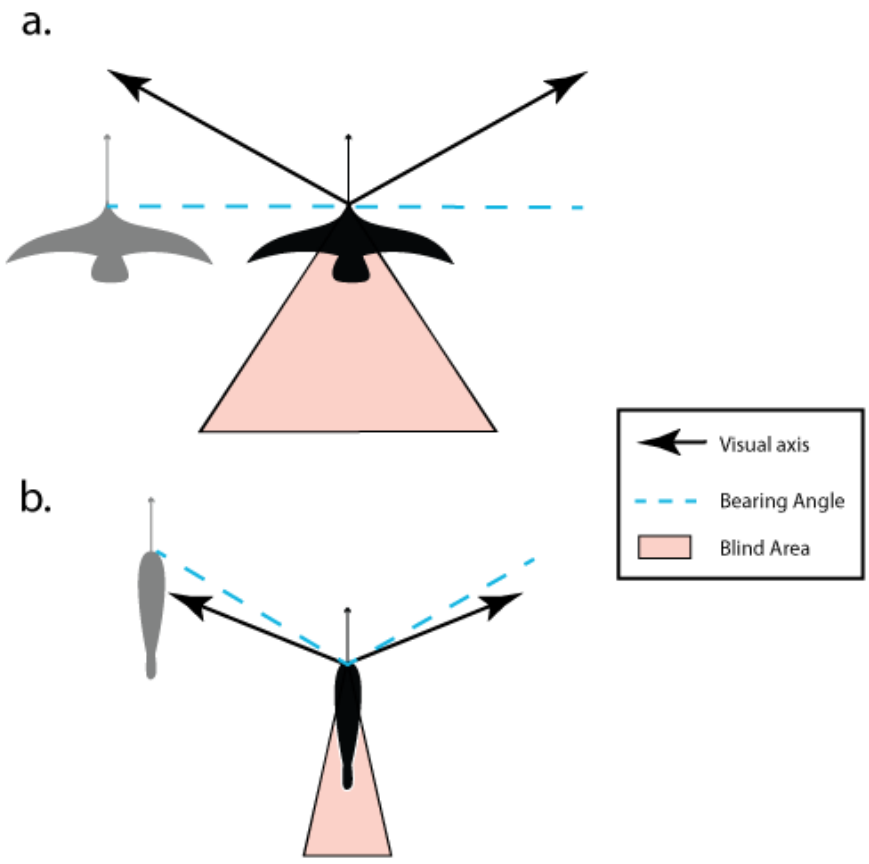

Figure A2. Schematic representation comparing the typical configuration of an individual in a group along the horizontal plane of the body. The angle of the nearest neighbor's position (i.e., bearing angle) and the of the projection of the center of acute vision (i.e., visual axis) are represented on the focal individual depicted in black, while its nearest neighbor is depicted in grey. a. European starlings have a 90° bearing angle and 60° visual axis from their forward directional heading and b. golden shiners have a 60° bearing angle and 67° visual axis.

References:

Ballerini, M., Cabibbo, N., Candelier, R., Cavagna, a, Cisbani, E., Giardina, I., et al. (2008). Interaction ruling animal collective behavior depends on topological rather than metric distance: evidence from a field study. *Proc. Natl. Acad. Sci. U. S. A.* 105, 1232–1237. doi:10.1073/pnas.0711437105.

Butler, S. R., Fernandez-Juricic, E., and Fernández-Juricic, E. (2014). European starlings recognize the location of robotic conspecific attention. *Biol. Lett.* 10, 20140665. doi:10.1098/rsbl.2014.0665.

Collin, S. P., and Pettigrew, J. D. (1988). Retinal ganglion cell topography in teleosts: A comparison between nissl-stained material and retrograde labelling from the optic nerve. *J. Comp. Neurol.* 276, 412–422. doi:10.1002/cne.902760306.

Croft, D. P., James, R., Ward, A. J. W., Botham, M. S., Mawdsley, D., and Krause, J. (2005). Assortative interactions and social networks in fish. *Oecologia* 143, 211–219. doi:10.1007/s00442-004-1796-8.

Hughes, A. (1977). "The topography of vision in mammals of contrasting life style: comparative optics and retinal organization," in *The visual system in vertebrates* (New York: Springer), 613–756.

Katz, Y., Tunstrøm, K., Ioannou, C. C., Huepe, C., Couzin, I. D., Tunstrom, K., et al. (2011). Inferring the structure and dynamics of interactions in schooling fish. *Proc. Natl. Acad. Sci.* 108, 18720–18725. doi:10.1073/pnas.1107583108.

Pettigrew, J. D., Dreher, B., Hopkins, C. S., McCall, M. J., and Brown, M. (1988). Peak density of ganglion cells in the retinae of michiropteran bats: implications for visual acuity. *Brain. Behav. Evol.* 32, 39–56.

Pita, D., Moore, B. A., Tyrrell, L. P., and Fernández-Juricic, E. (2015). Vision in two cyprinid fish: implications for collective behavior. *PeerJ* 3, e1113. doi:10.7717/peerj.1113.

Tyrrell, L. P., Moore, B. A., Loftis, C., and Fernández-Juricic, E. (2013). Looking above the prairie: localized and upward acute vision in a native grassland bird. *Sci. Rep.* 3, 3231. doi:10.1038/srep03231.

Williams, D. R., and Coletta, N. J. (1987). Cone spacing and the visual resolution limit. *J. Opt. Soc. Am. A* 4, 1514. doi:10.1364/JOSAA.4.001514.

APPENDIX B

Section 1: Visual field configuration and apparatus design

We scaled down the visual field apparatus design of (Martin, 1984) to allow for the observation of the retinal reflex with an ophthalmoscope (Figure B1). This was accomplished by reducing the diameter of circular rotating arm to 24 cm. The apparatus was configured such that 90° and 270° were directly in front and behind of the animal, respectively, along the horizontal plane, while 0° and 180° represented the vertical plane above and below the animal, respectively (Figure 2.1C, D).

Fish were measured immediately after euthanasia and were fixed on top of two metal prongs located at the center of the coordinate system of the apparatus (Figure B2). We maintained the position of the animal such that the body was parallel to the ground (i.e. 90° horizontal plane). The adjustment dial on the side of the apparatus allowed the observer to measure the visual field across various elevations about the animal. We recorded the visual field configuration across all angles around the head along 10° increments in elevation. The elevations 160°-270° were obtained such that the dorsal side of the fish was 0° and the ventral side was 180°. Complete rotation of the circular arm was obstructed along the elevations of 170°-260°; in order to record the visual field along this region, we rotated the body of the animal along the x-axis, 180° such that the dorsal side of the fish faced 180° and the ventral side faced 0°.

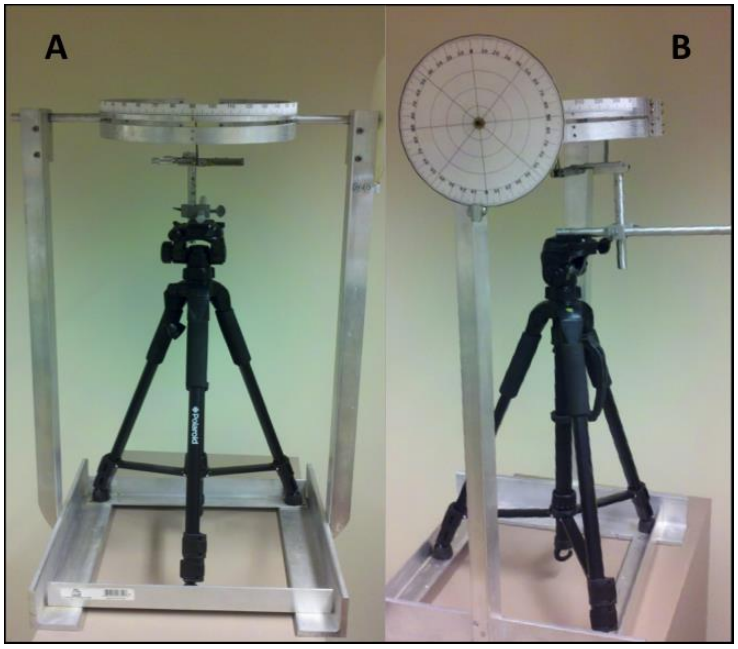

Figure B1. The visual field apparatus designed to measure the retinal visual field in fish. (A) front view and (B) side view of the apparatus with circular dial in view

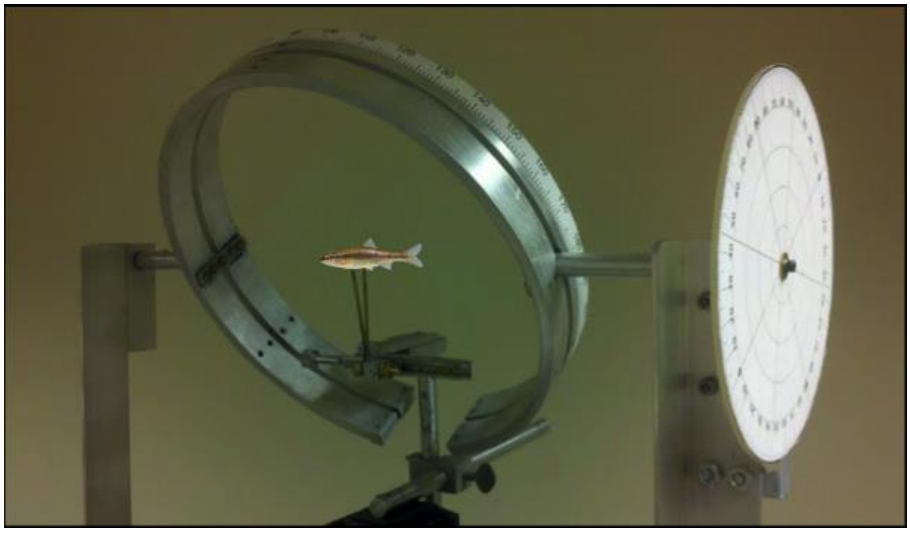

Figure B2. Closeup of the apparatus with fish model in view. For accurate measurement, the fish is placed in the center of the apparatus where the head and body are aligned in the horizontal plane, 90°-270°. The circular rotating metal arm has angular coordinates along the outer perimeter, used for determining the width of the visual field along various elevations around the head.

APPENDIX C

Section 1: Experimental arena:

We used two cameras to record the behavior of the live fish in response to the video playback of the virtual fish (
Figure C1).

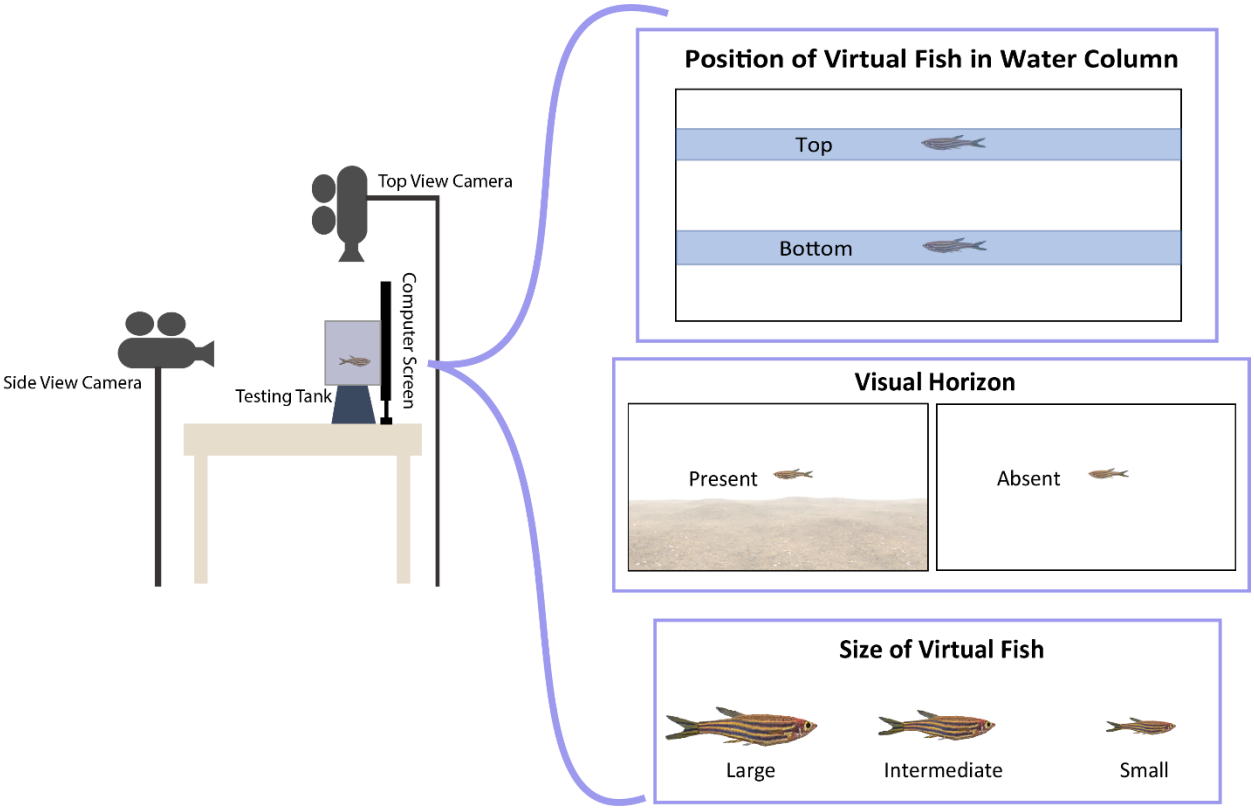

Figure C1. Experimental arena and camera setup during video playback.

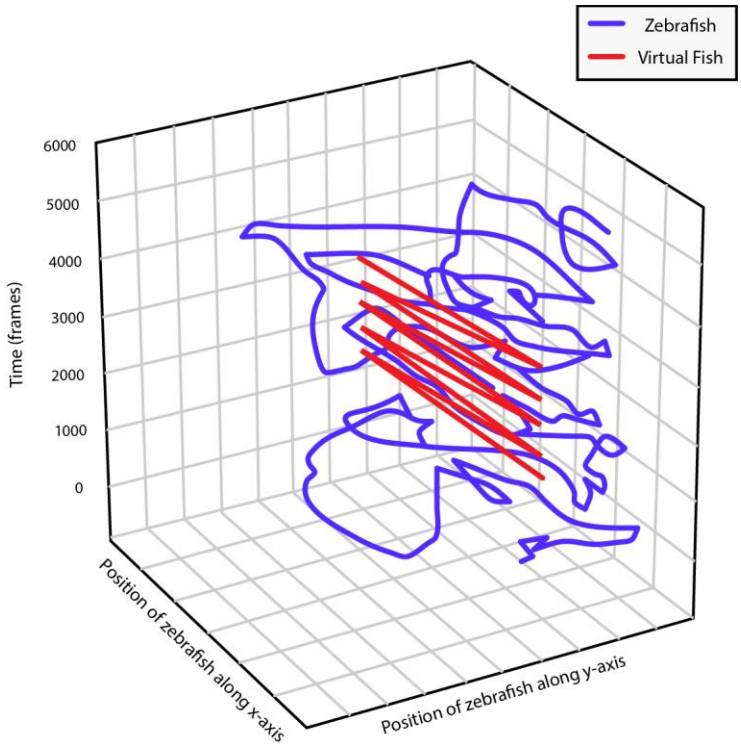

Figure C2. Representative sample of the movement trajectory of the zebrafish (x and y position) before, during and after the virtual fish treatment exposure. Data for the figure was generated using the videotracking software idTracker (http://www.idtracker.es/) from the side view camera recording. Additional data available upon request.

Section 2: Code used for the statistical analyses:

We conducted our general linear mixed models using ProcMixed in SAS. The code used for each variable is presented here.

Dependent variable: Interaction distance

```
proc mixed data=ddd;
class StimSize StimHeight Substrate ID;
model Separation_Distance = StimSize StimHeight Substrate Order StimSize*StimHeight StimSize*Substrate StimHeight*Substrate/solution outp=preds ddfm=bw;
random ID StimSize(ID) StimHeight(ID) Substrate(ID) / V VCorr;
  lsmeans StimSize StimHeight Substrate StimSize*StimHeight StimHeight*Substrate/diff;
proc plot data=preds; plot resid*pred;
proc univariate data=preds plot normal;  var resid;
run;
```

Dependent variable: Interaction time

```
proc mixed data=ddd;
```

```
class StimSize StimHeight Substrate ID;
model Approach_Duration = StimSize StimHeight Substrate Order StimSize*StimHeight StimSize*Substrate StimHeight*Substrate/solution outp=preds ddfm=bw;
random ID StimSize(ID) StimHeight(ID) Substrate(ID) / V VCorr;
  lsmeans StimSize StimHeight Substrate StimSize*StimHeight StimHeight*Substrate/diff;
proc plot data=preds; plot resid*pred;
proc univariate data=preds plot normal;  var resid;
run;
```

Dependent variable: probability of using the center of acute vision

```
proc glimmix data= ddd method=rspl;
 class StimSize StimHeight Substrate ID;
model COAV = StimSize  StimHeight Substrate Order StimSize*StimHeight StimSize*Substrate StimHeight*Substrate
/ dist=binomial link=logit solution ddfm=bw;
 random ID StimSize(ID) StimHeight(ID) Substrate(ID) / type=ar(1);
 lsmeans StimSize StimHeight Substrate;
run;
```

Abbreviation of other factors:
- StimSize: the size of the virtual conspecific (large, intermediate, small).
- StimHeight: the perceived social risk (top, bottom position of the virtual conspecific in the water column).
- Substrate: the perceived depth (presence, absence of the visual horizon).
- COAV: use of center of acute vision (high acuity vision) or retinal periphery (low acuity vision).
- ID: identity of the individual zebrafish.
- Order: order in which each individual zebrafish approached the virtual fish.

Section 3: Estimation of resolution limits:

Visual acuity is positively associated with the density of retinal ganglion cells, which summate information from other retinal cell types into an electrical signal that is sent to the brain, and eye size (Pettigrew et al., 1988; Pettigrew and Manger, 2008). Typically, higher visual acuity or spatial resolving power leads to a greater capacity to resolve objects of a finer scale at a given distance. Additionally, higher spatial resolving power allows animals to resolve objects from farther away. We estimated the distances at which zebrafish would be able to resolve the eye size and the stripe width of a conspecific (i.e., resolution limits) (Table 1). Retinal ganglion cell estimates of acuity were calculated from a previous paper (Pita et al., 2015), which were then incorporated into the following equation to calculate spatial resolving power: $\frac{RMF}{2}\sqrt{\frac{2D}{3}}$, where D represents the density of retinal ganglion cells and RMF represents the retinal magnification factor. The RMF was calculated as: $\frac{2\pi\ x\ PND}{360}$, where PND is the posterior nodal distance, which is calculated by multiplying the radius of the zebrafish lens by 2.55 (Williams and Coletta, 1987; Collin and Pettigrew, 1988). Final spatial resolving power values are in units of cycles per degree. We estimated visual acuity using the retinal ganglion cell density of the center of acute vision (high

acuity vision) as 1.89 cycles/degree, and the periphery of the retina (low acuity vision) as 0.81 cycles/degree. Actually, our low acuity vision estimates of spatial resolving power were similar to previous estimates based on photoreceptor densities (0.87 cycles/degree; Haug et al. 2010) and behavioral measurements (0.60 cycles/degree; Tappeiner et al. 2012; Cameron et al. 2013). Therefore, for the calculations in the next section we only used the ones we estimated from retinal ganglion cells (high and low acuity vision).

We then utilized the equation from (Tyrrell et al., 2013), $d = \frac{r}{\tan\frac{\alpha}{2}}$, to calculate the maximum distance (d) that zebrafish could resolve conspecific social cues using the radius (r) of the eyes and stripes, with α being the inverse of the spatial resolving power. This equation assumes maximum visual contrast and optimal ambient light conditions.

We estimated the distances zebrafish would be able to resolve the eye and stripes of conspecifics with different sizes of the virtual fish and compared those distances to the averaged neighbor distances they maintained during the experiment (Figure C3). We considered resolution distances when the live fished used high acuity vision (Figure C3a) and low acuity vision (Figure A3b). These results suggest that zebrafish appeared to maintain a distance that allowed them to resolve the eyes and stripes with high acuity vision for all virtual fish sizes (Figure C3a). However, the separation distance maintained by zebrafish would only allow for social cue resolution with low acuity vision for the large and intermediate conspecific sizes, but not necessarily for the small virtual fish sizes (Figure C3b). When live fished interacted with the small virtual fish, they maintained a separation distance that would allow for the resolution of the eye and it was at the margin of the limits for resolving the stripes.

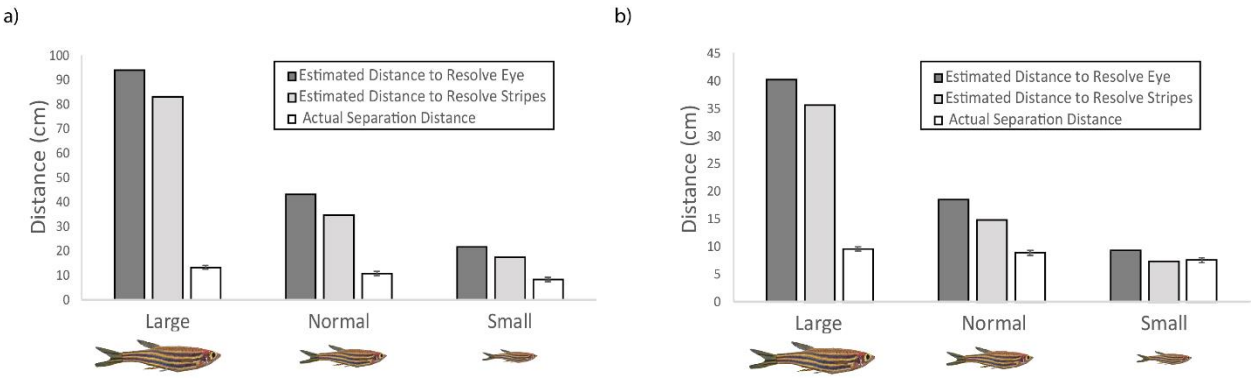

Figure C3. Distance at which zebrafish could resolve the eye and stripes of a conspecific (gray bars) relative to the averaged actual separation distance measured during the experiment for three sizes of the virtual conspecific (large, intermediate, small) considering resolution limits calculated using (a) high acuity vision and (b) low acuity vision.

References:

Cameron, D. J., Rassamdana, F., Tam, P., Dang, K., Yanez, C., Ghaemmaghami, S., et al. (2013). The optokinetic response as a quantitative measure of visual acuity in zebrafish. *J. Vis. Exp.*, 1–6. doi:10.3791/50832.

Collin, S. P., and Pettigrew, J. D. (1988). Retinal ganglion cell topography in teleosts: A comparison between nissl-stained material and retrograde labelling from the optic nerve. *J. Comp. Neurol.* 276, 412–422. doi:10.1002/cne.902760306.

Pettigrew, J. D., Dreher, B., Hopkins, C. S., McCall, M. J., and Brown, M. (1988). Peak Density and Distribution of Ganglion Cells in the Retinae of Microchiropteran Bats: Implications for Visual Acuity. *Brain. Behav. Evol.* 32, 48–56. doi:10.1159/000316042.

Pettigrew, J. D., and Manger, P. R. (2008). Retinal ganglion cell density of the black rhinoceros (*Diceros bicornis*): calculating visual resolution. *Vis. Neurosci.* 25, 215–20. doi:10.1017/S0952523808080498.

Pita, D., Moore, B. A., Tyrrell, L. P., and Fernández-Juricic, E. (2015). Vision in two cyprinid fish: implications for collective behavior. *PeerJ* 3, e1113. doi:10.7717/peerj.1113.

Tappeiner, C., Gerber, S., Enzmann, V., Balmer, J., Jazwinska, A., and Tschopp, M. (2012). Visual acuity and contrast sensitivity of adult zebrafish. *Front. Zool.* 9, 10. doi:10.1186/1742-9994-9-10.

Tyrrell, L. P., Moore, B. A., Loftis, C., and Fernández-Juricic, E. (2013). Looking above the prairie: localized and upward acute vision in a native grassland bird. *Sci. Rep.* 3, 3231. doi:10.1038/srep03231.

Williams, D. R., and Coletta, N. J. (1987). Cone spacing and the visual resolution limit. *J. Opt. Soc. Am. A* 4, 1514. doi:10.1364/JOSAA.4.001514.

APPENDIX D

Section 1: Animated Color Treatments

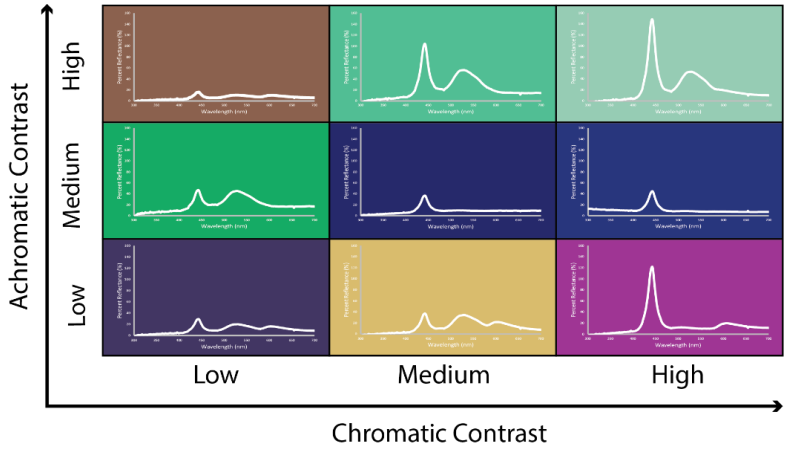

Figure D1. Reflectance spectra of the 9 animated colors used in the experiment represented across categories of low, medium and high chromatic and achromatic contrast.

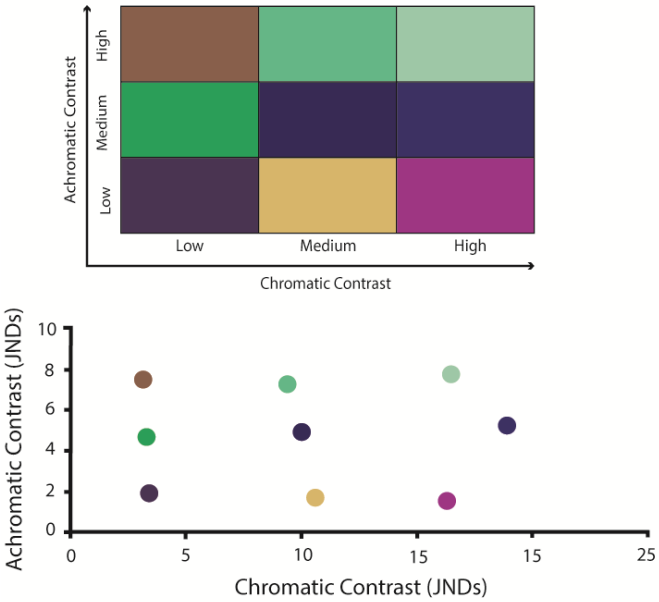

Figure D2. Representation of the 9 RGB animated colors according to zebrafish visual contrast perception. Visually saliency is represented in units of just noticeable difference (JND) calculated using the receptor noise limited model (Vorobyev and Osorio, 1998). A JND less than 1 is considered indistinguishable from the visual background while a JND above 3 is considered easily distinguishable (Siddiqi et al., 2004).

Section 2: Reflectance of Zebrafish body regions

The reflectance of 5 adult wildtype zebrafish were measured from 300 to 700 nm, averaged and interpolated into 1 nm increments in order to calculate the percent reflectance. Prior to measurement, the zebrafish were euthanized via the rapid cooling method which exposes zebrafish to an ice water bath for 20 minutes (Wilson et al., 2009). Measurements of the 7 different body regions were measured 5 times per region per individual.

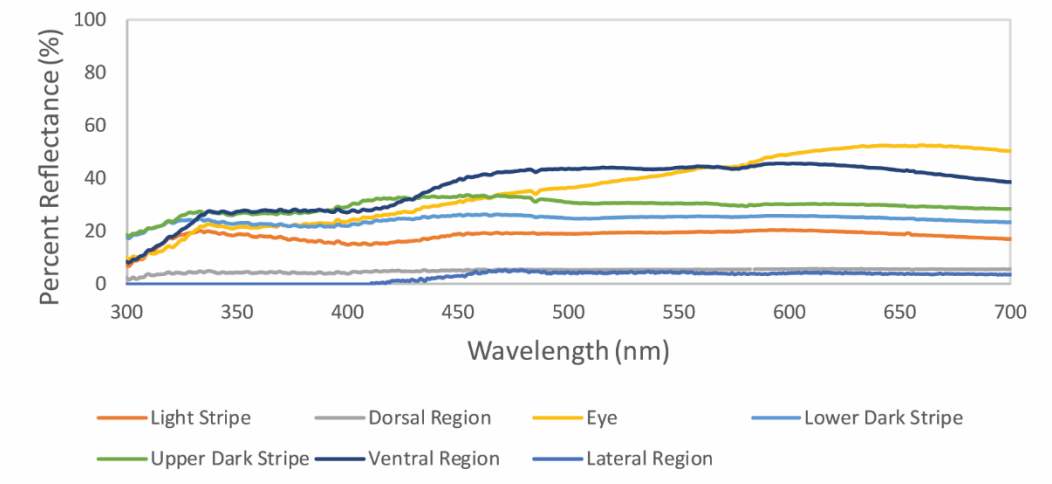

Figure D3. Percent reflectance of zebrafish body regions taken with spectrometer.

Section 3: Code used for statistical analyses:

We analyzed the data using general linear mixed models in R (v. 4.0.2) with the packages lme4 and afex. The data were log transformed to satisfy model assumptions for normality of the residuals and homogeneity of variance.

Background Manipulation Experiment - Dependent Variable: Separation Distance (log transformed):

```
Lbkdistancet <- mixed(log_Separation_Distance ~ Chromatic + Achromatic + Chromatic*Achromatic +(Chromatic + Achromatic||ID), data = zebrafish, method = "KR",
                control = lmerControl(optCtrl = list(maxfun = 1e6)), expand_re = TRUE)
anova(Lbkdistancet)
```

Background Manipulation Experiment - Dependent Variable: Interaction Duration (log transformed):

```
Lbkdurationt <- mixed(log_Duration ~ Chromatic + Achromatic + Chromatic*Achromatic +(Chromatic + Achromatic||ID), data = zebrafish, method = "KR",
                control = lmerControl(optCtrl = list(maxfun = 1e6)), expand_re = TRUE)
anova(Lbkdurationt)
```

Conspecific Manipulation Experiment - Dependent Variable: Separation Distance (log transformed):

```
Lbkdistancet <- mixed(log_Separation_Distance ~ Chromatic + Achromatic + Chromatic*Achromatic +(Chromatic + Achromatic||ID), data = zebrafish, method = "KR",
                control = lmerControl(optCtrl = list(maxfun = 1e6)), expand_re = TRUE)
anova(Lbkdistancet)
```

References:

Siddiqi, A., Cronin, T. W., Loew, E. R., Vorobyev, M., and Summers, K. (2004). Interspecific and intraspecific views of color signals in the strawberry poison frog *Dendrobates pumilio*. *J. Exp. Biol.* 207, 2471–2485. doi:10.1242/jeb.01047.

Vorobyev, M., and Osorio, D. (1998). Receptor noise as a determinant of colour thresholds. *Proc. Biol. Sci.* 265, 351–358. doi:10.1098/rspb.1998.0302.

Wilson, J. M., Bunte, R. M., and Carty, A. J. (2009). Evaluation of rapid cooling and tricaine methanesulfonate (MS222) as methods of euthanasia in zebrafish (*Danio rerio*). *J. Am. Assoc. Lab. Anim. Sci.* 48, 785–789.